2-3-2014

The Known MyoD Enhancers are Largely Dispensable for Proper Embryonic Expression and Cells of the MyoD Expressing Lineage are Multipotent in the Trunk but Not the Limbs of Amyogenic Embryos

James R. Camp
University of Connecticut - Storrs, james.camp@uconn.edu

The Known *MyoD* Enhancers are Largely Dispensable for Proper Embryonic Expression

And

Cells of the *MyoD* Expressing Lineage are Multipotent in the Trunk but Not the Limbs of Amyogenic Embryos

by

James Camp, PhD

University of Connecticut, 2014

In the developing vertebrate embryo, multipotent cells of the paraxial mesoderm form epithelial spheres called somites that physically define the segmentation pattern of the embryo. *MyoD* is transcribed in the myogenic precursor cells of the developing somite and is essential for proper hypaxial muscle formation. Whether *MyoD* is a determination factor or downstream member of the myogenic program had yet to be shown and the cis-transcriptional control of this important gene was incompletely defined.

By permanently labeling cells that have transcribed the *MyoD* locus in *MyoD*$^{-/-}$/*Myf-5*$^{-/-}$ embryos, where myogenesis does not occur, the determination state of presumptive myoblasts has been revealed. Previous studies used a temporary cell labeling system and suggested that in *MyoD*$^{-/-}$/*Myf-5*$^{-/-}$ embryos, cells of the *MyoD* lineage apoptose and do not contribute to other cell types. This suggests that the *MyoD* lineage is committed to myogenesis before myoblasts form. In the results presented herein, cells that have activated the

MyoD locus persist until birth and contribute to bone, brown adipose tissue and connective tissue demonstrating the multipotent nature of premyogenic cells prior to *MyoD* activation.

The genetic regulatory elements controlling *MyoD* expression were thought to be the core enhancer (CE) and distal regulatory region (DRR), where the CE initiates *MyoD* expression and the DRR maintains it. Deletion of either the CE or DRR from the mouse genome resulted in only mild phenotypes and suggested more complexity in *MyoD* regulation. Here, we deleted both the CE and DRR to determine if the enhancers have compensatory abilities or if other unknown regulatory elements exist. *In situ* hybridization for *MyoD* mRNA in our new line of mouse embryos shows that removal of both enhancers does not seriously alter the *MyoD* expression profile. The phenotypes seen in the individual knockout embryos are both present when the CE and DRR are removed. Genomic database analysis implicates the introns of *MyoD* as the uncharacterized enhancers.

The Known *MyoD* Enhancers are Largely Dispensable for Proper Embryonic Expression

And

Cells of the *MyoD* Expressing Lineage are Multipotent in the Trunk but Not the Limbs of Amyogenic Embryos

by

James Camp, B.S. University of Connecticut, 2001

A Dissertation

Submitted in Partial Fulfillment of the

Requirements of the Degree of

Doctor of Philosophy

at the

University of Connecticut, 2014

Approval Page

Doctor of Philosophy Dissertation

The Known *MyoD* Enhancers are Largely Dispensable for Proper Embryonic Expression and Cells of the *MyoD* Expressing Lineage are Multipotent in the Trunk but Not the Limbs of Amyogenic Embryos

Presented by

James Camp, B.A.

Major Advisor_____
David Goldhamer

Associate Advisor_____
Michael O'Neill

Associate Advisor_____
Charles Giardina

Associate Advisor_____
David Knecht

Associate Advisor_____
Joseph LoTurco

University of Connecticut

2014

University of Connecticut

2014

Acknowledgements

I would like to begin by expressing my gratitude to Dr. David Goldhamer for the immense learning experience I underwent during my graduate career. I never intended to pursue a PhD, and frankly, I didn't think I was able to. As a Masters student, I met David and he quickly drew me into the vast world of higher education. Thinking back on me as I came into this program is comparable to thinking of a different person. I have grown, learned, and matured during my PhD career, and David played a major role in my growth.

I also want to thank the members of my Ph.D. committee, Drs. Charles Giardina, David Knecht, Michael J. O'Neill, and Joseph LoTurco who found time along their busy schedules to accommodate me and guide me with their helpful input along the way. They have supported me, made me sweat, and forced me to change my view of my work and the scientific field as a whole.

Cathy Cogswell met me on my first day in the lab as a trainer and mentor, and quickly became my friend. She has been with me throughout the entirety of my time as a PhD student, and has never failed to support me, help me, or console me. She deserves a lot of credit and praise. Her husband, John, is also pretty awesome.

Masakazu Yamamoto is one of the smartest people I have ever met. Together we solved many problems, sometimes through intensive interaction, but also through brief comments he would make about my work. I took his

comments to heart and pursued them to great results. He is an innovator, a creator, and a diligent scientist. I view his work ethic as something I wish to emulate.

Onur Kanisicak, my Turkish brother, taught me too many things to list. We shared so many important times and big moments of our lives together. It has been over a year since he and his family drove from Ohio to Connecticut to see me get married and I miss them terribly. The truth is, I know he will always support me, love me, and help me fight whatever needs fighting at the time, and for that I am grateful. He is a lovely man, a great husband, and an awesome father. Esra, Kaya and Alev...and the new one....you are in good hands.

Julio Mendez, my other long term lab companion, has also helped me to get where I am. He has a good heart, an endless curiosity, and the ability to let his passions drive him wherever he wishes. If you get him outside of the lab to have some fun, he excels in that arena as well. I will not forget the times we spent together.

My parents, maw and paw, or Bob and Carol, have always supported me and only want me to be happy. During the past years, I have not always been happy, but they gave me so much support and love that I made it through to the other side because of them.

My brother, and friend, Bob. Let us paint this town some color. Family doesn't always get along, but when it does, it's great. I can always count on him for ANYTHING. He led the family into higher education and I always saw him as

a brave pioneer. From grade school on, if I saw him do something, it gave me the courage to try. Thanks Bob.

Carmen Santiago, my lovely wife and life companion, I wouldn't have been able to finish my degree without your love, support, and dedication. I see your passion for teaching, your drive to succeed, and I can't help but try to do the same. You are a source of inspiration, strength, and happiness. Because of you, I can finally wear that PhD T-shirt you got me. I love you.

I used to sweat every time I had to kill a mouse. Sorry about that little guys.

And to Molly, you furry dog, who's a good girl? Oh right, dogs can't read.

Table of Contents

List of Figures

Chapter 1: Introduction

Skeletal myogenesis is vital for motility, and the transcriptional regulation of a potent myogenic transcription factor, *MyoD*, and the determination state of embryonic cells poised to enter the myogenic program have yet to be fully explained. This thesis focuses on *MyoD* in the hopes that basic scientific knowledge of its function and regulatory elements can advance the field toward a more nuanced understanding of myogenesis. This introduction will provide background knowledge on the genes involved and the process of embryonic myogenesis.

1.1 Identification of the Myogenic Regulatory Factors:

Embryologists, and now stem cell biologists, have been interested in finding what gene products could convert multipotent progenitor cells to become developmentally restricted to a single cell type. Early insight into the genes controlling skeletal muscle formation was gleaned by experiments where 10T1/2 fibroblasts were converted to differentiated skeletal muscle cells by treatment with the DNA demethylating agent 5-azacytidine (Constantinides, 1977). 5-azacytidine is a cytosine nucleotide analog that can not be methylated and was introduced into dividing fibroblasts. To find what transcripts were responsible for the phenotypic change in fibroblasts, subtractive hybridization was performed

between the two populations, revealing a cDNA, that when ectopically expressed, was capable of converting 10T1/2 fibroblasts, nerve, pigment, fat, and liver cells muscle (Davis et al., 1987; Weintraub et al., 1989). The gene activated due loss of methylation and responsible for the fate switches when over expressed was named *MyoD* for 'myogenic determination gene'.

Subsequent to the identification of *MyoD,* three other genes possessing the ability to convert non-muscle cells to muscle were identified. Looking for related transcription factors, MyoD cDNA was used as a probe in low stringency conditions to fish for transcripts in myogenic cells lines and from mRNA extracted from adult rat muscle. The three genes found were, *Myogenin* (Olson et al., 1990; Wright et al., 1989), *Myf-5* (Braun et al., 1989), and *Mrf4*(Braun et al., 1990; Miner and Wold, 1990). These four genes are expressed only in skeletal muscle or mesodermal precursor cells and encode highly related transcription factors containing 95% amino acid homology within a centrally located 70 amino acid basic helix-loop-helix (bHLH) domain which is necessary for DNA binding and dimerization (Ishibashi et al., 2005; Olson et al., 1990).

1.2 Myogenic Regulatory Factor Function:

Formation of function skeletal muscle occurs via two broad phases, determination and differentiation. Determination occurs when a multipotent progenitor becomes committed to the myogenic fate and contributes to the proliferative progenitor pool of myoblasts. During differentiation, myoblasts fuse

with each other to form multinucleated myotubes that will eventually become muscle fibers.

Muscle based mobility is essential for life in non-sedentary organisms and there would be no muscle fibers without the determination of the myogenic lineage and formation of myoblasts. *MyoD*, *Myf-5*, and *Mrf4* are the three genes currently shown to be involved in myoblast formation. Absence of the protein products from the *MyoD*, *Myf-5*, and *Mrf4* genes in the developing mouse embryo results in new born mice devoid of skeletal muscle (Rudnicki et al., 1993). Importantly, not only was mature skeletal muscle absent, but cells expressing markers of myoblasts, the single cell proliferative precursors of muscle fibers, were absent as well (Kablar et al., 2003). The original *Myf-5* knock out allele, $Myf\text{-}5^{Neo}$, unknowingly blocking transcription of *Mrf4* during early development (Kassar-Duchossoy et al., 2004). A more recent knock out allele, $Myf\text{-}5^{loxP}$, does not affect *Mrf4* transcription and paraxial mesoderm cells form myosin heavy chain positive muscle cells in the absence of only *MyoD* and *Myf-5*. However, *Mrf4* is not capable of establishing a robust myogenic population and $MyoD^{-/-}$;$Myf\text{-}5^{-/-}$ embryos are born largely devoid of skeletal muscle. Removal of either *MyoD* or *Myf-5* results in transient defects or delays in myogenesis, and ultimately ends with a viable mouse with functional muscle (Braun et al., 1992; Rudnicki et al., 1992). *MyoD* and *Myf-5* may appear to have grossly overlapping functions, evidenced by the single and double knock out phenotypes, but they have differing genomic targets and specific functions during myogenesis. Real time PCR expression data shows that *MyoD* is much more efficient at activating

differentiation genes than *Myf-5*, while both proteins were shown to activate growth phase target genes (Ishibashi et al., 2005). Also, *Myf-5*$^{-/-}$ myoblasts differentiate prematurely in vitro, at the expense of proliferation, (Montarras et al., 2000) while *MyoD*$^{-/-}$ myoblasts divide quickly and differentiate poorly (Sabourin et al., 1999). A more in depth review of MyoD function can be found in the following sections.

Myogenin controls myogenic differentiation due to the fact that in *Myogenin* knock out embryos, there are severe differentiation defects and embryos die a birth, while myoblasts and primary myogenesis occurs normally (Venuti et al., 1995). Historically, *Mrf4* has been thought to be a differentiation factor as *Mrf4* null animals have normal muscle determination and differentiation, but there is a four fold increase in *Myogenin* expression, likely a compensation mechanism (Braun and Arnold, 1995). However, as stated above, *Mrf4* can play a role in myoblast formation.

1.3 MyoD; Structure and Function:

MyoD belongs to a subfamily of bHLH transcription factors involved in myogenesis. The bHLH family of transcription factors falls into two broad categories. One is called Class I, and are broadly expressed in many cell types and contain the E protein family. Class II bHLH factors, that the MRFs are members of, expression is restricted in a tissue specific manner. As mentioned previously, forced *MyoD* expression in differentiated non muscle cells in vitro can

be converted to muscle (Weintraub et al., 1989). For this to happen, genes must be silenced, new genes activated, and chromatin remodeled. MyoD has the ability to perform all of these functions and deserves a detailed description of its structure, and more broadly the structure of bHLH transcription factors, and the signaling pathways involving MyoD to describe its function.

1.3.1 Structure:

MyoD and the other MRFs share two domains with each other and with other bHLH (basic helix-loop-helix) transcription factors, the DNA binding and dimerization domains. Variability among these factors lies in the presence, absence, or combination of activation domains and repressive domains. The common element is comprised of approximately 60 amino acids containing the DNA binding region (basic) followed by two alpha-helices, separated by a variable loop region (HLH) (Ferre-D'Amare et al., 1993). The HLH domain allows for dimerization between two HLH containing factors, either through homodimerization, which is uncommon, or through heterodimerization (Kadesch, 1993). Once dimerized, the basic regions of the two transcription factors bind specific DNA sequences. During myogenesis, the MRF's bind E-boxes, whose consensus sequence is CANNTG, where N can be any nucleotide. MyoD has a strong, single transcriptional activation domain at the amino terminal end and a histine-cystine rich domain containing a tryptophan amino acid necessary for interaction with the Pbx/Meis complex, a known transcriptional activator (Okada

et al., 2003; Tapscott, 2005). The strong transactivation domain of MyoD has been used in a fusion protein with the DNA binding domain of Oct4 for a 50 fold increase in production of induced pluripotent stem cells (iPSCs), partly due to the chromatin remodeling ability of MyoD (Hirai et al., 2010).

1.3.2 Function:

MyoD is a master transcription factor that remodels chromatin and recruits activating transcriptional complexes to the loci of many genes involved in all aspects of myogenesis. MyoD does not perform all of its functions at once, rather there is a temporal specificity to its actions, with some genes influenced immediately, and others influenced within days of initiation of expression (Lin et al., 1994; Zhao et al., 2002). MyoD has been shown to directly bind both early and late genomic targets via CHiP data in a fibroblast cell line containing an estrogen induced *MyoD* allele (Bergstrom et al., 2002). The proposed cause of this phenomenon is a feed-forward mechanism, where early targets of MyoD are needed to cooperate with MyoD to activate the next temporal level of genes (Penn et al., 2004). Acetylation of the MyoD protein has also been shown to affect target gene selection (Di Padova et al., 2007).

The simplified description of MyoD function is that it heterodimerizes with the structurally similar, but broadly expressed, E-proteins through their shared HLH domains. Specifically, MyoD is shown to heterodimerize with E12 and E47 to activate myogenic genes, and this activation ability is at least partly governed

by the MAP kinase p38 (Watada et al., 1995). p38 phosphorylates E47 at serine 140, and this modification is essential for association with MyoD (Lluis et al., 2005). Then, through a combination of the lone activation domain of MyoD and the variable activation/repression domains of the E-proteins, target genes are activated or repressed. Strangely, the target DNA sequence of MyoD is short, (CANNTG) and occurs frequently through out the mammalian genome. A large amount of regulation via protein interactions are therefore required to obtain target gene and temporal specificity. Specificity is achieved either by tandem E boxes, or a combination of E boxes and binding sites for cooperative factors that directly interact with the activation domain of MyoD, such as Mef2, Pbx, Meis, and Sp1 (Knoepfler et al., 1999; Sartorelli et al., 1997; Sartorelli et al., 1990) (Tapscott, 2005).

An essential family of transcription factors needed for activation of essentially all myogenic genetic loci, is the MEF2 (myocyte enhancement factor) family. In mice, there are four members of the MEF2 family, and they are required for the differentiation, but not specification of the myogenic lineage (Black and Olson, 1998). Although MyoD and the MEF2 family bind different consensus DNA sequences, both sequences are found at almost every skeletal muscle genes promoter region, and efficient transcription of those genes only occurs when both factors are bound (Dodou et al., 2003; Li and Capetanaki, 1994; Malik et al., 1995).

1.3.2.1 Chromatin Modification and Remodeling:

Part of the temporal specificity in MyoD mediated myogenesis is due to binding sites being hidden via inaccessible chromatin states. Many of the E-box targets of MyoD and the other MRFs, are hidden by unfavorable chromatin at time specific loci, or loci initially targeted at the onset of myogenesis. MyoD has the ability to alter the epigenome of myogenic cells, by directly interacting with the histone acetyltransferases (HATs), p300 and CBP (Bannister and Kouzarides, 1996; Ogryzko et al., 1996). Addition of acetyl groups to histone tails negates their positive charge resulting in the weakening of their interaction with the negatively charged DNA, allowing access to the DNA sequence. The MyoD/p300/CBP complex can recruit another HAT, p300/CBP-associated factor (PCAF), resulting in a complex with two differing acetyltransferase abilities and specificities (Puri et al., 1997; Sartorelli et al., 1997). p300 acetylates histone proteins, weakening the protein-DNA interaction, allowing that region of DNA to be accessible to transcription factors. PCAF acetylates the MyoD protein at two lysine residues just outside of the DNA binding domain, increasing the transcriptional activation ability of MyoD (Polesskaya et al., 2000) (Dilworth et al., 2004).

Besides associating with histone modifying proteins, MyoD also recruits protein complexes known to remodel chromatin. The large ATP-dependent SWI/SNF complex, actively moves histones or switches out nucleosome histone subunits to facilitate transcription of previously silent local genes (de la Serna et

al., 2005; Hirschhorn et al., 1992). The SWI/SNF complex directly interacts with MyoD via the BAF60c subunit (Forcales, 2012).

1.3.2.2 Association with RNA Helicases:

MyoD has been shown to interact with two different RNA helicases, p68 and p72. Generally, RNA helicases are enzymes that alter RNA structure and are therefore involved in all aspects of RNA structure modification during transcription, splicing, and translation (Abdelhaleem, 2004). RNA helicases mediate conversion between single stranded RNA and double stranded RNA, and also affects the affinity of RNA for specific proteins. For a comprehensive review, see (Jarmoskaite and Russell, 2011; Pan and Russell, 2010). The role of RNA helicases involved in controlling cell determination or differentiation comes from work showing a direct interaction between MyoD and p68 and p72. When p68 and p72 are knocked down in HeLa cells or the immortal myoblast line, C2C12, myogenic differentiation is severely diminished, such that multinucleated myotubes never from in vitro and the cells fail to express myosin heavy chain, a hallmark of differentiating skeletal muscle. The proposed mechanism for the inhibition of myogenic differentiation is through the lack of effective transcriptional initiation complex formation at the promoters of myogenic genes, and also through a failure of chromatin remodeling (Fuller-Pace and Ali, 2008).

1.3.2.3 Transcriptional Repression by MyoD:

As a pioneer transcription factor, MyoD must remodel chromatin to access target genes that are physically hidden, and then activate transcription of those genes. By virtue of MyoD's ability to convert non-muscle cell types to the myogenic lineage, it would be logical to assume that MyoD can repress genes expressed in the cell type before myogenic conversion.

microRNAs (miRNA) are short, approximately 20 nucleotides in length, single stranded RNAs that negatively impact gene expression by directing degradation of specific mRNAs or inhibiting translation (Luo et al., 2013). Three miRNAs, miR-1, 133, and 206 are all restricted to muscle cells and may be controlled by the MRFs. MyoD has been shown to directly activate the transcription of mIR-206, that suppress translation of transcripts expressed in fibroblasts. Two genes expressed in fibroblasts, utrophin (Utrn) and follistatin-like 1 (Fstl1) have their mRNA reduced after the onset of MyoD expression due to the fact that MyoD directly binds an E box near the genomic locus of miR-206. The miR-206 locus is next to a gene activated by MyoD, AK132452, and mIR-206 may be a result of processing of that gene. miR-206 then complementary base pairs the 3' UTR of Fstl1 transcripts, targeting them for destruction (Rosenberg et al., 2006). It is also suggested that MyoD activates transcription of miR-133 and miR-1. These miRNAs target the destruction of a histone deacetylase, HDAC4, a transcriptional repressor, and serum response factor (SRF), an anti-mitotic protein (Chen et al., 2006). The action of MyoD via

miRNAs promotes cell proliferation and gene expression at certain loci, while repressing transcripts characteristic of non-myogenic lineages.

Another method of transcriptional repression via MyoD is through histone deacetylase complexes (HDACs). MyoD recruits HDACs to genetic loci where histones will be modified such that the genes close by will be repressed (Puri et al., 2001). This phenomenon may be part of the temporal regulation of MyoD target genes, as these repressive complexes are also seen at the *Myogenin* promoter, a locus known to be activated by MyoD. While a myoblast is proliferating, some MyoD target genes will be activated at a later time, and need to be temporarily repressed to avoid premature differentiation, and association with HDACs is one pathway to achieve this effect.

1.4 Embryonic Myogenesis:

1.4.1 Somitogenesis:

During early embryogenesis, the neural tube and notochord lie at the center of the embryo and define the anterior-posterior axis by their action as signaling centers that induce surrounding tissues to adopt certain fates through secreted factors and direct cell-cell interactions. On both sides of the neural tube resides the paraxial mesoderm, a mesenchyme of multipotent cells that eventually give rise to skeletal muscle, the axial skeleton, and the dermis of the trunk. Somites are epithelial spheres formed from segmentation of the paraxial

mesoderm with a fixed periodicity starting at the anterior region of the embryo and steadily progressing toward the posterior. Somites form with a fixed periodicity governed by a 'molecular clock'. Many factors control the periodicity of somite formation such as FGF8 (fibroblast growth factor 8) and Wnt3a (Dubrulle et al., 2001) (Aulehla et al., 2003). Cycling expression of Notch family members and their receptor components play an integral role in the segmentation clock in all vertebrates (Gridley, 2006). The morphological boundary between each somite in mice is controlled by two bHLH transcription factors, MesP2, regulated by Notch, and Paraxis (Sosic et al., 1997). If either of these genes is removed from the mouse genome, the paraxial mesoderm fails to undergo the mesenchymal to epithelial transition, and somites fail to form. These mutations are lethal at birth due to fused vertebra and disorganized axial muscle. Interestingly, the cell types found in a normal proper somite still form, but segmentation and patterning are lethally incorrect. MesP2 directly activates *Eph4A*, a gene involved in cell-cell interaction, specifically cell-cell repulsion, an action vital to somite formation (Burgess et al., 1996; Saga et al., 1997; Takahashi et al., 2005). The initial somite is plastic in regards to what somitic lineage it will become, as shown in somite rotation experiments (Dockter and Ordahl, 2000). Within a few hours of somite formation, the epithelial sphere begins to change as lineage specification occurs. The dorsal portion of the somite maintains its epithelial nature and forms the dermomyotome, while the ventral portion form the mesenchymal sclerotome (discussed below).

The dermomyotome is a transient structure, where cells on the end of the epithelial sheet delaminate, or lose their epithelial shape to become mesenchymal. Factors secreted from the overlying ectoderm (Wnts1 and 7A) (Tajbakhsh et al., 1998) induce myogenesis in dermomyotomal cells, while the lateral plate mesoderm inhibits myogenesis in other cells types via BMP4. The premyogenic cells activate *MyoD* or *Myf-5* and migrate immediately medially to populate the area under the dermomyotome, forming the myotome, the first skeletal muscle of the embryo (Kalcheim et al., 1999). Subsequently, the dermomyotome provides progenitor cells for all trunk and limb musculature. The dermomyotome also produces trunk dermis, and limb endothelial cells (Kardon et al., 2002a). The ventro-medial portion of the somite loses its epithelial nature to return to a mesenchyme and becomes the sclerotome, and gives rise to the ribs, vertebra, and tendons of the axial skeleton(Wilting et al., 1994). This cell structure conversion is controlled by Sonic Hedgehog (Shh), produced by the notochord and floorplate of the neural tube by activating *Pax1* in the future sclerotome, and along with BMP4, the early formation of the axial skeleton begins (Murtaugh et al., 1999).

1.4.2 Myogenic Lineages:

All skeletal muscle in the embryo is not formed through an identical pathway. At different anatomical locations in the body, there are differing

environments and embryonic signaling centers regulating MRF expression. The three major sites of skeletal muscle determination are the head, limbs and trunk.

1.4.2.1 Craniofacial Myogenesis:

Skeletal muscle of the head does not originate from somites, but from unsegmented prechordal mesoderm located cranially to the first somite and from the branchial arches. The branchial arches, a subset of the craniofacial muscle population, are embryonic structures evolved from gill structures in fish, and in mammals their derivatives still control feeding and breathing. *MyoD* is transcriptionally regulated differently in head muscles than in the body. In the body, *Myf-5* and *Pax3* are genetically upstream of *MyoD* because in their absence, *MyoD* is not expressed. In these mutant embryos, *MyoD* expression occurs normally in the head and myogenesis occurs (Tajbakhsh et al., 1997). In the absence of *Myf-5* and *MyoD*, some trunk musculature forms due to *Mrf4* expression, but *Mrf4* is not expressed in the head and as a result, no myofibers form in the head, demonstrating the differing upstream activators in the two populations (Kassar-Duchossoy et al., 2004).

MyoR and *Capsulin* are bHLH factors related to the four major myogenic bHLH transcription factors, and are expressed in migratory myogenic precursors that travel from the unsegmented paraxial mesoderm to the branchial arches. (Hacker and Guthrie, 1998; Noden, 1983; Noden et al., 1999) Specific head muscles controlling mastication are missing in embryos missing functional *MyoR*

(*Msc* or *Musculin*) and *Capsulin* (*TCF21* or *epicadian*) genes. *MyoD* and *Myf-5* are not turned on in the first branchial arch in the absence *MyoR* and *Capsulin* (Lu et al., 2002). *Tbx1* and *Pitx2* also regulate myogenesis in the branchial arches due to resulting muscle defects when either gene is missing (Dong et al., 2006; Kelly et al., 2004). These phenotypes are restricted to the head, supporting the fact that head and body myogenesis differ significantly.

1.4.2.2 Epaxial Myogenesis:

Muscle of the trunk and limbs arise from the dermomyotome of the maturing somite and are broken down into two categories; epaxial and hypaxial musculature. Epaxial muscle progenitors originate from the dorso-medial aspect of the dermomyotome and form deep back muscles (Ordahl and Le Douarin, 1992), while hypaxial muscle precursors delaminate from the ventro-lateral portion of the dermomyotome and give rise to ventral body wall muscle, and at limb level somites, to the limb musculature(Christ B, 1977).

Formation of the early musculature in the embryo is a multiphase process. Initially, a small group of cells at the dorso-medial lip of the dermomyotome, closest to the neural tube, lose their epithelial nature, activate *Myf-5* via Wnt1 and Shh (Cossu et al., 1996a), and migrate ventrally to create the primary myotome. Timely myotome formation is dependent on *Myf-5*,as there is a one day delay in myotome formation in *Myf-5* null embryos(Arnold and Braun, 1996; Braun et al., 1992). *Pax3* is initially expressed throughout the somite, but its

expression becomes limited to the dermomyotome. Ectopic *Pax3* expression can activate *MyoD* and *Myf-5* in mesoderm and neural tube explants (Daston et al., 1996; Williams and Ordahl, 1994). These early myotomal cells form the pioneer fibers that become the scaffold for the new myogenic cells which begin to arrive from all sides of the dermomyotome (Kahane et al., 2007). Ultimately, the central dermomyotome breaks down and Pax3/7 expressing cells enter the myotome directly.

1.4.2.3 Hypaxial Myogenesis:

The hypaxial lineage comprises abdominal wall muscles, the diaphragm, and limb musculature (Kablar and Rudnicki, 2000). *MyoD* is activated in the hypaxial domain of the dermomyotome via Wnt7a (Cossu et al., 1996b). MyoD controls timely formation of hypaxial muscle lineages, as $MyoD^{-/-}$ embryos have a one day delay in hypaxial myogenesis (Kablar et al., 2003). At inter limb levels, the hypaxial myotome matures into intercostal and abdominal wall muscle. At limb levels, a different phenomenon occurs where single cells are released from the lateral portion of the dermomyotome, do not express any of the MRFs, and migrate directly to the limb buds where they will activate the MRFs, proliferate and eventually differentiate.

Many genes are known to control the delamination and migration of these cells. *Pax3* is arguably the most important gene as mutant mice lacking this gene have no limb muscle, while trunk myogenesis is not affected (Bober et al.,

1994). *Pax3* is positively regulated by *Dach2*, the vertebrate analog of the Drosphila gene *dachshund* which is involved in the eye formation pathway (Kardon et al., 2002b). Two members of a six member gene family are also involved in proper migration of limb myogenic precursors are *Six1* and *Six4* (Grifone et al., 2005). These two genes are genetically upstream of *Pax3*, as are *Eya1* and *Eya2* (Grifone et al., 2007). If either the *Eya* gene pair or *Six* gene pair is knocked out, *Pax3* is not activated in the hypaxial dermomyotome, resulting in a lack of limb musculature. Interestingly, the *Six* and *Eya* genes are homologous to Drosophila genes that interact synergistically to control eye development. In vertebrates, they still interact synergistically, but these specific members control migration, while other members control other organ development.

The lack of limb muscle phenotype in *Pax3* mutants, or upstream activator mutants, is due to a migration defect. *Pax3* directly activates *c-met*, (Yang et al., 1996) a transmembrane tyrosine kinase receptor located on the cells that will migrate to the limb. The ligand for this receptor is scatter factor/hepatocyte growth factor (SF/HGF) and is produced by cells of the limb bud (Bladt et al., 1995). Removal of the c-met gene causes limb myogenesis to fail due to a lack of migration (Heymann et al., 1996) and ectopic activation of SF/HGF causes delamination of cells from the dermomyotome of interlimb somites, which normally do not produce lateral migratory precursors (Brand-Saberi et al., 1996). *Pax7* and *Lbx1* are also expressed in the migrating population of premyogenic cells. *Lbx1* is another target of *Pax3*, as its

expression is absent in *Pax3* knockout embryos (Dietrich et al., 1998). *Lbx1* is only expressed in the lateral portion of the dermomyotome while cells are delaminating and is turned off slightly after the cell arrives in the limb field. In *Lbx1* knock out embryos, cells delaminate but do not migrate properly. Interestingly, there is a difference of phenotype between the forelimb and hindlimb muscles. All hindlimb muscles are missing, while in the forelimb, only the extensor muscles of the forearm muscle are missing, indicating that *Lbx1* allows for cells to know their positional identity (Schafer and Braun, 1999). Two other genes regulated by *Pax3* in migratory precursors are *Sp5* and *CXCR4*. *Sp5* is a transcription factor and vertebrate homologue of the Drosophila gene, *buttonhead.* The function of Sp5 is unknown, and no phenotype is produced when it is knocked out, but that may be due to the presence of seven other Sp factors (Sahara et al., 2007) that may compensate for the lack of *Sp5*. *CXCR4* is a chemokine receptor whose ligand, *Sdf1*, is expressed in the limb mesenchyme. In *CXCR4* null mice, fewer progenitor cells reach the limb and there is an increase in apoptosis (Vasyutina et al., 2005). Migratory cells also express *Pitx2,* a factor involved in the organization of the muscle anlagen once the progenitors reach the limb (Campbell et al., 2012).

There are numerous factors expressed in myogenic progenitor cells before they leave the dermomyotome for the limb. These cells may already be specified to myogenesis before arriving at the limb bud and activating the MRFs. The data in this thesis suggests these migratory cells are largely determined to myogenesis by factors present in the somite.

1.5 Transcriptional control of MyoD expression:

Defining regulatory DNA elements of powerful transcription factors is of ultimate importance in understanding transcriptional pathways and in designing transgenic mouse lines. Enhancer mutations may result in ectopic or altered expression of a gene and result in various pathologies depending on the specific gene (Bastianutto et al., 2002; Fuhrmann et al., 1999; Majumdar and Diamandis, 1999). It has been shown that *MyoD*$^{-/-}$ myoblasts serve as better transplant material than wild type myoblasts in mice (Asakura et al., 2007) which may be applicable to humans with muscle wasting diseases.

There are only two known enhancer elements positively controlling *MyoD* expression. These elements, the Core Enhancer (CE) and Distal Regulatory Region (DRR) lie 20kb and 5 kb upstream of *MyoD*, respectively. In *in vitro* assays, these two enhancers exhibit activity in non-muscle cell types, contrasted by the precise control of MyoD expression in muscle lineages *in vivo* (Goldhamer et al., 1992). In a developing embryo, there are probably repressive signals involved in *MyoD* expression. One method to hide these positively acting control elements is the surrounding chromatin state.

Enhancers were identified with constructs containing various restriction digest fragments of the 24 kb of human genomic sequence upstream of *MyoD*. The fragments were ligated to the chlorampenicol acetyltransferase (CAT) gene and stably transfected into various cell lines. The amount of enzymatic activity in the cell lines represented the positive transcriptional ability of the DNA sequence

in question. The most powerful fragment was F3, a 4kb segment containing the 258bp CE (Goldhamer et al., 1992). The CE and DRR share extremely high sequence similarity and genomic position between human and mice (Asakura et al., 1995; Goldhamer et al., 1995b). The highly conserved DRR maintains all putative binding sites between the two species, which are four E-boxes (CANNTG) and two MEF-2 sites (Chen et al., 2001). E-boxes are the DNA elements which bHLH transcription factor family members bind to, while MEF-2 sites are bound by 'myocyte enhancement factors'. This family of transcription factors are calcium dependent transcription factors involved in cellular differentiation and proliferation (McKinsey et al., 2002). The sequence similarities between the CE's of humans and mice is approximately 90% and all putative binding sites are maintained, including four E-boxes, an AP-1 site, and a H4TF-1 site (Goldhamer et al., 1995b).

In the trunk, but not the limbs, *Myf-5* lies genetically upstream of *MyoD*, and *Pax3;Myf-5* double mutants fail to activate *MyoD* at all in the body (Tajbakhsh et al., 1997). As mentioned previously, *Six1/4* are upstream of *Pax3*, and in *Six1/4;Myf-5* triple knockouts *MyoD* fails to activate as well (Relaix et al., 2013). Another positive regulator of *MyoD* is *SRF* (serum response factor), and when inhibited in myoblasts or differentiating myotubes, the *MyoD* locus is rapidly shut down (Gauthier-Rouviere et al., 1996). Another group of interacting factors is Sp1, YY1 and p300/CBP which are involved in chromatin remodeling (L'Honore et al., 2003; Roth et al., 2003; Wilson and Rotwein, 2006). Cell-based assays and in vitro studies show a partnership between Fox03, Pax3, and Pax7

in the recruitment of RNA Polymerase II during the formation of the pre-initiation complex at the MyoD locus in myoblast cultures. *Fox03* is further implicated as a direct activator of *MyoD* through *Fox03* knock out experiments, where *MyoD* is down regulated in regenerating muscle (Hu et al., 2008).

Recent findings regarding the transcriptional control of *MyoD* have shown many factors bind the CE directly. Six1/4 regulates *MyoD* by binding the CE (Relaix et al., 2013), as does CLOCK and BMAL1, regulators of the circadian rhythm of *MyoD* expression (Zhang et al., 2011). A limb specific activator of *MyoD*, *Pitx2*, has also been shown to bind the CE (L'Honore et al., 2010). Repression of MyoD expression has also been linked to the CE as Sim2 and YB1/p32 bind to the CE and repress the locus by both gain and loss of function experiments (Havis et al., 2012; Song and Lee, 2010).

In vitro cell culture analysis shows the histone variant H3.3, associated with transcriptionally active genes, is required to become associated with the CE for proper expression of MyoD in myoblasts and differentiating myotubes (Yang et al.), showing a role for epigenetic remodeling in the activation of the MyoD locus via the CE.

1.5.1 Transgenic experiments:

Using upstream regions of *MyoD* to drive lacZ or CAT expression have revealed two distinct elements, the Core Enhancer (Goldhamer et al., 1995a) (CE) and the Distal Regulatory Region (DRR) (Asakura et al., 1995). 24

kilobases of DNA sequence upstream of *MyoD*, containing the CE and DRR, drives lacZ expression in a spatio-temporal pattern that fully mimics MyoD mRNA expression. Transgenic analysis indicates that the CE controls initiation of expression in newly forming myoblasts, while the DRR maintains expression in differentiating muscle. CE-lacZ transgenic embryos exhibit activity in a manner similar to MyoD mRNA detection (Faerman et al., 1995; Goldhamer et al., 1992). DRR-lacZ transgene expression is limited to sites of differentiating muscle (Asakura et al., 1995). In *MyoD*$^{-/-}$;*Myf-5*$^{-/-}$ embryos, where no myoblasts form, the CE transgene is active while the DRR is not (Kablar et al., 1999) indicating the ability of the CE to initiate de novo *MyoD* expression. The 2.5 kilobases immediately upstream of the transcriptional start site, including the proximal promoter does not contribute to specificity of expression. The herpes simplex virus promoter exhibited nearly identical activity in myoblasts as the native *MyoD* promoter (Goldhamer et al., 1992). The genomic region upstream of *MyoD* that had the highest activity was referred to as 'fragment 3' and contains the 258 base pair long Core Enhancer (Goldhamer et al., 1992). When comparing the expression profile of the -24lacZ construct, which fully copies endogenous *MyoD* expression, to a similar construct which lacks the F3 fragment, there is only a delay in expression in the hypaxial myotome and limb buds up to E115, after which a normal expression profile is regained (Chen et al., 2001).

1.5.2 Deletion of Enhancers:

Given the data showing the sufficiency of the CE and DRR to regulate *MyoD* expression, it is surprising to see these elements are not individually necessary. In embryos lacking the CE, *MyoD* expression initiates properly in the epaxial lineage while there is a 1 day delay of expression in the branchial arches and limb buds (Chen and Goldhamer, 2004b). This shows the initial timely activation of *MyoD* is CE dependent in only a subset early myogenic cells, and that ultimately, initiation of *MyoD* expression is CE independent. Targeted removal of the DRR resulted in persistent *MyoD* expression in differentiating embryonic muscle, and this expression continues into adulthood, but with an approximate 60% reduction in mRNA levels, showing continued *MyoD* expression in differentiated muscle occurs without the DRR. DRR knock out embryos exhibit a general reduction in MyoD levels at E10.5 (Chen et al., 2002). The differences between transgenic and knock out experimental results can be explained in two ways. The first is that the CE and DRR have overlapping or compensatory abilities to regulate MyoD expression, such that when one is removed, only transient or minor defects are observed, due to the presence of the other enhancer. The second is that another, uncharacterized DNA regulatory element exists. In this thesis, I resolve the two hypotheses by removing both the CE and DRR on the same chromosome. Here, targeting of the CE for deletion was performed on mouse embryonic stem cells already lacking the DRR. The expression profile of *MyoD* will be monitored in this new mouse line.

Myf-5 initiates *MyoD* expression in the body, as there is a 2 day delay in *MyoD* expression in *Myf-5* mutants (Tajbakhsh et al., 1997). *MyoD* expression is eventually rescued in *Myf-5* mutants through a *Pax3* dependent mechanism. Delayed *MyoD* expression is also seen in mice lacking *Myf-5* and the CE or DRR, implying that both enhancers are responsive to *Myf-5* dependent activation. The kinetics of *Pax3* dependent *MyoD* expression is the same in embryos with both enhancers present or embryos lacking either the CE or the DRR (Chen et al., 2002) (Chen and Goldhamer, 2004a) (Tajbakhsh et al., 1997), demonstrating that neither the CE or DRR are exclusive targets of *Pax3* dependent activation.

1.6 References:

Abdelhaleem, M., Over-expression of RNA Helicases in Cancer. Vol. 24, 2004, pp. 3951-3954.

Arnold, H. H., Braun, T., 1996. Targeted inactivation of myogenic factor genes reveals their role during mouse myogenesis: a review. Int J Dev Biol. 40**,** 345-53.

Asakura, A., et al., 2007. Increased survival of muscle stem cells lacking the MyoD gene after transplantation into regenerating skeletal muscle. Proc Natl Acad Sci U S A. 104**,** 16552-7.

Asakura, A., et al., 1995. The regulation of MyoD gene expression: conserved elements mediate expression in embryonic axial muscle. Dev Biol. 171**,** 386-98.

Aulehla, A., et al., 2003. Wnt3a Plays a Major Role in the Segmentation Clock Controlling Somitogenesis. Developmental cell. 4**,** 395-406.

Bannister, A. J., Kouzarides, T., 1996. The CBP co-activator is a histone acetyltransferase. Nature. 384, 641-3.

Bastianutto, C., et al., 2002. A Novel Muscle-Specific Enhancer Identified within the Deletion Overlap Region of Two XLDC Patients Lacking Muscle Exon 1 of the Human Dystrophin Gene. Genomics. 80, 614-620.

Bergstrom, D. A., et al., 2002. Promoter-specific regulation of MyoD binding and signal transduction cooperate to pattern gene expression. Mol Cell. 9, 587-600.

Black, B. L., Olson, E. N., 1998. Transcriptional control of muscle development by myocyte enhancer factor-2 (MEF2) proteins. Annu Rev Cell Dev Biol. 14, 167-96.

Bladt, F., et al., 1995. Essential role for the c-met receptor in the migration of myogenic precursor cells into the limb bud. Nature. 376, 768-71.

Bober, E., et al., 1994. Pax-3 is required for the development of limb muscles: a possible role for the migration of dermomyotomal muscle progenitor cells. Development. 120, 603-12.

Brand-Saberi, B., et al., 1996. Scatter factor/hepatocyte growth factor (SF/HGF) induces emigration of myogenic cells at interlimb level in vivo. Dev Biol. 179, 303-8.

Braun, T., Arnold, H. H., 1995. Inactivation of Myf-6 and Myf-5 genes in mice leads to alterations in skeletal muscle development. Embo J. 14, 1176-86.

Braun, T., et al., 1990. Myf-6, a new member of the human gene family of myogenic determination factors: evidence for a gene cluster on chromosome 12. Embo J. 9, 821-31.

Braun, T., et al., 1989. A novel human muscle factor related to but distinct from MyoD1 induces myogenic conversion in 10T1/2 fibroblasts. Embo J. 8, 701-9.

Braun, T., et al., 1992. Targeted inactivation of the muscle regulatory gene Myf-5 results in abnormal rib development and perinatal death. Cell. 71, 369-82.

Burgess, R., et al., 1996. Requirement of the paraxis gene for somite formation and musculoskeletal patterning. Nature. 384, 570-573.

Campbell, A. L., et al., 2012. Regulation of Motility of Myogenic Cells in Filling Limb Muscle Anlagen by Pitx2. PLoS ONE. 7, e35822.

Chen, J.-F., et al., 2006. The role of microRNA-1 and microRNA-133 in skeletal muscle proliferation and differentiation. Nat Genet. 38**,** 228-233.

Chen, J. C., Goldhamer, D. J., 2004a. The core enhancer is essential for proper timing of MyoD activation in limb buds and branchial arches. Dev Biol. 265**,** 502-12.

Chen, J. C., et al., 2001. Two upstream enhancers collaborate to regulate the spatial patterning and timing of MyoD transcription during mouse development. Dev Dyn. 221**,** 274-88.

Chen, J. C., et al., Essential and redundant functions of the MyoD distal regulatory region revealed by targeted mutagenesis. Vol. 245, 2002, pp. 213 - 223.

Chen, J. C. J., Goldhamer, D. J., 2004b. The core enhancer is essential for proper timing of MyoD activation in limb buds and branchial arches. Developmental Biology. 265**,** 502-512.

Christ B, J. H., Jacob M., 1977. Experimental analysis of the origin of the wing musculature in avian embryos. Anat. Embryology. 150**,** 16.

Constantinides, 1977. Functional striated muscle cells from non-myoblast precursors following 5-azacytidine treatment. Nature. 267**,** 3.

Cossu, G., et al., 1996a. Activation of different myogenic pathways: myf-5 is induced by the neural tube and MyoD by the dorsal ectoderm in mouse paraxial mesoderm. Development. 122**,** 429-37.

Cossu, G., et al., 1996b. How is myogenesis initiated in the embryo? Trends Genet. 12**,** 218-23.

Daston, G., et al., Pax-3 is necessary for migration but not differentiation of limb muscle precursors in the mouse. Vol. 122, 1996, pp. 1017-1027.

Davis, R. L., et al., 1987. Expression of a single transfected cDNA converts fibroblasts to myoblasts. Cell. 51**,** 987-1000.

de la Serna, I. L., et al., 2005. MyoD targets chromatin remodeling complexes to the myogenin locus prior to forming a stable DNA-bound complex. Mol Cell Biol. 25**,** 3997-4009.

Di Padova, M., et al., 2007. MyoD Acetylation Influences Temporal Patterns of Skeletal Muscle Gene Expression. Journal of Biological Chemistry. 282**,** 37650-37659.

Dietrich, S., et al., 1998. Specification of the hypaxial musculature. Development. 125, 2235-49.

Dilworth, F. J., et al., 2004. In vitro transcription system delineates the distinct roles of the coactivators pCAF and p300 during MyoD/E47-dependent transactivation. Proc Natl Acad Sci U S A. 101, 11593-8.

Dockter, J., Ordahl, C. P., 2000. Dorsoventral axis determination in the somite: a re-examination. Development. 127, 2201-6.

Dodou, E., et al., 2003. mef2c is activated directly by myogenic basic helix-loop-helix proteins during skeletal muscle development in vivo. Mechanisms of Development. 120, 1021-1032.

Dong, F., et al., 2006. Pitx2 promotes development of splanchnic mesoderm-derived branchiomeric muscle. Development. 133, 4891-9.

Dubrulle, J., et al., 2001. FGF Signaling Controls Somite Boundary Position and Regulates Segmentation Clock Control of Spatiotemporal Hox Gene Activation. Cell. 106, 219-232.

Faerman, A., et al., 1995. The distal human myoD enhancer sequences direct unique muscle-specific patterns of lacZ expression during mouse development. Dev Biol. 171, 27-38.

Ferre-D'Amare, A. R., et al., 1993. Recognition by Max of its cognate DNA through a dimeric b/HLH/Z domain. Nature. 363, 38-45.

Forcales, S. V., 2012. The BAF60c-MyoD complex poises chromatin for rapid transcription. Bioarchitecture. 2012 May 1;2(3):104-109.

Fuhrmann, G., et al., 1999. The MYC dualism in growth and death. Mutation Research/Reviews in Mutation Research. 437, 205-217.

Fuller-Pace, F. V., Ali, S., 2008. The DEAD box RNA helicases p68 (Ddx5) and p72 (Ddx17): novel transcriptional co-regulators. Biochem Soc Trans. 2008 Aug;36(Pt 4):609-12.

Gauthier-Rouviere, C., et al., Expression and activity of serum response factor is required for expression of the muscle-determining factor MyoD in both dividing and differentiating mouse C2C12 myoblasts. Vol. 7, 1996, pp. 719-729.

Goldhamer, D. J., et al., 1995a. Embryonic activation of the myoD gene is regulated by a highly conserved distal control element. Development. 121, 637-49.

Goldhamer, D. J., et al., Embryonic activation of the myoD gene is regulated by a highly conserved distal control element. Vol. 121, 1995b, pp. 637 - 649.

Goldhamer, D. J., et al., 1992. Regulatory elements that control the lineage-specific expression of myoD. Science. 256**,** 538-42.

Gridley, T., 2006. The long and short of it: Somite formation in mice. Developmental Dynamics. 235**,** 2330-2336.

Grifone, R., et al., 2007. Eya1 and Eya2 proteins are required for hypaxial somitic myogenesis in the mouse embryo. Dev Biol. 302**,** 602-16.

Grifone, R., et al., 2005. Six1 and Six4 homeoproteins are required for Pax3 and Mrf expression during myogenesis in the mouse embryo. Development. 132**,** 2235-49.

Hacker, A., Guthrie, S., A distinct developmental programme for the cranial paraxial mesoderm in the chick embryo. Vol. 125, 1998, pp. 3461-3472.

Havis, E., et al., 2012. Sim2 prevents entry into the myogenic program by repressing MyoD transcription during limb embryonic myogenesis. Development. 139**,** 1910-20.

Heymann, S., et al., 1996. Regulation and function of SF/HGF during migration of limb muscle precursor cells in chicken. Dev Biol. 180**,** 566-78.

Hirai, H., et al., 2010. Structure and functions of powerful transactivators: VP16, MyoD and FoxA. Int J Dev Biol. 2010;54(11-12):1589-96. doi: 10.1387/ijdb.103194hh.

Hirschhorn, J. N., et al., Evidence that SNF2/SWI2 and SNF5 activate transcription in yeast by altering chromatin structure. Vol. 6, 1992, pp. 2288-2298.

Hu, P., et al., 2008. Codependent Activators Direct Myoblast-Specific MyoD Transcription. Developmental Cell. 15**,** 534-546.

Ishibashi, J., et al., 2005. MyoD induces myogenic differentiation through cooperation of its NH2- and COOH-terminal regions. J Cell Biol. 171**,** 471-82.

Jarmoskaite, I., Russell, R., 2011. DEAD-box proteins as RNA helicases and chaperones. Wiley Interdisciplinary Reviews: RNA. 2**,** 135-152.

Kablar, B., et al., 2003. Myf5 and MyoD activation define independent myogenic compartments during embryonic development. Dev Biol. 258**,** 307-18.

Kablar, B., et al., 1999. Myogenic determination occurs independently in somites and limb buds. Dev Biol. 206**,** 219-31.

Kablar, B., Rudnicki, M. A., 2000. Skeletal muscle development in the mouse embryo. Histol Histopathol. 15**,** 649-56.

Kadesch, T., Consequences of heteromeric interactions among helix-loop-helix proteins. Vol. 4, 1993, pp. 49-55.

Kahane, N., et al., 2007. Medial pioneer fibers pattern the morphogenesis of early myoblasts derived from the lateral somite. Dev Biol. 305**,** 439-50.

Kalcheim, C., et al., 1999. Myotome formation: a multistage process. Cell Tissue Res. 296**,** 161-73.

Kardon, G., et al., 2002a. Local extrinsic signals determine muscle and endothelial cell fate and patterning in the vertebrate limb. Dev Cell. 3**,** 533-45.

Kardon, G., et al., 2002b. Pax3 and Dach2 positive regulation in the developing somite. Dev Dyn. 224**,** 350-5.

Kassar-Duchossoy, L., et al., 2004. Mrf4 determines skeletal muscle identity in Myf5:Myod double-mutant mice. Nature. 431**,** 466-71.

Kelly, R. G., et al., 2004. The del22q11.2 candidate gene Tbx1 regulates branchiomeric myogenesis. Hum Mol Genet. 13**,** 2829-40.

Knoepfler, P. S., et al., 1999. A conserved motif N-terminal to the DNA-binding domains of myogenic bHLH transcription factors mediates cooperative DNA binding with pbx-Meis1/Prep1. Nucleic Acids Res. 27**,** 3752-61.

L'Honore, A., et al., MyoD distal regulatory region contains an SRF binding CArG element required for MyoD expression in skeletal myoblasts and during muscle regeneration. Vol. 14, 2003, pp. 2151 - 2162.

L'Honore, A., et al., Pitx2 defines alternate pathways acting through MyoD during limb and somitic myogenesis. Vol. 137, 2010, pp. 3847-3856.

Li, H., Capetanaki, Y., 1994. An E box in the desmin promoter cooperates with the E box and MEF-2 sites of a distal enhancer to direct muscle-specific transcription. Embo J. 13**,** 3580-9.

Lin, Z., et al., 1994. Sequential appearance of muscle-specific proteins in myoblasts as a function of time after cell division: evidence for a conserved myoblast differentiation program in skeletal muscle. Cell Motil Cytoskeleton. 29**,** 1-19.

Lluis, F., et al., 2005. E47 phosphorylation by p38 MAPK promotes MyoD/E47 association and muscle-specific gene transcription. Embo J. 24**,** 974-84.

Lu, J.-r., et al., Control of Facial Muscle Development by MyoR and Capsulin. Vol. 298, 2002, pp. 2378-2381.

Luo, W., et al., 2013. MicroRNAs Involved in Skeletal Muscle Differentiation. Journal of Genetics and Genomics. 40**,** 107-116.

Majumdar, S., Diamandis, E. P., 1999. The promoter and the enhancer region of the KLK 3 (prostate specific antigen) gene is frequently mutated in breast tumours and in breast carcinoma cell lines. Br J Cancer. 79**,** 1594-602.

Malik, S., et al., 1995. The role of the CANNTG promoter element (E box) and the myocyte-enhancer-binding-factor-2 (MEF-2) site in the transcriptional regulation of the chick myogenin gene. Eur J Biochem. 230**,** 88-96.

McKinsey, T. A., et al., 2002. MEF2: a calcium-dependent regulator of cell division, differentiation and death. Trends in Biochemical Sciences. 27**,** 40-47.

Miner, J. H., Wold, B., 1990. Herculin, a fourth member of the MyoD family of myogenic regulatory genes. Proc Natl Acad Sci U S A. 87**,** 1089-93.

Montarras, D., et al., 2000. Cultured myf5 null and myoD null muscle precursor cells display distinct growth defects. Biol Cell. 92**,** 565-72.

Murtaugh, L. C., et al., Sonic hedgehog promotes somitic chondrogenesis by altering the cellular response to BMP signaling. Vol. 13, 1999, pp. 225-237.

Noden, D. M., 1983. The role of the neural crest in patterning of avian cranial skeletal, connective, and muscle tissues. Developmental Biology. 96**,** 144-165.

Noden, D. M., et al., 1999. Differentiation of avian craniofacial muscles: I. Patterns of early regulatory gene expression and myosin heavy chain synthesis. Dev Dyn. 216**,** 96-112.

Ogryzko, V. V., et al., 1996. The transcriptional coactivators p300 and CBP are histone acetyltransferases. Cell. 87**,** 953-9.

Okada, Y., et al., Homeodomain proteins MEIS1 and PBXs regulate the lineage-specific transcription of the platelet factor 4 gene. Vol. 101, 2003, pp. 4748-4756.

Olson, E., et al., 1990. Myogenin is in an evolutionarily conserved linkage group on human chromosome 1q31-q41 and unlinked to other mapped muscle regulatory factor genes. Genomics. 8, 427-34.

Ordahl, C. P., Le Douarin, N. M., 1992. Two myogenic lineages within the developing somite. Development. 114, 339-53.

Pan, C., Russell, R., 2010. Roles of DEAD-box proteins in RNA and RNP Folding. RNA Biology. 7, 667-676.

Penn, B. H., et al., 2004. A MyoD-generated feed-forward circuit temporally patterns gene expression during skeletal muscle differentiation. Genes Dev. 18, 2348-53.

Polesskaya, A., et al., 2000. CREB-binding Protein/p300 Activates MyoD by Acetylation. Journal of Biological Chemistry. 275, 34359-34364.

Puri, P. L., et al., 2001. Class I histone deacetylases sequentially interact with MyoD and pRb during skeletal myogenesis. Mol Cell. 8, 885-97.

Puri, P. L., et al., 1997. Differential roles of p300 and PCAF acetyltransferases in muscle differentiation. Mol Cell. 1, 35-45.

Relaix, F. d. r., et al., 2013. Six Homeoproteins Directly Activate <italic>Myod</italic> Expression in the Gene Regulatory Networks That Control Early Myogenesis. PLoS Genet. 9, e1003425.

Rosenberg, M. I., et al., 2006. MyoD inhibits Fstl1 and Utrn expression by inducing transcription of miR-206. J Cell Biol. 175, 77-85.

Roth, J.-F., et al., 2003. Differential role of p300 and CBP acetyltransferase during myogenesis: p300 acts upstream of MyoD and Myf5. EMBO J. 22, 5186-5196.

Rudnicki, M. A., et al., 1992. Inactivation of MyoD in mice leads to up-regulation of the myogenic HLH gene Myf-5 and results in apparently normal muscle development. Cell. 71, 383-90.

Rudnicki, M. A., et al., 1993. MyoD or Myf-5 is required for the formation of skeletal muscle. Cell. 75, 1351-9.

Sabourin, L. A., et al., 1999. Reduced differentiation potential of primary MyoD-/- myogenic cells derived from adult skeletal muscle. J Cell Biol. 144, 631-43.

Saga, Y., et al., Mesp2: a novel mouse gene expressed in the presegmented mesoderm and essential for segmentation initiation. Vol. 11, 1997, pp. 1827-1839.

Sahara, S., et al., 2007. Sp8 exhibits reciprocal induction with Fgf8 but has an opposing effect on anterior-posterior cortical area patterning. Neural Dev. 2**,** 10.

Sartorelli, V., et al., 1997. Molecular mechanisms of myogenic coactivation by p300: direct interaction with the activation domain of MyoD and with the MADS box of MEF2C. Mol Cell Biol. 17**,** 1010-26.

Sartorelli, V., et al., 1990. Muscle-specific expression of the cardiac alpha-actin gene requires MyoD1, CArG-box binding factor, and Sp1. Genes Dev. 4**,** 1811-22.

Schafer, K., Braun, T., 1999. Early specification of limb muscle precursor cells by the homeobox gene Lbx1h. Nat Genet. 23**,** 213-216.

Song, Y. J., Lee, H., 2010. YB1/p32, a nuclear Y-box binding protein 1, is a novel regulator of myoblast differentiation that interacts with Msx1 homeoprotein. Experimental Cell Research. 316**,** 517-529.

Sosic, D., et al., 1997. Regulation of paraxis expression and somite formation by ectoderm- and neural tube-derived signals. Dev Biol. 185**,** 229-43.

Tajbakhsh, S., et al., 1998. Differential activation of Myf5 and MyoD by different Wnts in explants of mouse paraxial mesoderm and the later activation of myogenesis in the absence of Myf5. Development. 125**,** 4155-62.

Tajbakhsh, S., et al., 1997. Redefining the genetic hierarchies controlling skeletal myogenesis: Pax-3 and Myf-5 act upstream of MyoD. Cell. 89**,** 127-38.

Takahashi, Y., et al., Differential contributions of Mesp1 and Mesp2 to the epithelialization and rostro-caudal patterning of somites. Vol. 132, 2005, pp. 787-796.

Tapscott, S. J., 2005. The circuitry of a master switch: Myod and the regulation of skeletal muscle gene transcription. Development. 132**,** 2685-95.

Vasyutina, E., et al., 2005. CXCR4 and Gab1 cooperate to control the development of migrating muscle progenitor cells. Genes Dev. 19**,** 2187-98.

Venuti, J. M., et al., 1995. Myogenin is required for late but not early aspects of myogenesis during mouse development. J Cell Biol. 128**,** 563-76.

Watada, H., et al., 1995. Ubiquitous, but variable, expression of two alternatively spliced mRNAs encoding mouse homologues of transcription factors E47 and E12. Gene. 153**,** 255-9.

Weintraub, H., et al., 1989. Activation of muscle-specific genes in pigment, nerve, fat, liver, and fibroblast cell lines by forced expression of MyoD. Proc Natl Acad Sci U S A. 86**,** 5434-8.

Williams, B. A., Ordahl, C. P., 1994. Pax-3 expression in segmental mesoderm marks early stages in myogenic cell specification. Development. 120**,** 785-96.

Wilson, E. M., Rotwein, P., Control of MyoD Function during Initiation of Muscle Differentiation by an Autocrine Signaling Pathway Activated by Insulin-like Growth Factor-II. Vol. 281, 2006, pp. 29962-29971.

Wilting, J., et al., 1994. Kinetics and differentiation of somite cells forming the vertebral column: studies on human and chick embryos. Anat Embryol (Berl). 190**,** 573-81.

Wright, W. E., et al., 1989. Myogenin, a factor regulating myogenesis, has a domain homologous to MyoD. Cell. 56**,** 607-17.

Yang, J.-H., et al., Myogenic transcriptional activation of MyoD mediated by replication-independent histone deposition. 2010.

Yang, X. M., et al., 1996. Expression of the met receptor tyrosine kinase in muscle progenitor cells in somites and limbs is absent in Splotch mice. Development. 122**,** 2163-71.

Zhang, X., et al., A non-canonical E-box within the MyoD core enhancer is necessary for circadian expression in skeletal muscle. Vol. 40, 2011, pp. 3419-3430.

Zhao, P., et al., 2002. Slug is a novel downstream target of MyoD. Temporal profiling in muscle regeneration. J Biol Chem. 277**,** 30091-101.

Chapter 2: The *MyoD* expressing lineage remains multipotent in the trunk but not the limbs of amyogenic embryos

2.1 Abstract:

Using the *MyoD*$^{iCre/+}$;*R26*$^{lacZ/+}$ genetic cell labeling system, we have for the first time performed permanent lineage tracing of presumptive myoblasts in a genetic background where no myoblasts or muscle fibers form. Recombined cells persist until birth and in the trunk, labeled cells change their fate and become cartilage, bone, and brown fat. In the limbs, myogenic progenitors migrate properly and pattern themselves in a manner similar to wild type embryos. Recombined limb cells do not express *Pax7* or *CD31* and only contribute to the loose connective tissue found in the limbs of amyogenic embryos. The majority of these cells are surrounded by ER-TR7 positive extracellular matrix and many recombined cells express *Tcf4*, a transcription factor and fibroblast marker. The results suggest the *MyoD* expressing lineage of presumptive trunk myoblasts can adopt alternate fates in the absence of primary myogenesis while limb progenitors appear to be fibroblastic.

2.2 Introduction:

MyoD is a pioneer transcription factor whose expression is restricted to the skeletal muscle lineage. Forced *MyoD* expression from a retroviral vector in hepatocytes, adipocytes, and fibroblasts, transforms them into muscle cells (Weintraub et al., 1989) *MyoD* belongs to a highly conserved myogenic family of basic helix-loop-helix (bHLH) transcription factors along with *Mrf4* (Miner and Wold, 1990), *Myogenin* (Wright et al., 1989) and *Myf-5* (Braun et al., 1989). These four factors are collectively referred to as the Myogenic Regulatory Factors (MRFs). *MyoD* and *Myf-5* function earlier in skeletal muscle development than *Myogenin* based on knock out experiments, while *Mrf4* is expressed throughout myogenesis (Kassar-Duchossoy et al., 2004). Single knock outs of either *MyoD* (Rudnicki et al., 1992) or *Myf-5* (Braun et al., 1992) result in mild, transient delays in muscle development, and animals are born with skeletal muscle and are viable. Embryos lacking *MyoD*, *Myf-5* and *Mrf4* develop no skeletal muscle, or their determined precursors, myoblasts (Rudnicki et al., 1993) (Kablar et al., 2003) and the fate of these presumptive myoblasts is investigated here. *Myogenin*$^{-/-}$ embryos exhibit severe differentiation defects, while myoblasts and primary myogenesis occurs normally (Venuti et al., 1995). *Mrf4* knock out embryos show normal muscle formation, but there is a four fold increase in *Myogenin* expression (Braun and Arnold, 1995). Initially, myoblast formation was thought to be controlled by *MyoD* and *Myf-5* only, however, the *Myf-5* knockout allele, *Myf-5*^{Neo}, transcriptionally silenced the nearby *Mrf4* gene.

The newer, *Myf-5*^{loxP} allele allows for *Mrf4* expression, and in *MyoD*$^{-/-}$;*Myf-5*$^{loxP/loxP}$ embryos, some skeletal muscle is produced, but not enough to support life as embryos die at birth due to the absence of the diaphragm (Kassar-Duchossoy et al., 2004). It has never been demonstrated that cells that activate the *MyoD* locus in an amyogenic embryo can form other cell types, leaving the status of presumptive myoblast determination in question.

All skeletal muscle of the trunk and limbs arise from somites, transient embryonic structures flanking the neural tube. *MyoD* and *Myf-5* are expressed in a subset of somitic cells and form muscle, while the rest of the somite forms dermis and the axial skeleton (Christ and Ordahl, 1995). *MyoD* and *Myf-5* have been shown to function as master transcription factors, activating numerous muscle specific genes, but it has been proposed that myogenic progenitor cells are indeed determined before the onset of MRF expression (Tajbakhsh et al., 1997), specifically in the migratory precursors of the limb (Kablar et al., 1999b).

Myogenic progenitors of the limb arise from the somites at limb level, but migrate directly to the limb bud without entering the myotome and without expressing any MRF's (Tajbakhsh and Buckingham, 1994). Whether this migratory cell population is determined in the somite without MRF expression, or migrate in a multipotent state and are determined upon MRF activation by signaling factor gradients present in the limb bud will be addressed. Support for the view that migratory cells are determined in the somite includes selective limb muscle group hypoplasia in mouse mutants lacking genes expressed in the somite, ie; *Lbx1* and the *Six1/4* transcription factors, (Grifone et al., 2005) (Gross

et al., 2000) (Brohmann et al., 2000) *CXCR4* (Vasyutina et al., 2005) and *Pitx2* (Campbell et al., 2012). Also, limb bud grafts at interlimb levels induce the local somites to provide migratory cells to populate the ectopic limb muscle niche (Hayashi and Ozawa, 1995). The dual population hypothesis is supported by gene knockout experiments, where *MyoD*$^{-/-}$ embryos exhibit a delay in hypaxial and limb myogenesis, while *Myf-5*$^{-/-}$ embryos have a delay in epaxial myogenesis (Kablar et al., 1997). However, there is also data suggesting that premyogenic cells are not determined, and migrate to the limb, where endothelial or myogenic fates are determined by the signaling factors in the limb (Kardon et al., 2002a).

Our hypothesis is that multipotent cells of the somite become determined to myogenesis upon *MyoD* or *Myf-5* activation. To directly asses whether these genes function as determination factors, *MyoD*$^{Cre/-}$*;Myf-5*$^{Neo/Neo}$ mouse embryos containing a *Cre*-dependent reporter, will have cells that would have expressed *MyoD* permanently labeled via *Cre*-dependent recombination. Recombination results in heritable, continuous reporter gene production allowing for long term lineage tracing. Contribution of labeled cells to other lineages show the cells of the MyoD expressing lineage are not determined prior to MRF expression.

As described above *MyoD*$^{-/-}$*;Myf-5*$^{Neo/Neo}$ embryos produce no myoblasts (Rudnicki et al., 1993). The premyogenic population in these mice could have died, or changed fate based on observations of brown fat expansion in the back, and excess ‘amorphous loose connective tissue’ in the limbs of these double mutants (Rudnicki et al., 1993) (Rot-Nikcevic et al., 2006). Transgenic experiments using *Myf-5* regulatory regions to drive lacZ expression in

amyogenic embryos showed that the *Myf-5* expressing population could change fate and contribute to cartilage of the axial skeleton. Similar transgenic experiments using *MyoD* regulatory regions to control lacZ expression show the labeled population undergoing apoptosis, not contributing to other lineages, and the eventual loss of lacZ detection by E13.5 (Kablar et al., 2003). Here, we show recombined cells of the *MyoD* expressing lineage to contribute to the axial skeleton and the expanded interscapular brown fat in $MyoD^{Cre/-};Myf\text{-}5^{Neo/Neo};R26^{lacZ}$ embryos and persist until birth, indicating that myogenic progenitors with an active *MyoD* locus remain multipotent in the absence of *MyoD* and *Myf-5*.

In contrast to the multipotent cells in the trunk, the limb population of recombined cells is associated with no distinct structures. The premyogenic cells migrate to the limb and pattern themselves into structures similar to muscle beds. Recombined cells are found in the limb at birth, P0, and are only associated with the connective tissue found in large quantities in the limbs. Immunofluorescent detection of Pax7, an upstream factor of the MRF's, is lacking in mutant limbs. The recombined cells express *Tcf4*, a marker of fibroblastic cells (Mathew et al., 2011), and are surrounded by a connective tissue extracellular matrix, that is positive for ER-TR7 antibody reactivity. The fluorescent Cre dependent reporter, $R26^{EYFP}$, was used in conjunction with fluorescent detection of these proteins in $MyoD^{Cre/-};Myf\text{-}5^{Neo/Neo};R26^{EYFP}$ embryonic limbs.

2.3 Materials and Methods:

Mouse breeding and genotyping

All mouse handling, breeding, and sacrificing were done in accordance with our IACUC animal care protocol. All separate lines were maintained by breeding to FVB mice. Experimental mice were generated by crossing *MyoD*$^{iCre/+}$*;Myf-5*$^{Neo/+}$ males with *MyoD*$^{Neo/+}$*;Myf-5*$^{Neo/+}$*;R26*$^{lacZ/lacZ}$ (Jax# 003309) or *R26*$^{EFYP/EYFP}$ females. The *MyoD*^{iCre} allele was detected by PCR using a forward primer (5′-GCGGATCCGAATTCGAAGTTCC-3′) that lies at the 3′ end of the icre/+2pA cassette and a reverse primer in intron 1 of *MyoD* (5′-TGGGTCTCCAAAGCGACTCC-3′), generating a product of 149 bp. *MyoD*^{iCre} animals were bred to *Myf-5*^{Neo} (Jax# 002522) animals to produce *MyoD*$^{iCre/+}$*;Myf5*$^{Neo/+}$ males. These males were bred to *MyoD*$^{Neo/+}$*;Myf-5*$^{Neo/+}$*;R26*$^{lacZ/lacZ}$ females in order to produce *MyoD*$^{iCre/Neo}$*;Myf-5*$^{Neo/Neo}$*;R26*^{lacZ} embryos with an estimated frequency of 1 in 16. The *MyoD*^{Neo} allele was detected with the forward primer 5'- TGGATGTGGAATGTGTGCGAG-3' and the reverse primer 5'- TCACTGTAGTAGGCGGTGTCGTAG-3' to create a 420 bp product. *R26*^{lacZ} was detected with the primers 5'-CCGAAATCCC GAATCTCTATC-3' and 5'-TTGGCTTCATCCACCACATAC-3' to create a 333 bp product. The *R26*^{EYFP} allele was detected using the primers 5'-GACGTAAACGGCCACAAGTT-3' and 5'-GGTCTTGTAGTTGCCGTCGT-3'. The *Myf-5*^{Neo} allele was detected using the primers 5'-CGTTGG

CTACCCGTGATATT-3' and 5'- CAGCTCAGCTTTGTGTGCTC-3' creating a 410 bp product. *Myf-5* wild type allele used forward primer 5'-TGAAGGATGGACATGACGGAC-3' and reverse 5'-TGACCTTCTTCAGG CGTCTACG-3' to create a 300bp product

All PCR reactions followed standard conditions and 30 cycles, with the following annealing temperatures; $MyoD^{iCre}$, $Myf\text{-}5^{Neo}$, $MyoD^{Neo}$, and $R26^{EYFP}$ at 57°C and $R26^{lacZ}$ at 55°C.

X-Gal Staining

Embryos were collected in PBS and fixed in 2% paraformaldehyde/ 0.25% glutaraldehyde/ in PBS pH 7.4 for 3 hours on ice, followed by several rinses in PBS for 2 hours to overnight, all in individual screw cap tubes. Staining solution was prepared in PBS and contained 2 mM MgCl2, 5 mM K3Fe(CN)6, 5 mM K4Fe(CN)6, 0.01% Tween, 0.1% sodium deoxycholate and 0.1% X-gal. The staining solution was added to the embryos, and were placed in the dark at 37°C overnight with gentle rocking. Following staining, embryos were washed in four changes of PBS over several hours and stored in 1% paraformaldehyde at 4°C.

Paraffin Sectioning

X-Gal stained embryos were processed and paraffin embedded using standard procedures, then serially sectioned at 10µm and counter stained with Nuclear Fast Red (Vector labs)

Cryostat sectioning

Embryos were isolated and fixed with 4% paraformaldehyde for 3.5 hours at 4^{o}C. The embryos were rinsed with cold PBS 4 times at 20 minutes each. The fixed muscle was processed through a sucrose gradient of 15% sucrose in PBS overnight, followed by 30% sucrose in PBS overnight. The processed tissue was placed into OCT compound and quickly frozen in dry ice cooled isopentane. The frozen tissue was cryosectioned at 10 microns and either stored at -80^{o}C, or immediately processed for observation.

Immunofluorescence

Slides for EYFP detection were blocked in PBSMT (2% powdered milk, 0.5% Tween in PBS) followed by rabbit anti-GFP antibody at a 1:500 dilution. For Pax7 detection, slides underwent an antigen retrieval process of 6 minutes in -20^{o}C methanol followed by boiling sodium citrate for 30 minutes. Vector labs Mouse on Mouse block was used according to manufacturers recommendations (Vector # BMK-2202). Pax7 supernatant (Developmental Studies Hybridoma Bank) was applied 1:1 in PBMST overnight at 4^{o}C. Tcf4 detection used only boiling sodium citrate for antigen retrieval and a standard block (1% BSA, 10% goat serum, 0.1% Tween in PBS). Rabbit anti-Tcf4 (Cell Signaling 2569P) was applied at a 1:100 dilution in block, and incubated overnight at 4^{o}C. Perillipin was detected using standard block, with the rabbit anti-perillipin (Sigma P1783)

applied at a 1:500 dilution. ER-TR7 (Santa Cruz sc-73355) was detected using standard block and a 1:400 dilution and incubated overnight at 4^{o}C. Osterix was detected using a standard 2 hour block (1% BSA, 10% goat serum, 0.1% Tween in PBS) followed by an overnight incubation of the primary antibody, rabbit anti-osterix (abcam# ab22552), at a 1:250 dilution. The surface antigen, CD34, was detected using standard conditions with a 2 hour primary incubation, using rat-anti CD34 (abcam# ab8185)at a 1:200 dilution.

Secondary antibodies were used at a 1:500 and dilution and are goat anti-rabbit Alexafluor 488 (GFP) (Invitrogen A11008), goat anti rat 568 (ER-TR7) (Invitrogen A11077) and for all other applications, goat anti rabbit 555 (Invitrogen A21428)

.

Imaging

Whole mount images were taken using a Lecia MZ FLIII and sections were viewed using a Nikon Eclipse E600. Images were captured using a Spot 25.2 2 Mp Color Mosaic camera using Spot Software V4.6 by Diagnostic Instruments. Images were modified using Photoshop CS2.

2.4 Results:

2.4.1 Time Course of Cell Labeling During late Embryogenesis

MyoD$^{iCre/Neo}$;*Myf-5*$^{Neo/Neo}$ embryos, referred to as 'mutant' for brevity, harboring a Cre-dependent reporter, were collected from E13.5 until birth, postnatal day zero, or P0. E13.5 is the chosen starting point as it's when cells were 'lost' in previous experiments using *lacZ* transgenes for lineage tracing (Kablar et al., 2003). Using a Cre-dependent reporter, we are able to permanently label any cell that has activated the *MyoD* locus, and this label is passed on to all daughter cells. The Cre-dependent reporter, *R26*^{lacZ}, was used for most developmental stages, while *R26*^{EYFP} was used for the P0 time point due to a lack of reagent penetration during X-Gal staining and for the ease of fluorescent immunological detection of cell specific markers in conjunction with a fluorescent reporter. Both reporter constructs are identical except for the reporter gene that gets activated following Cre mediated recombination. E13.5 mutant embryos show a massive decrease in lacZ positive cells compared to phenotypically wild type embryos (Figure 2-1). This result can be expected when no myoblasts form, causing a lack of cell proliferation and fusion into muscle fibers. However, a relatively large number of β-Gal positive cells persist in embryos lacking all primary MRF activity in both the epaxial and hypaxial domains.

Recombined cells in the developing cranial region were largely ignored in this analysis due to the many differences known to exist between head and body myogenesis, resulting in difficulties in interpretation of the results. These differences include head muscle progenitors arising from prechordal mesoderm, not from somites, unique regulation of *MyoD* (Tajbakhsh et al., 1997), and other distinct factors that drive myogenesis solely in the head, such as *MyoR*, *Pitx2*, *Tbx1*, and *Capsulin* (Lu et al., 2002) (Noden and Francis-West, 2006) (Grifone and Kelly, 2007).

Embryos collected at E14.5, 15.5, 18.5, and newborns, denoted P0, show that recombined cells persist (Figure 2-2 A and B), and do so until E18.5 (Figure 2-2 C). P0 embryos contain the enhanced yellow fluorescent protein gene, *EYFP* as a readout of Cre-dependent recombination. Due to the size of newborn mice, and low fluorescent levels of *EYFP*, whole mount images are not informative and have been omitted. Identification of cell position and cell type marker expression in the newborn mice is achieved by cryosectioning and immunofluorescent antibody detection. *MyoD* is a lineage specific marker, and finding cells that normally would have expressed *MyoD* changing their fates and not undergoing apoptosis, provides firm evidence that the *MyoD* expressing lineage of presumptive myoblasts remains multipotent in the amyogenic embryo.

We have shown that presumptive myogenic cells persist and do not apoptose in the absence of MRFs. Previous lineage tracing experiments (Kablar et al., 1997; Kablar et al., 1999a) were inconclusive because reporter gene expression was only temporary, and the absence of labeled cells meant either

the transgene was silenced, or the cells died. Using a permanent cell labeling system, we now know the absence of signal was due to transcriptional silencing of the reporter transgene.

Figure 2-1

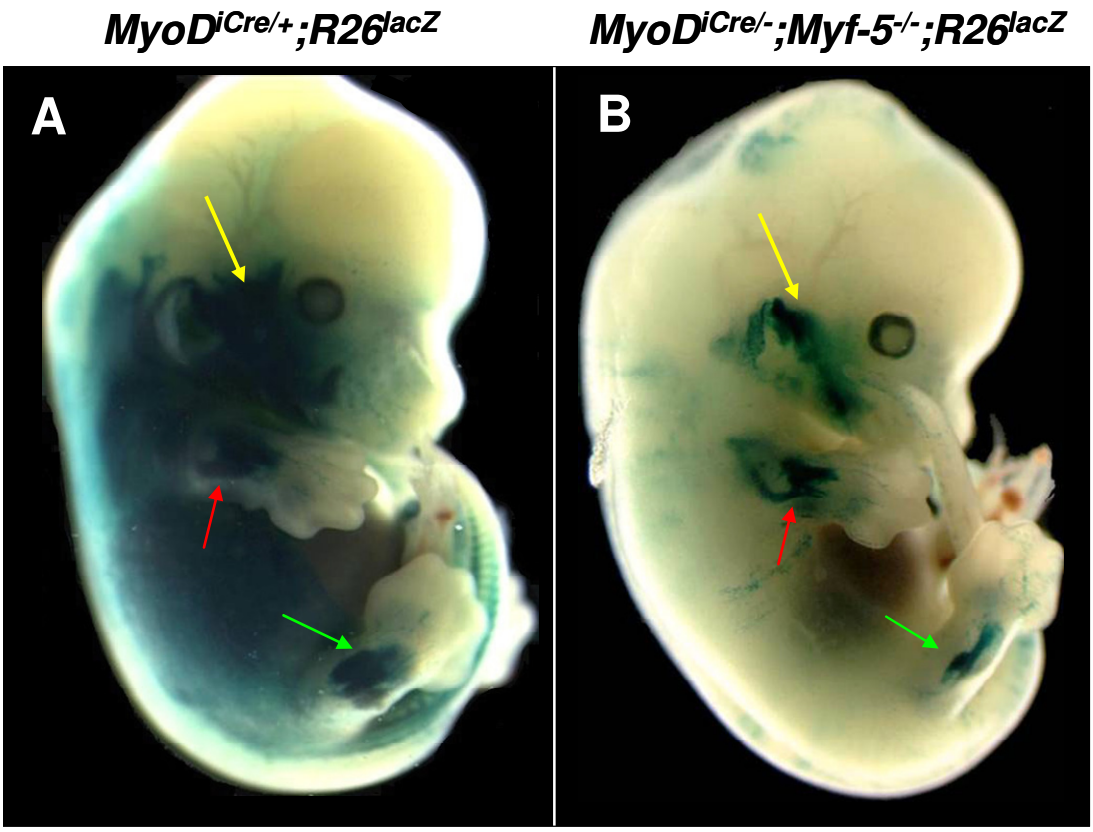

Figure 2-1. X-Gal staining in E13.5 wild type and mutant embryos

Observation of labeled myoblasts and muscle fibers in phenotypicaly normal *MyoD*$^{iCre/+}$;*R26*^{lacZ} embryos (A) and cells that have activated the *MyoD* locus in *MyoD*$^{iCre/Neo}$;*Myf-5*$^{Neo/Neo}$;*R26*^{lacZ} embryos (B). There is a marked decrease of recombined cells in the mutant, particularly in the trunk. Branchial arch derived myogenic progenitors activate the MyoD locus and remain in large numbers in the mutant (yellow arrows). Labeled cells in the limbs of mutants maintain a physical pattern reminiscent of wild type in the fore (red arrows) and hind limbs (green arrows).

Figure 2-2

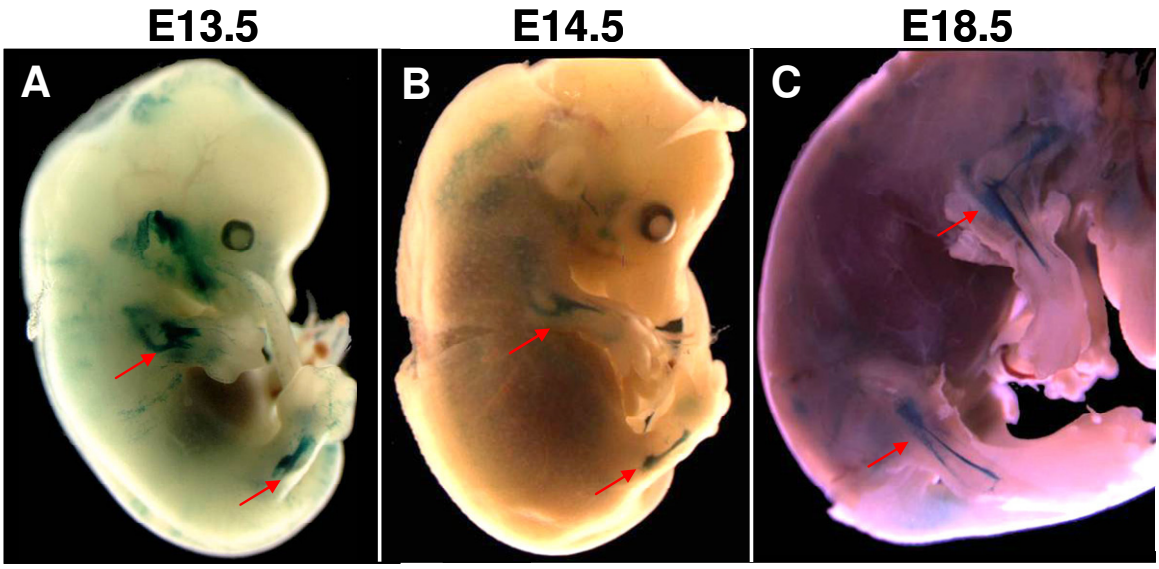

Figure 2-2. Time course of recombined cell staining during late embryonic and fetal development in *MyoD$^{iCre/Neo}$;Myf-5$^{Neo/Neo}$;R26^{lacZ}* mice

Labeled cells persist through E18.5 in *MyoD$^{iCre/Neo}$;Myf-5$^{Neo/Neo}$;R26^{lacZ}* embryos. Limb staining shows a clear progression of recombined cell patterning from one developmental stage to the next (red arrows). Quantity and patterning of labeled cells was consistent between embryos at similar developmental time points. Recombined cells in the trunk are difficult to see due to their low number and density.

2.4.2 Fate changes in recombined cells in the trunk of E13.5 *MyoD$^{iCre/Neo}$;Myf-5$^{Neo/Neo}$;R26^{lacZ}* embryos

In the absence of the primary MRF's, recombined cells contribute to cartilage in the forming scapula (Figure 2-4 A, red arrow) and vertebra (Figure 2-4 B red arrow) and are histologically identical to their non recombined neighbors. While many labeled cells contribute to the endochondral ossification process, many more remain as loose connective tissue, found in place of skeletal muscle surrounding the bones (Figure 2-4 A and B, black arrows). In *MyoD$^{iCre/+}$;R26^{lacZ}* embryos, recombined cells contribute only to skeletal muscle, and their precursor myoblasts.

Interscapular brown fat pads, a major source for non-shivering thermogenesis in neonates, from both mutant and wild type embryos were isolated and sectioned. A large number of recombined cells are found in the fat pads of mutant embryos (Figure 2-4 C) and appear histologically indistinguishable from their non-recombined neighbors. Interestingly, in the dorsal portion of the trunk, there is a large amount of fluid underneath the skin, making it prone to tearing. Sectioning embryos shows empty pockets where cells are absent. No recombined cells were found in the fat pads of *MyoD$^{iCre/+}$;R26^{lacZ}* embryos.

Figure 2-3

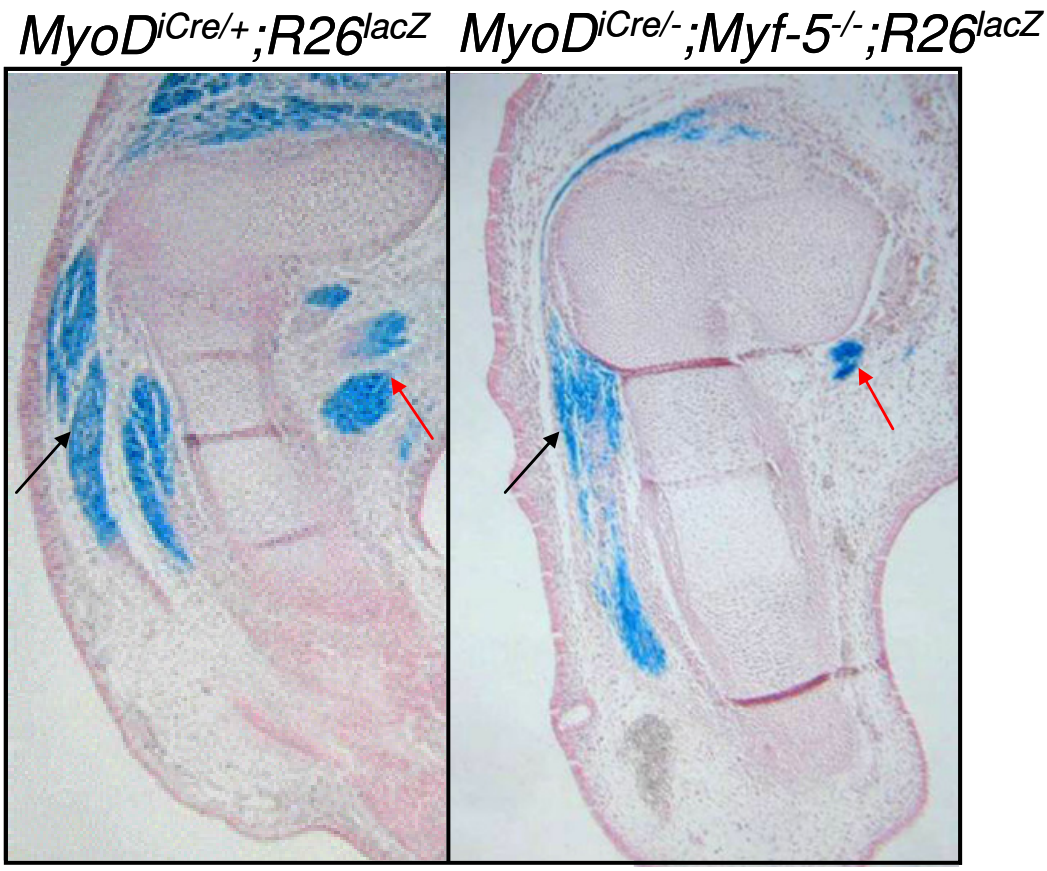

Figure 2-3. Recombined cell patterning in forelimbs

10 µm transverse paraffin sections of limbs in E13.5 mutant (B) and wild type (A) embryos. In A, migratory myogenic precursors populate the limbs and pattern themselves into developing muscle beds. In B, recombined cells do not undergo myogenesis, but position themselves in a manner similar to myoblasts. Red arrows indicate the medial portion of the limb, while black arrows indicate the lateral portion. The distal portion of the limb is located at the bottom of the image. Nuclear fast red used as counter stain.

2.4.3 Limb Phenotype in *MyoD$^{iCre/Neo}$;Myf-5$^{Neo/Neo}$;R26^{lacZ}* embryos

Myogenic progenitors of the limb in *MyoD$^{iCre/Neo}$;Myf-5$^{Neo/Neo}$;R26^{lacZ}* embryos not only migrate from limb level somites properly, they also pattern themselves in a manner similar to wild type embryos (Fig 2-3), and these cells persist past E18.5 (Figure 2-2 C) until birth (Figure 2-10 B and E). The limb patterning results are reproducible at each stage, indicating precise activation of the *MyoD* locus in the limbs. It has previously been shown that cells migrate to the limb prior to MRF expression, so this result is not surprising. The fact that these cells persist, and continue to maintain a reproducible pattern until birth is novel. Labeled cells do not contribute to any identifiable structures in the limb, such as bone and skin.

The amyogenic phenotype has been reported in other studies, but descriptions of the limb have been lacking. With no muscle in the limb, fibroblasts proliferate and make up almost the entire volume of the limb. These delicate, fibrous cells are not durable and prone to damage during skinning, embryo manipulation. During sectioning, the delicate nature of the tissue causes section tearing. It is possible to see the bones of the limb through this delicate tissue (Fig 2-7B red arrows). Quality sectioning of embryos is difficult due to the lack of a strong cellular structure. In the forelimbs, the radius and ulna are much closer together in mutant versus wild type embryos (Fig 2-8), as are the tibia and fibula in the hindlimbs.

Figure 2-4

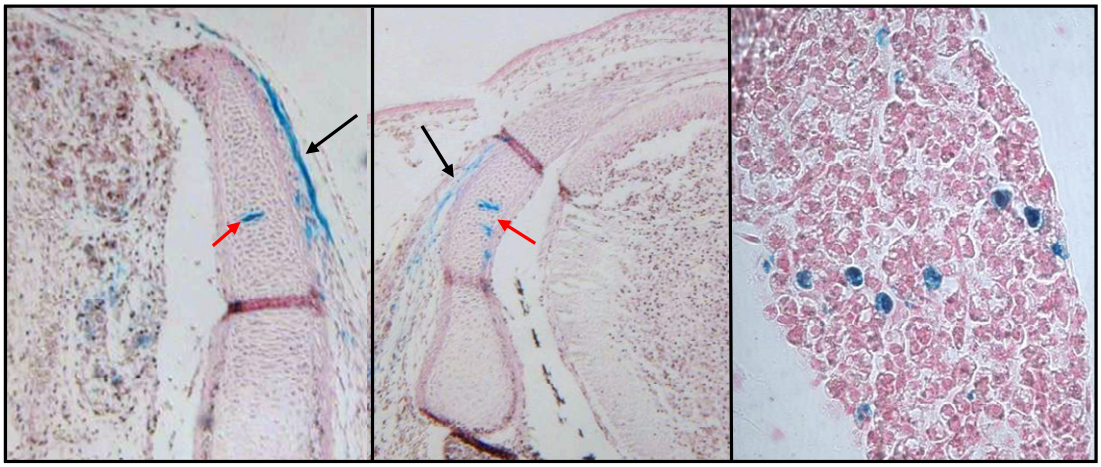

Scapula Vertebra Interscapular Brown Fat

Figure 2-4. Labeled cells contribute to non myogenic lineages in the trunk

10 µm paraffin cross sections of E13.5 *MyoD*$^{iCre/Neo}$*;Myf-5*$^{Neo/Neo}$*;R26*^{lacZ} embryos. The cartilage condensations of the developing scapula (A) and vertebra (B) contain lacZ+ cells only in *MyoD*$^{iCre/Neo}$*;Myf-5* $^{Neo/Neo}$*;R26*^{lacZ} embryos (red arrows). Recombined cells also populate the area surrounding the developing bone (black arrows). Labeled cells are also present in the interscapular brown fat pads from E13.5 to birth (C).

Figure 2-5

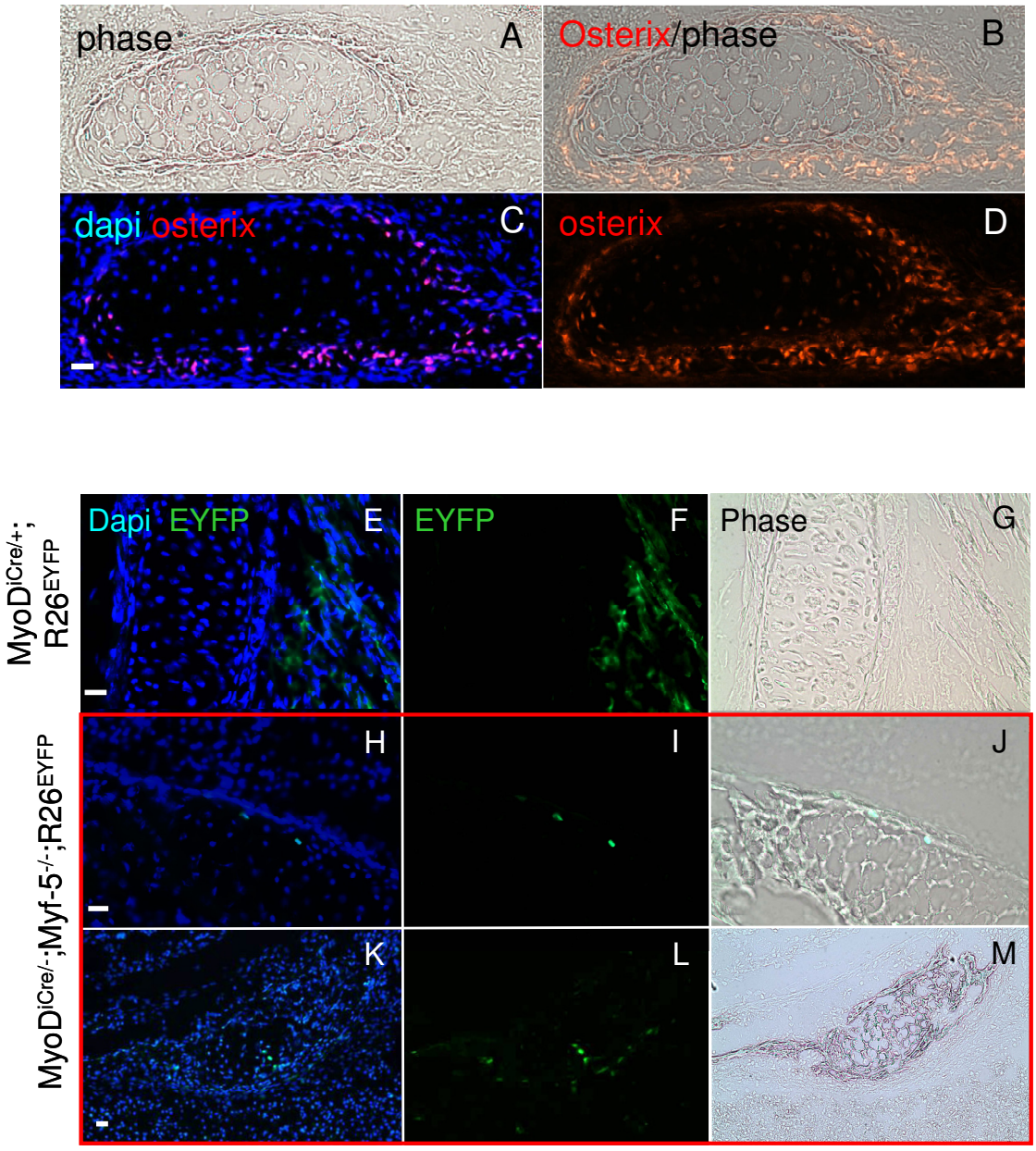
phase
A
Osterix/phase
B
dapi osterix
C
osterix
D
MyoDiCre/+; R26EYFP
Dapi EYFP
E
EYFP
F
Phase
G
MyoDiCre/-;Myf-5-/-;R26EYFP
H
I
J
K
L
M

Figure 2-5. Recombined cells in the trunk contribute to bone at P0

Serial 10µm cryosections of *MyoD*$^{iCre/Neo}$*;Myf-5*$^{Neo/Neo}$*;R26*^{EYFP} embryo (A-D and H-M). Panels A-D show Osterix positive bone cells (red) of the rib rudiments. Phase contrast image (A) is characteristic of bone morphology in phase panels G, J, and M. Dapi (C, E, H, K) was used to visualize nuclei. Panels F, I, and L show EYFP+ cells in different rib rudiments. Panels E-G are from a *MyoD*$^{iCre/+}$*;R26*^{EYFP} embryos and show no EYFP detection in bone, only in the surrounding muscle. Scale bars represent 30 µm.

Figure 2-6

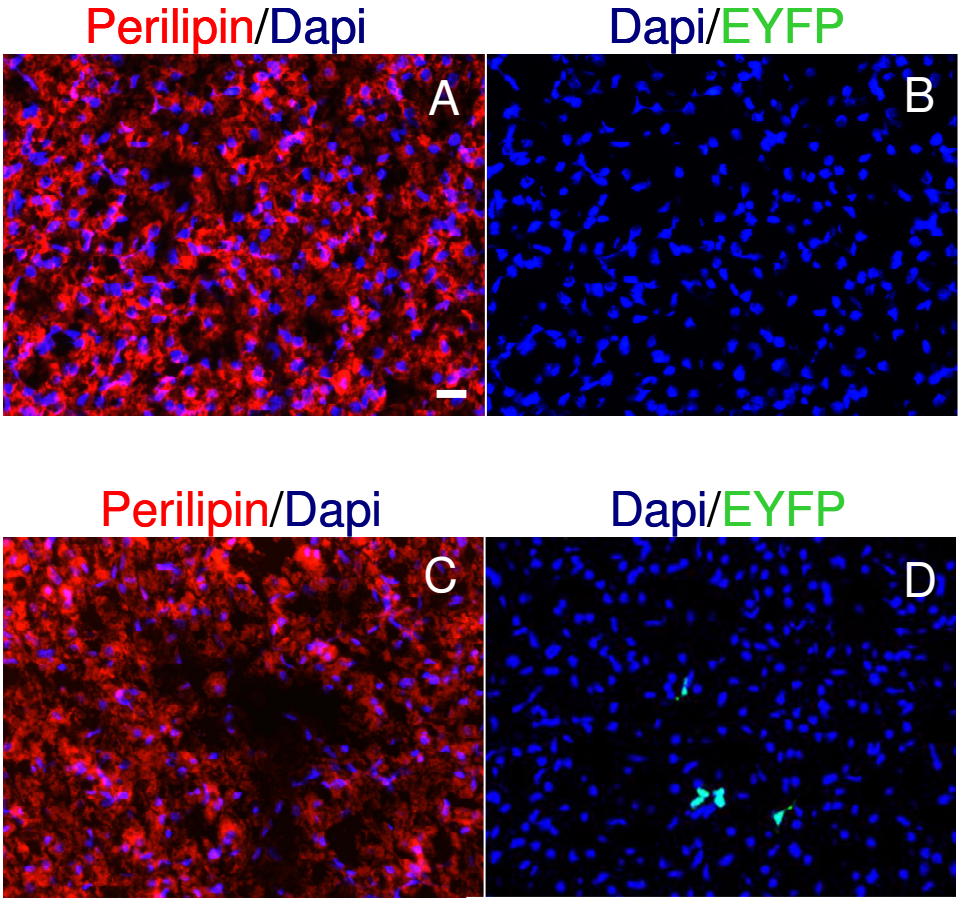

Figure 2-6. Recombined cells contribute to brown fat in P0 *MyoD$^{iCre/Neo}$;Myf-5$^{Neo/Neo}$;R26^{EYFP}* animals

10 µm serial cryosections of *MyoD$^{iCre/+}$;R26^{EYFP}* (A and B) and *MyoD$^{iCre/Neo}$;Myf-5$^{Neo/Neo}$;R26^{EYFP}* newborns(C and D). Perilipin (red in A and C), a fat specific marker, was used along with section location to identify interscapular brown fat pads. In serial sections from *MyoD$^{iCre/Neo}$;Myf-5$^{-/-}$;R26^{EYFP}* embryos, EYFP+ cells contribute to perilipin positive brown fat (C). Dapi used to visualize nuclei. Scale bar represents 30 µm.

2.4.4 Fate of recombined cells in the trunk and limbs at P0 in *MyoD*$^{iCre/Neo}$;*Myf-5*$^{Neo-Neo}$;*R26*^{EYFP} embryos

There are differing results in the fate of labeled cells in the trunk versus the limbs in mutant embryos. In the trunk, fate changes take place, and cells that would normally form muscle express perillipin and contribute to brown fat (Fig 2-6), while others are osterix positive and contribute to bone (Fig 2-5). Due to the low level of EYFP expression, antibody detection is used to enhance the signal. Serial cryosections were used for antibody detection of other markers.

In the limb, labeled cells do not contribute to bone or vasculature, and instead, the vast majority remain clustered in a 'rod' aligned along the proximal-distal axis (Fig 2-7) with some recombined cells remaining outside of the rod. Some EYFP positive cells express *Tcf4*, a fibroblastic marker (Mathew et al., 2011), and are surrounded by an ER-TR7 (Van Vliet et al., 1986) positive extra cellular matrix (Fig 2-9). It can be safely assumed that these cells have become fibroblastic or are stalled in their developmental pathway.

Not all of the EYFP+ cells express *Tcf4*, so if some of our cells of interest remain poised for myogenesis, they should express the early myogenic marker, Pax7 (Halevy et al., 2004). However, no Pax7 positive cells were found in mutant limbs, either in the EYFP positive or negative areas (Fig 2-10 E and F). In wild type limbs, *Pax7* is expressed in satellite cells, the tissue specific stem cell used in muscle growth and repair (Fig 2-10 A and B).

While no EYFP+ cells were found in the bones of the limb, and some EYFP+ cells are phenotypically fibroblastic, we investigated whether recombined cells could contribute to endothelial vascular cells, the other major limb cell type present. In the mutant limbs, there is a severe reduction in the amount of CD31+ vasculature (Fig 2-10 G and H) in comparison to wild type (Fig 2-10 C and D). Of the rare CD31+ cells found in the mutant, none of them were EYFP+.

Figure 2-7

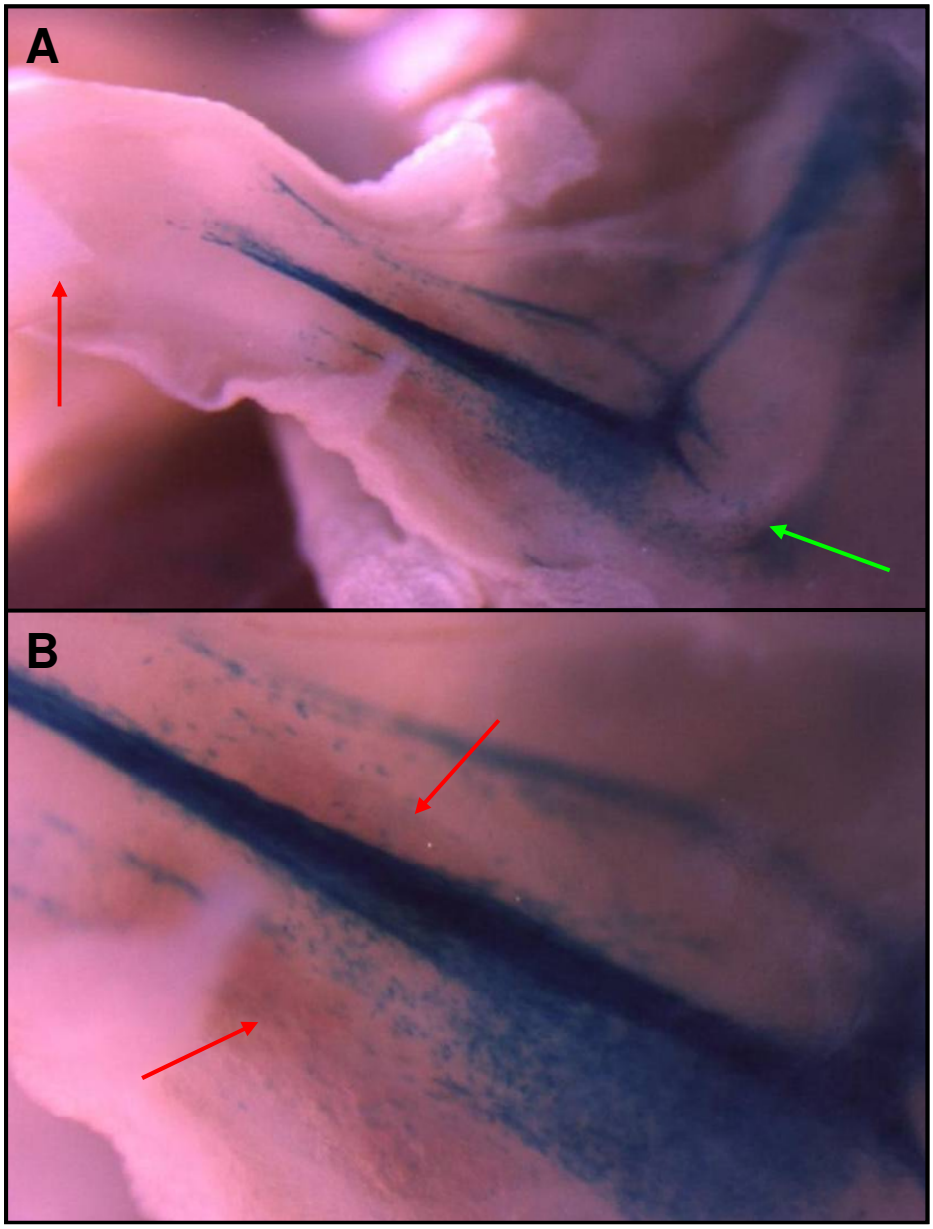

Figure 2-7. Forelimb close up of E18.5 *MyoD$^{iCre/Neo}$;Myf-5$^{Neo/Neo}$;R26^{lacZ}* embryo

Limbs contain no muscle fibers and are largely transparent, allowing visualization of limb bones (red arrows show radius and ulna in B). (B) is a higher magnification image of the limb in (A). Loose connective tissue comprises the majority of soft tissue in the limb and is quite fragile. In (A), the green arrow indicated the distal paw, while red arrow points to proximal elbow.

Figure 2-8

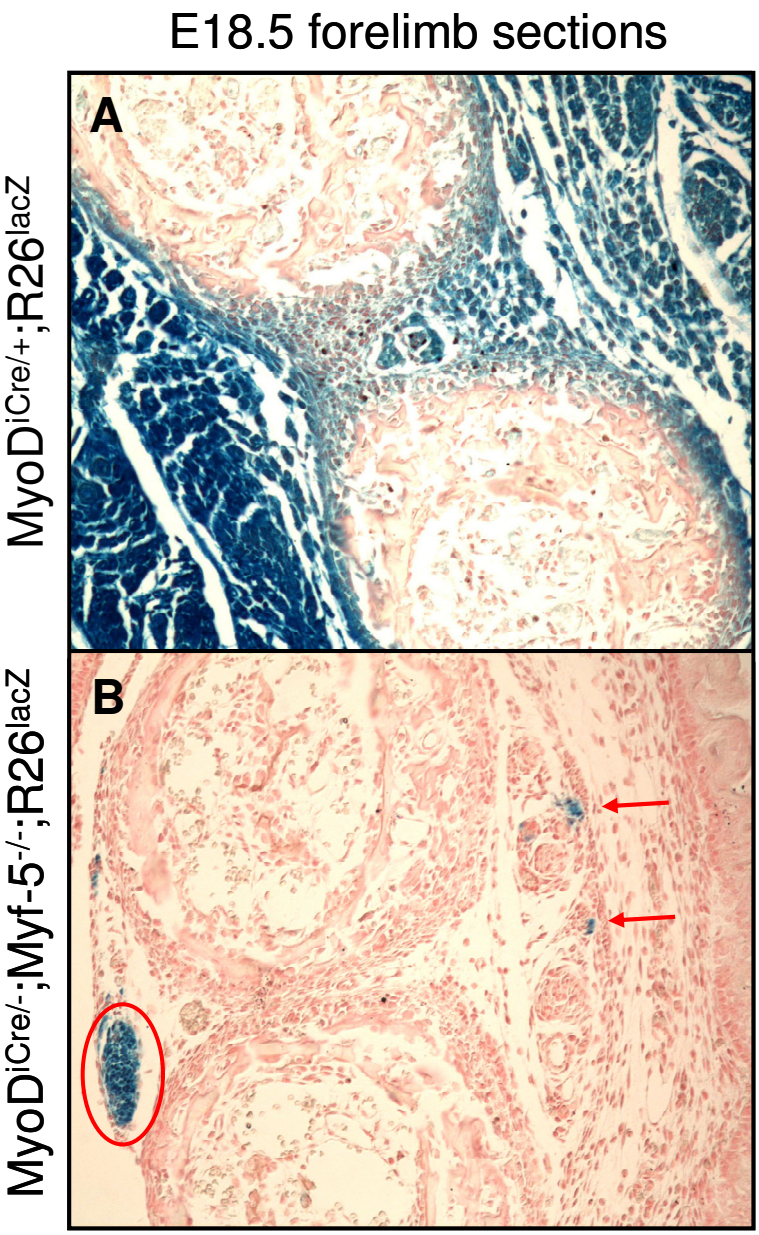
E18.5 forelimb sections
A
B
MyoD$^{iCre/+}$;R26^{lacZ}
MyoD$^{iCre/-}$;Myf-5$^{-/-}$;R26^{lacZ}

Figure 2-8. Paraffin sections of E18.5 forelimbs

10 μm paraffin sections of *MyoD$^{iCre/+}$;R26^{lacZ}* (A) and *MyoD$^{iCre/Neo}$;Myf-5$^{Neo/Neo}$;R26^{lacZ}* (B) E18.5 forelimbs. The distance between the radius and ulna is smaller in B compared to A. In both panels, blue cells have historically activated the MyoD locus. The thick 'rod' of cells seen in Figure 2-7 is shown in cross section (in B, red circle). Other, less concentrated, β-Gal positive cells are also seen in B (red arrows).

Figure 2-9

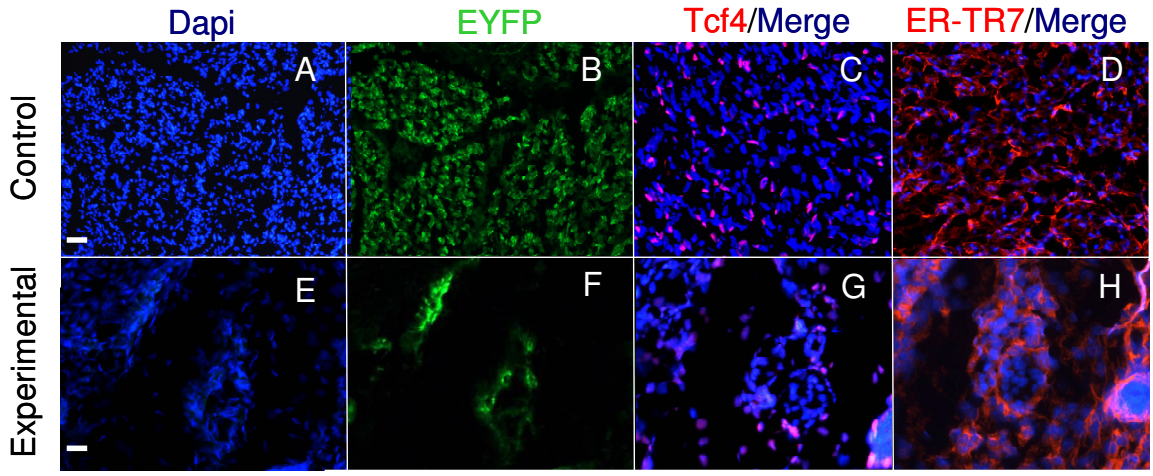
Dapi
EYFP
Tcf4/Merge
ER-TR7/Merge
Control
Experimental
A
B
C
D
E
F
G
H

Figure 2-9. Fibroblastic recombined cells in P0 limb sections

EYFP+ cells in the limb of *MyoD*$^{iCre/+}$*;R26*^{lacZ} embryo cryosections (A-D) show EYFP+ skeletal muscle and position of fibroblasts. *MyoD*$^{iCre/Neo}$*;Myf-5*$^{Neo/Neo}$*;R26*^{EYFP} embryos (E-H) show the dense packing of cells seen in Figures 2-7 and 2-8. In serial sections, EYFP+ areas are surrounded by the extracellular matrix protein, ER-TR7 (H) and some cells express the fibroblastic marker *Tcf4* (G). Scale bar represents 30 μm.

Figure 2-10

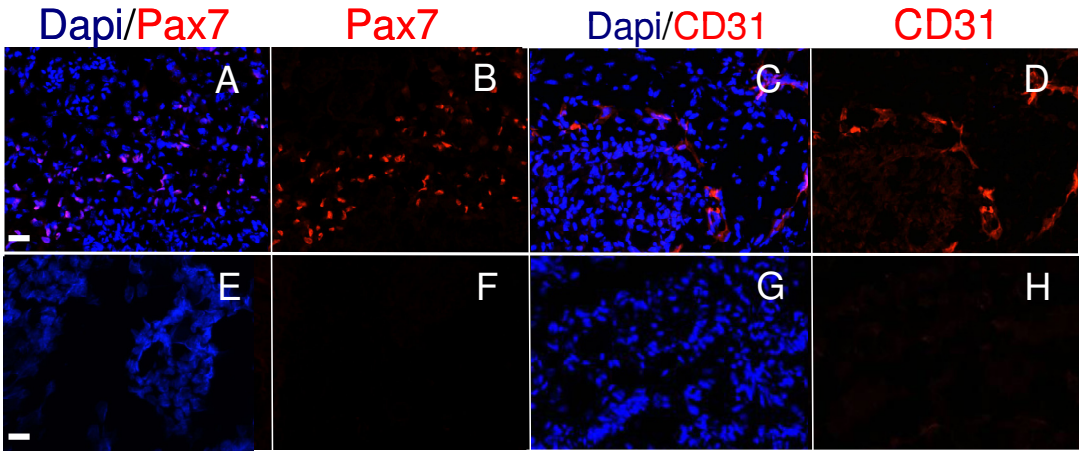

Figure 2-10. Recombined cells in mutant embryos do not express Pax7 or CD31 at P0

Pax7, a marker of pre and early myogenic cells, is found only in *MyoD*$^{iCre/+}$*;R26*^{EYFP} sections (A and B) and nowhere in *MyoD*$^{iCre/-}$*;Myf-5*$^{Neo/Neo}$*;R26*^{EYFP} sections (E and F). CD31, an endothelial cell marker, is greatly reduced in mutant (G and H) versus control (C and D) limb sections. Also, no EYFP+ cells in the mutant were CD31+. Scale bar represents 30 μm.

2.5 Discussion:

MyoD is such a potent transcription factor that its trans-activation domain has been fused to other DNA binding domains in order to increase the efficiency of forming iPS cells (Hirai et al., 2012) and cardiomyocytes (Hirai et al., 2013) in culture. MyoD has incredible chromatin remodeling abilities and activates transcription at many downstream loci. MyoD directly recruits the SWI/SNF chromatin remodeling complex to specific sites(de la Serna et al., 2005), leading to muscle specific E box binding (an excellent review (Tapscott, 2005)).

However, there has been no classical experimental evidence proving MyoD is a determination factor. To prove a cell is determined, transplantation of the cells in question to an ectopic site in the embryo is performed. If the transplanted cells maintain their original identity, they were determined to a fate at the time of transplant. Myoblast transplants in mice to ectopic sites form skeletal muscle, but myoblasts have already expressed MyoD, and the results are not informative (Irintchev et al., 1998). Somite rotation experiments in the developing chicken embryo show that cells of the somite are plastic in newly formed somites, as well as the two sets located cranially (Dockter and Ordahl, 2000). Some of the cells in the somite have already expressed *Myf-5*, but not *MyoD*, at the time of rotation, but early in somite maturation, appropriate gene expression requires continuous exposure to signaling centers in the embryo (Pownall et al., 2002).

The questions addressed here are if the *MyoD* expressing lineage remains multipotent in the absence of myogenesis and if the lineage remains multipotent in epaxial (trunk) and hypaxial (limb) myogenic fields. Given the complex, and still largely unknown, upstream activators of *MyoD*, cells may be determined by one or more upstream factors before the onset of *MyoD* expression and myogenesis. Here, we analyzed the fate of cells that have activated the *MyoD* locus, in the absence of *MyoD* and the other primary MRFs, while all upstream signaling pathways are unperturbed.

Previous lineage tracing studies using transgenes have only followed Myf-5lacZ+ cells through E15.5, and MyoDlacZ+ cells to E13.5 in amyogenic embryos (Kablar et al., 2003; Kablar et al., 1999a). The conclusion from these reports, along with an increase in the number of apoptotic cells, was that cells of the *MyoD* lineage apoptose and do not contribute to other lineages, while cells in the *Myf-5* lineage remain and contribute to other cell lineages, such as cartilage. Using *Cre recombinase* we show the *MyoD* lineage persists and the loss of signal was due to transcriptional silencing of the transgene. Our current findings demonstrate that myogenic progenitors in the trunk abandon myogenesis before E13.5, and instead are able to progress down different lineages, such as cartilage, bone, and brown fat. In the limbs, our labeled population survives and contributes only to the fibroblastic-like cells of the limbs.

A common hypothesis was that *MyoD* and *Myf-5* control myogenesis in two different cell lineages as opposed to single cells expressing both factors. Recent supporting experiments used diphtheria toxin (DTA) driven lineage

ablation, to kill *Myf-5* expressing cells, yet skeletal muscle still forms (Haldar et al., 2008) demonstrating that a *Myf-5* independent lineage exists. However, when the *MyoD* expressing lineage is ablated, no muscle remains in embryos at E18.5 (preliminary data in chapter 4) (Wood et al., 2013). Also, it has been shown that all satellite cells, muscle specific stem cells, express *MyoD* prenatally (Kanisicak et al., 2009). Taken together, these results show that all cells in the myogenic lineage express *MyoD*, while not every cells expresses *Myf-5*. This means that the fate changes seen in Myf-5lacZ amyogenic embryos are accounted for in this study. Our results show that cells that have activated the *MyoD* locus persist until birth, and take on different fates.

There are differing observations of cell fate plasticity in trunk versus limb myogenic progenitor cells. These two populations are quite different, as trunk myogenesis begins earlier and limb progenitors migrate directly from the dermomyotome, without entering the myotome. Cells that populate the limb express several genes that trunk progenitors do not, such as *c-met* and *Lbx1* (Mennerich and Braun, 2001). Expression of the transcription factors *Pax3, Pitx2, Dach2, Eya2,* and *Six1/4* remains only in the hypaxial edge of the dermomyotome and in migratory limb progenitors (Grifone et al., 2007; Heanue et al., 1999; Kardon et al., 2002b; L'Honore et al., 2010). These migratory cells don't express any MRFs until they reach the limb field. As they are the only source of skeletal muscle for the limbs, they are possibly already specified for the myogenic fate as they leave the somite. Trunk myoblasts and bone progenitors share a common somitic origin, while the bones of the limb derive from lateral

plate mesoderm. This may explain the inability of recombined limb cells to contribute to osteogenesis. The other fate change, recombined brown fat cells, may be linked to a common origin as well. *Prdm16* has been shown to control a switch between skeletal muscle and brown fat fate decisions, such that over expression of *Prdm16* can convert myoblasts to brown fat (Seale et al., 2008). Brown fat progenitors have been shown to activate the *Myf-5* locus (Shan et al., 2013), and *MyoD;Igf2* double null animals have an increase in brown fat development (Borensztein et al., 2012). However, limb myogenic progenitors share a dermomyotomal origin with limb endothelial cells, but there was no fate change noted. This may be due to specification in the somite followed by signaling molecules in the limb regulating fate decisions (Kardon et al., 2002a).

As previously stated, the $MyoD^{iCre}$ labeling system labels the entire embryonic population of myoblasts, while $Myf\text{-}5^{Cre}$ does not. While this project was underway, this fact was not yet known. Therefore, $MyoD^{iCre/Neo}$;$R26^{lacZ}$ embryos were analyzed for any fate changes in the absence of *MyoD* only, as *MyoD* and *Myf-5* might control myogenesis in two different cell lineages. All recombined cells contributed to muscle in these embryos, and the data was excluded. In retrospect, if the DTA experiments reflect the actual biology, then some premyogenic cells do not express *Myf-5*, and are dependent on *MyoD* or *Mrf4* for access to the myogenic program. In $MyoD^{iCre/Neo};R26^{lacZ}$ embryos, *MyoD* expressing cells do not contribute to other fates, perhaps due expression of *Myf-5* and *Mrf4*. If there is a *MyoD* dependent myogenic lineage, its close proximity

to *Myf-5* and *Mrf4* expressing myogenic cells may lead to fusion into the forming muscle fibers.

2.6 References

Borensztein, M., et al., 2012. Double Myod and Igf2 inactivation promotes brown adipose tissue development by increasing Prdm16 expression. The FASEB Journal. 26**,** 4584-4591.

Braun, T., Arnold, H. H., 1995. Inactivation of Myf-6 and Myf-5 genes in mice leads to alterations in skeletal muscle development. Embo J. 14**,** 1176-86.

Braun, T., et al., 1989. A novel human muscle factor related to but distinct from MyoD1 induces myogenic conversion in 10T1/2 fibroblasts. Embo J. 8**,** 701-9.

Braun, T., et al., 1992. Targeted inactivation of the muscle regulatory gene Myf-5 results in abnormal rib development and perinatal death. Cell. 71**,** 369-82.

Brohmann, H., et al., 2000. The role of Lbx1 in migration of muscle precursor cells. Development. 127**,** 437-45.

Campbell, A. L., et al., 2012. Regulation of Motility of Myogenic Cells in Filling Limb Muscle Anlagen by Pitx2. PLoS ONE. 7**,** e35822.

Christ, B., Ordahl, C. P., 1995. Early stages of chick somite development. Anat Embryol (Berl). 191**,** 381-96.

de la Serna, I. L., et al., 2005. MyoD targets chromatin remodeling complexes to the myogenin locus prior to forming a stable DNA-bound complex. Mol Cell Biol. 25**,** 3997-4009.

Dockter, J., Ordahl, C. P., 2000. Dorsoventral axis determination in the somite: a re-examination. Development. 127**,** 2201-6.

Grifone, R., et al., 2007. Eya1 and Eya2 proteins are required for hypaxial somitic myogenesis in the mouse embryo. Dev Biol. 302**,** 602-16.

Grifone, R., et al., 2005. Six1 and Six4 homeoproteins are required for Pax3 and Mrf expression during myogenesis in the mouse embryo. Development. 132**,** 2235-49.

Grifone, R., Kelly, R. G., 2007. Heartening news for head muscle development. Trends Genet. 23**,** 365-9.

Gross, M. K., et al., 2000. Lbx1 is required for muscle precursor migration along a lateral pathway into the limb. Development. 127**,** 413-24.

Haldar, M., et al., 2008. Two cell lineages, myf5 and myf5-independent, participate in mouse skeletal myogenesis. Dev Cell. 14**,** 437-45.

Halevy, O., et al., 2004. Pattern of Pax7 expression during myogenesis in the posthatch chicken establishes a model for satellite cell differentiation and renewal. Dev Dyn. 231**,** 489-502.

Hayashi, K., Ozawa, E., Myogenic cell migration from somites is induced by tissue contact with medial region of the presumptive limb mesoderm in chick embryos. Vol. 121, 1995, pp. 661-669.

Heanue, T. A., et al., 1999. Synergistic regulation of vertebrate muscle development by Dach2, Eya2, and Six1, homologs of genes required for Drosophila eye formation. Genes Dev. 13**,** 3231-43.

Hirai, H., et al., 2012. Efficient iPS Cell Production with the MyoD Transactivation Domain in Serum-Free Culture. PLoS ONE. 7**,** e34149.

Hirai, H., et al., 2013. Accelerated direct reprogramming of fibroblasts into cardiomyocyte-like cells with the MyoD transactivation domain. Cardiovascular Research.

Irintchev, A., et al., 1998. Ectopic skeletal muscles derived from myoblasts implanted under the skin. Journal of Cell Science. 111**,** 3287-3297.

Kablar, B., et al., 2003. Myf5 and MyoD activation define independent myogenic compartments during embryonic development. Dev Biol. 258**,** 307-18.

Kablar, B., et al., 1997. MyoD and Myf-5 differentially regulate the development of limb versus trunk skeletal muscle. Development. 124**,** 4729-38.

Kablar, B., et al., 1999a. Myogenic determination occurs independently in somites and limb buds. Dev Biol. 206**,** 219-31.

Kablar, B., et al., Myogenic determination occurs independently in somites and limb buds. Vol. 206, 1999b, pp. 219 - 231.

Kanisicak, O., et al., 2009. Progenitors of skeletal muscle satellite cells express the muscle determination gene, MyoD. Dev Biol. 332**,** 131-41.

Kardon, G., et al., 2002a. Local extrinsic signals determine muscle and endothelial cell fate and patterning in the vertebrate limb. Dev Cell. 3**,** 533-45.

Kardon, G., et al., 2002b. Pax3 and Dach2 positive regulation in the developing somite. Dev Dyn. 224**,** 350-5.

Kassar-Duchossoy, L., et al., 2004. Mrf4 determines skeletal muscle identity in Myf5:Myod double-mutant mice. Nature. 431**,** 466-71.

L'Honore, A., et al., Pitx2 defines alternate pathways acting through MyoD during limb and somitic myogenesis. Vol. 137, 2010, pp. 3847-3856.

Lu, J.-r., et al., Control of Facial Muscle Development by MyoR and Capsulin. Vol. 298, 2002, pp. 2378-2381.

Mathew, S. J., et al., 2011. Connective tissue fibroblasts and Tcf4 regulate myogenesis. Development. 138**,** 371-384.

Mennerich, D., Braun, T., 2001. Activation of myogenesis by the homeobox gene Lbx1 requires cell proliferation. Embo J. 20**,** 7174-83.

Miner, J. H., Wold, B., 1990. Herculin, a fourth member of the MyoD family of myogenic regulatory genes. Proc Natl Acad Sci U S A. 87**,** 1089-93.

Noden, D. M., Francis-West, P., 2006. The differentiation and morphogenesis of craniofacial muscles. Dev Dyn. 235**,** 1194-218.

Pownall, M. E., et al., 2002. Myogenic regulatory factors and the specification of muscle progenitors in vertebrate embryos. Annu Rev Cell Dev Biol. 18**,** 747-83.

Rot-Nikcevic, I., et al., 2006. Myf5-/- :MyoD-/- amyogenic fetuses reveal the importance of early contraction and static loading by striated muscle in mouse skeletogenesis. Dev Genes Evol. 216**,** 1-9.

Rudnicki, M. A., et al., 1992. Inactivation of MyoD in mice leads to up-regulation of the myogenic HLH gene Myf-5 and results in apparently normal muscle development. Cell. 71**,** 383-90.

Rudnicki, M. A., et al., 1993. MyoD or Myf-5 is required for the formation of skeletal muscle. Cell. 75**,** 1351-9.

Seale, P., et al., 2008. PRDM16 controls a brown fat/skeletal muscle switch. Nature. 454**,** 961-7.

Shan, T., et al., 2013. Distinct populations of adipogenic and myogenic Myf5-lineage progenitors in white adipose tissues. Journal of Lipid Research. 54**,** 2214-2224.

Tajbakhsh, S., Buckingham, M. E., 1994. Mouse limb muscle is determined in the absence of the earliest myogenic factor myf-5. Proc Natl Acad Sci U S A. 91**,** 747-51.

Tajbakhsh, S., et al., 1997. Redefining the genetic hierarchies controlling skeletal myogenesis: Pax-3 and Myf-5 act upstream of MyoD. Cell. 89**,** 127-38.

Tapscott, S. J., 2005. The circuitry of a master switch: Myod and the regulation of skeletal muscle gene transcription. Development. 132**,** 2685-95.

Van Vliet, E., et al., 1986. Reticular fibroblasts in peripheral lymphoid organs identified by a monoclonal antibody. Journal of Histochemistry & Cytochemistry. 34**,** 883-90.

Vasyutina, E., et al., 2005. CXCR4 and Gab1 cooperate to control the development of migrating muscle progenitor cells. Genes Dev. 19**,** 2187-98.

Venuti, J. M., et al., 1995. Myogenin is required for late but not early aspects of myogenesis during mouse development. J Cell Biol. 128**,** 563-76.

Weintraub, H., et al., 1989. Activation of muscle-specific genes in pigment, nerve, fat, liver, and fibroblast cell lines by forced expression of MyoD. Proc Natl Acad Sci U S A. 86**,** 5434-8.

Wood, W. M., et al., 2013. MyoD-expressing progenitors are essential for skeletal myogenesis and satellite cell development. Dev Biol. 384**,** 114-27.

Wright, W. E., et al., 1989. Myogenin, a factor regulating myogenesis, has a domain homologous to MyoD. Cell. 56**,** 607-17.

Chapter 3: Embryonic transcriptional regulation of *MyoD* is largely independent of the Core Enhancer and Distal Regulatory Region

3.1 Abstract:

Transgenic experiments identified two enhancers of the muscle specific gene, *MyoD*. These enhancers, called the core enhancer (CE) and distal regulatory region (DRR), control the initiation and maintenance of expression, respectfully. However, deletion of CE results in only a mild expression delays in the limb buds and branchial arches, while deletion of the DRR results in lowered postnatal expression levels. Here, we have removed both enhancers via homologous recombination to address the functional redundancy between the two enhancers. In homozygous embryos with both enhancers removed ($MyoD^{\Delta CEDRR/\Delta CEDRR}$), *MyoD* expression continues with a one day delay in hypaxial lineage expression, reminiscent of $CE^{loxP/loxP}$ embryos who only lack the CE (Chen and Goldhamer, 2004a). An even milder delay in early myotome expression is the only novel phenotype in $MyoD^{\Delta CEDRR/\Delta CEDRR}$ embryos. In additon, the removal of the 15 kb of DNA between the CE and DRR, ($MyoD^{\Delta CE15DRR/\Delta CE15DRR}$) resulted in identical expression kinetics. In the absence of *Myf-5*, *MyoD* expression is dependent on *Pax3*. The rescue kinetics in these new lines are identical to wild type embryos. Ultimately, the CE and DRR are not necessary for largely normal *MyoD* expression.

In an attempt to identify the new enhancers, a genomic approach was taken to analyze 2 Mbp surrounding *MyoD* for conserved sequences across species and for transcriptionally positive epigenetic markers. We found the introns of *MyoD* contain positive epigenetic marks, are conserved across species, and have putative binding sites for several transcription factors.

3.2 Introduction:

MyoD is a pioneer transcription factor that activates genes necessary for myogenesis in a temporally regulated manner, remodels chromatin, promotes proliferation and orchestrates a complex cellular response. Two excellent reviews can be found here (Tapscott et al. 2005, Singh et al. 2013).

MyoD is one of four members of the myogenic family of bHLH transcription factors that control embryonic and postnatal myogenesis. Myoblast formation is controlled by *MyoD* and *Myf-5*, and to a lesser extent *Mrf4,* while myogenic differentiation and fiber formation is performed primarily by *Mrf4* and *Myogenin*. In the original $MyoD^{-/-};Myf\text{-}5^{-/-}$ embryos, myoblasts fail to form and myogenesis fails (Rudnicki et al., 1993). However, this phenotype was partly due to transcriptional silencing of the *Mrf4* locus by the $Myf\text{-}5^{Neo}$ allele. When a different *Myf-5* knockout allele is used, $Myf\text{-}5^{loxp}$, *Mrf4* expression is not compromised and some Myosin Heavy Chain positive cells form, but myogenesis is not robust enough to produce viable animals (Kassar-Duchossoy et al., 2004).

In order to understand the transcriptional regulation of *MyoD,* we must define it's enhancer regions. Enhancer mutations can result in ectopic or altered gene expression that results in various pathologies depending on the specific gene of interest (Sur et al., 2012) and reviewed (Pennacchio et al., 2013). It has been shown that *MyoD*$^{-/-}$ myoblasts serve as better transplant material in mice than wild type myoblasts (Asakura et al. 2007) and this finding may be applicable to humans with muscle wasting diseases. If *MyoD* can be temporarily transcriptionally repressed during in vitro culture and expansion of patients myoblasts, a useful number of cells can be generated for transplant.

Early knowledge of the upstream transcriptional regulators of *MyoD* expression comes from gross embryonic disruption of signaling centers, such as the notochord, neural tube, and surface ectoderm, impacting BMP, Shh and Wnt signaling pathways. (Reviewed by (Borycki and Emerson, 2000)). Removal of the neural tube from avian embryos causes MyoD expression to end, possibly due to a lack of Wnt signaling (Bober et al., 1994a). Members of the Wnt family of transcriptional activators are expressed in the neural tube, Wnt1 (Tajbakhsh et al., 1998), and surface ectoderm, Wnt7a (Cossu et al., 1996), and these two Wnt factors are shown to activate myogenesis in mesodermal cells. *Sonic Hedgehog* (Shh) is expressed in both the notochord and floorplate of the neural tube and has been shown to be promote myogenesis, while *Shh*$^{-/-}$ embryos exhibit myogenic defects (Marcelle et al., 1999). However, there has been no evidence of direct binding of these factors to the *MyoD* locus. The Wnt and Shh pathways may indirectly control *MyoD* expression.

To define the cis-acting DNA elements directing MyoD expression, transgenic experiments using human sequence of the upstream regions of *MyoD* to drive lacZ or CAT (chloramphenicol acetyltransferase) expression were performed. A transgene containing 24 kb of DNA upstream of the human *MyoD* gene was fused to the CAT gene and its transcriptional activity was tested in 23A2 myoblasts (Goldhamer et al., 1992). CAT was expressed at high levels, and the construct was reduced to smaller fragments to isolate discrete enhancers. A 4 kb portion called Fragment 3 (F3), lying 22 to 18 kb upstream of *MyoD*, directs reporter gene expression almost identically to the entire 24 kb construct. Removal of F3 from the original construct created -24ΔF3CAT, and expression levels dropped to baseline levels (Chen et al., 2001). -24lacZ and -24ΔF3lacZ constructs containing human DNA were also used to generate transgenic mouse embryos for *in vivo* analysis. -24lacZ embryos exhibited reporter gene expression in mouse embryos in a pattern that fully mimics endogenous MyoD mRNA expression (Goldhamer et al., 1992). -24ΔF3lacZ embryos exhibit delays and reduction of reporter expression at all myogenic locations (Chen et al., 2001) while F3lacZ constructs direct reporter gene expression in a manner faithful to *MyoD* mRNA in mouse embryos (Faerman et al., 1995). At the center of F3 is a 258bp element, the core enhancer (CE), largely responsible for the transcriptional activity of F3 (Goldhamer et al., 1995). Similar experiments identified a second enhancer, the distal regulatory region (DRR), 4kb 5' to *MyoD* (Asakura et al., 1995). The CE and DRR share sequence homology between mice and humans, explaining how human noncoding regions are capable of

driving proper expression in mouse embryos. The DRR is 71% identical, and all putative binding sites are preserved (Chen et al., 2001). Mutation of the YY1 and SRF binding sites in the DRR eliminates its enhancer activity *in vitro* (L'Honore et al., 2003). The CE is 87% identical and also maintains binding sites across species (Goldhamer et al., 1995). Transgenic analysis indicates that the CE controls initiation of expression in newly forming myoblasts, while the DRR maintains expression in differentiating muscle. In support of this idea, in *MyoD*$^{-/-}$;*Myf-5*$^{-/-}$ embryos, where no myoblasts form, the CE transgene is active while the DRR is not (Kablar et al., 1999). The drawbacks to these transgenic experiments are that the genomic regions of interest are assayed outside of their normal chromosomal context, and the results show only the sufficiency of these DNA elements in driving transcription of the reporter gene.

The necessity of the CE and DRR has been investigated by deletion of either enhancer from the mouse genome. Deletion of the CE resulted in *MyoD* expression initiating properly in the myotomes, while a 1 day delay of expression was observed in a subset of the hypaxial lineage, specifically the limb buds and branchial arches (Chen and Goldhamer, 2004b). This shows the CE is not necessary for initial activation of MyoD and that the CE controls timely activation in only a subset of myogenic cells. Targeted removal of the DRR resulted in a decrease of MyoD expression at E10 only. In adult muscle, *MyoD* expression continues, but with an approximate 60% reduction in mRNA levels, showing continued MyoD expression in differentiated muscle occurs without the DRR, albeit at reduced levels (Chen et al., 2002).

In summary, 24 kb of human DNA sequence upstream of MyoD can drive high levels of reporter gene expression in myoblasts in vitro and in developing mouse embryos. The same is true for CE and DRR driven transgenes as well. However, when the mouse equivalent of either of these enhancers are deleted, only mild changes in *MyoD* expression are seen. In -24ΔF3lacZ embryos, reporter gene expression shows a much more severe delay in limb expression than does *MyoD* expression in embryos lacking only the CE. Interestingly, there is no delay in branchial arch expression in -24ΔF3lacZ embryos, unlike embryos lacking the CE. These somewhat contradictory findings along with the difference between necessity and sufficiency of these enhancers regions may lie in the species difference between the transgenic and knock out experiments. Another possibility is that in the mouse, the CE and DRR have overlapping or compensatory abilities to regulate *MyoD* expression. The last possibility is that one or more uncharacterized DNA regulatory element exists. The best way to resolve the last two hypotheses is to remove both the CE and DRR on the same chromosome. In this chapter, targeted deletion of the CE was performed in mouse embryonic stem cells lacking the DRR.

A finer point of *MyoD* regulation investigated is the target of *Pax3* dependent rescue of *MyoD* expression. *MyoD* expression in the body is initially *Myf-5* dependent, and there is a delay in *MyoD* expression in *Myf-5* knock out embryos (Tajbakhsh et al. 1997) (Kassar-Duchossoy et al., 2004). *MyoD* expression is eventually rescued through a *Pax3* dependent mechanism, as *MyoD* is not activated in the trunk or limbs of *Myf-5/Pax3* double mutants

(Tajbakhsh et al., 1997). It should be noted however, that in *Pax3* mutant embryos, myogenic progenitors fail to migrate from the somite to the limb, and therefore may not receive the proper signals to activate *MyoD* (Daston et al., 1996b). A lacZ transgene, driven by the CE and promoter of *MyoD* called 258/-2.5lacZ is active in *Myf-5* null embryos and is a target of *Pax3* dependent rescue. Mutation of two, 15bp segments toward the 3' end of the CE results in poor lacZ expression in the trunk in *Myf-5* null embryos (Chen and Goldhamer, 2004a). Taken together, the CE is responsive to the *Pax3* pathway through a 30 bp internal segment. This internal segment is also a target of *Myf-5* activation, due to a lack of lacZ expression in *Pax3* null embryos (Kucharczuk et al., 1999). As mentioned above, the CE is sufficient to drive lacZ expression in either the absence of *Myf-5* or *Pax3*, but the CE is not necessary. The kinetics of *Pax3* dependent *MyoD* expression is the same in wild type embryos or those lacking the CE or the DRR, demonstrating that neither the CE nor the DRR are exclusive targets of *Pax3* dependent rescue of *MyoD* expression (Chen et al., 2002; Chen and Goldhamer, 2004b). Analysis of *MyoD* expression in the new mouse lines lacking both *MyoD* enhancers and *Myf-5* will asses whether there are other elements responsive to the *Pax3* pathway.

In order to fully understand the transcriptional control of *MyoD*, the regulatory regions must be identified and characterized. Because of the conflicting data from lacZ transgenic and knockout experiments in mice regarding the function of each enhancer, a CE and DRR double enhancer knock out line has been created, called $MyoD^{\Delta CEDRR}$. $MyoD^{\Delta CEDRR/\Delta CEDRR}$ embryos are assayed

for their *MyoD* expression profile to uncover any redundant transcriptional control abilities of the enhancers.

Given that 24kb of DNA upstream of MyoD drives transgene expression faithfully, and because other enhancers may exist between the CE and DRR, the 15kb of genomic DNA between the two enhancers, including the enhancer elements themselves, are deleted in a related mouse line named $MyoD^{\Delta CE15DRR}$

The two homozygous mutant lines, $MyoD^{\Delta CEDRR/\Delta CEDRR}$ and $MyoD^{\Delta CE15DRR/\Delta CE15DRR}$ exhibit the same MyoD expression profile as CE single knockouts, aside from a slight myotomal delay in expression. This shows at least one unknown enhancer exists, and it does not lie in the 15 kb of genomic DNA between the two enhancers. $MyoD^{\Delta CE15DRR/\Delta CE15DRR}$ and $MyoD^{\Delta CEDRR/\Delta CEDRR}$ embryos also exhibit the same kinetics of *Pax3* dependent rescue of *MyoD* expression as wild type embryos.

Knowing that other enhancers are controlling almost all aspects of embryonic *MyoD* expression, a computer database search was performed in an effort to identify evolutionarily conserved sequences and active histone modifications in the 2Mbp surrounding the *MyoD* locus. The results implicate the introns of *MyoD* as possible enhancers due to conservation across species, positive epigenetic modifications, and numerous binding sites for relevant transcriptional activators.

3.3 Materials and Methods:

MyoD CE targeting vector creation

All plasmid backbones are pBluescript II SK+ (Stratagene). A floxed (flanked by loxP sites) PGKNeo cassette was excised from the plasmid, ploxP-neo-1 (provided by Dr. Marissa Bartolomei) via EcoRI (5' end) and XhoI (3' end) double restriction enzyme digest. The resulting overhangs were filled in by Klenow (New England Biolabs cat# M0212S). This fragment was inserted and ligated in reverse orientation between two FRT sites in the loxP2-FRT2/BSIIPSK plasmid (provided by Dr. Mazakazu Yamamoto), previously blunt end linearized by EcoRV.

The FRT-loxP-PGKneo-loxP-FRT (FLneoLF) portion of the plasmid was removed via NotI and EcoRI sequential digests and inserted into p5'enh3'EB (created by Dr. Jennifer Chen (Chen and Goldhamer, 2004b)). This plasmid contains 7.3 kb of mouse genomic DNA containing the CE. The 258 bp core enhancer fragment was excised by BamHI and EcoRI sequential digests. The FLneoLF fragment was inserted and ligated into the space previously occupied by the CE, and was flanked by 3.7kb of genomic DNA on the 5' (upstream) side and 3.6kb on the 3' (downstream) side. The resulting ligation product was called p5'FLneoLF3'. A thymidine kinase (tk) cassette was added to the 3' end of p5'FLneoLF3' at the XhoI site.

The plasmid, p5'FLneoLF3'tk, was grown in NM544 electrocompetent bacteria and the plasmid was isolated using Qiagens EndoFree Maxi Kit, as per manufacturers' instructions.

Mouse chimera creation

The targeting vector was linearized by NotI and suspended in TE at a concentration of 1µg/µl and delivered to the University of Connecticut Health Center (UCHC) Gene Targeting and Transgenic Facility (GTTF) for electroporation into a custom line of mouse embryonic stem cells. The targeting of the core enhancer for homologous recombination occured on a chromosome already lacking the DRR. The GTTF created a hybrid ESC line by crossing mice lacking the DRR, maintained on a 129SvJ background, with 129SvEv mice. Blastocysts were collected to create the new ESC line. The CE targeting vector's homology arms come from the 129SvJ strain, with the intended purpose of enhanced targeting of the correct chromosome.

ESC clones were screened for proper recombination via BclI digest and Southern blot on the 5' side. The southern probe was PCR amplified from mouse genomic DNA using the forward primer 5'-GGCGGATCC TGAACAAAAGGGGATGAGATTCC-3' and reverse primer 5'-CGCGAATT CAGGAACCACCCTAAAGATCCACC-3'. The resulting fragment was subcloned in pBS SK+ plasmid.

The 3' end of the recombination event was assayed by nested long range PCR. The external PCR primer sequences are 5'-AGTAGAAGGTGGC GCGAAGG-3' and 5'-TCAAGCCGGCCACCATAAAG-3'. The internal PCR primers are 5'-TCATTCAGGAGAGCCTTTGTT-3' and 5'-TGGATGTGGA ATGTGTGCGAG-3'. The final amplicon is 4.6 kb in length. The Invitrogen Elongase system (cat # 10480-010) was used for long range PCR.

Mouse breeding

Chimeric mice were received from the UCHC GTTF and selected for breeding based on coat color composition as an indication of targeted cell contribution to the chimeric mice. Chimeras were mated with FVB (albino) mice in order to generate offspring with colored coats indicative of germline transmission. These pups were genotyped via tail snips, DNA isolation and PCR for both the CE^{Neo} and DRR^{loxP} alleles. Successful germline transmission also demonstrated if the correct chromosome was targeted such that if both alleles travel together , the correct chromosome was targeted.

CE^{Neo} male mice were crossed with HprtCre females (Jax stock #004302) and R26Flpe females(Jax stock #003946) to generate $MyoD^{\Delta CE15DRR/+}$ and $MyoD^{\Delta CEDRR/+}$ mice, respectively. Offspring harboring the recombined CE locus were interbred for expansion of stock animals and for staged collection. Timed matings were set up at night, with noon following the morning of a vaginal plug

considered E0.5. The separate knock out lines were also mated to Myf-5^{Neo} (S. Tajbakhsh) mice in order to create double heterozygous mice.

Embryo harvesting and staging

Pregnant female mice were sacrificed following IACUC approved protocols. Mice were anesthetized before cervical dislocation. The uterus was removed and placed into dishes filled with RNAse free PBS. Individual embryos were collected and placed into 2% PFA in PBS overnight at 4^{o}C on a shaker.

PCR analysis of genomic DNA from tail snips and embryo yolk sacs

The yolk sacs from each embryo were placed in 1.5ml tubes followed by Proteinase K digestion. The next day, DNA was purified via diatomaceous earth extraction.

PCR primers used for genotyping:

MyoD$^{\Delta CE15DRR}$ forward 5'- CTTGGAACCACACTACCTCAAGG-3' reverse 5'- CCAGA TAGATGTCTCCCAGGCTTG-3' to create 350 bp product

MyoD$^{\Delta CEDRR}$ forward 5'- CTTGGAACCACACTACCTCAAGG-3'

reverse 5'- GTTCCTCTCATGCCTGGTGTTTAGG-3' to create a 230 bp product

Myf-5Neo forward 5'-CGTTGGCTACCCGTGATATT-3' and reverse 5'-CAGCTCAGCTTTGTGTGCTC-3'to create a 670bp product.

Myf-5 Wild type forward 5'-TGAAGGATGGACATGACGGAC-3' and reverse 5'-TGACCTTCTTCAGGCGTCTACG-3' to create a 300bp product

DIG-labeled RNA probe creation for in situ hybridization

The plasmid, mMyoD-MS/BSIIPSK, contains the 3' portion of the MyoD cDNA, and was provided by Dr. Masakazu Yamamoto. The cDNA portion of the plasmid was PCR amplified using standard conditions, and used the M13 forward and reverse primers. The PCR product was run on an agarose gel. The product band was cut from the gel and purified, using the Macherey-Nagel NucleoSpin Gel and PCR clean-up kit, as per manufacturers instructions (ref # 740609.10). The purified product was PCR amplified as previously stated and repurified.

Digoxigenin labeled mRNA was created using the purified PCR product as the template, with a labeling kit by Roche (cat # 11 277 073 910) and using T3 and T7 polymerase to generate sense and anti-sense probes.

In situ hybridization for MyoD transcripts

Gentle rocking of embryos occurred during all following incubations. Embryos were fixed in 2% paraformaldehyde in PBS at 4℃ overnight. Embryos were rinsed and dehydrated in a gradient of methanol mixed with PBT (PBS with 0.1% Tween) (25%, 50%, 75% and 100% methanol) for 10 minutes each. Embryos were stored at -20℃ in 100% methanol until needed. Embryos were

returned to room temperature and rehydrated in a reverse gradient in methanol and PBT. For better probe penetration, embryos were digested in 10µg/ml ProteinaseK/PBT for 20 minutes, rinsed in PBT, then fixed in 0.2% glutaraldehyde/4% paraformaldehyde/PBT for 20 minutes. Following rinses in PBT, embryos were incubated in a 1:1 mix of PBT and prehybridization buffer, followed by 100% prehybridization buffer for over 1 hour (minimum 2 hours yielded best results) at 70°C. The prehybridization buffer is composed of 50% formimide, 5xSSC, 2%SDS, 2% Roche Blocking Reagent (cat#11096176001), 250µg/ml yeast tRNA, 100µg/ml heparin, in RNase free H_2O. Digoxygenin labeled RNA probe was then added to a concentration of .25µg/ml and incubated at 70°C overnight.

Embryos were washed in SolutionX (50% formamide, 2XSSC, 1% SDS) 5 times, 20 minutes per wash, at 70°C. Embryos were then incubated for 20 minutes as 70°C in a 1:1 mix of SolutionX and MABT (for 50ml of MABT mix .29g maleic acid, .218g NaCl, .5ml 10% Tween20, and H_20 to make 50 ml and adjusted pH to 7.5 with NaOH). Embryos were then washed 4 times at 5 minutes per wash in MABT at room temperature.

Embryos are incubated in 2% Roche Blocking Reagent (cat #11096176001) in MABT for 30 minutes at room temperature. Continue with a two hour room temperature block in 2% Roche Blocking Reagent/20% Fetal Bovine Serum in MABT. Anti-Digoxygenin-AP Fab were then added to a 1:2000 dilution and incubated at least 1 overnight (2 overnights gives best result) at 4°C.

Following incubation with the anti-DIG antibody, embryos were washed four times, at 1 hour per wash in MABT, followed by an overnight wash in MABT, all at room temperature.

Wash embryos in NTMT (100mM NaCl, 100mM TrisCl pH 9.5, 20mM $MgCl_2$, 0.2% Tween 20) three times, ten minutes per wash at room temperature. Replace NTMT with BM Purple (cat #11442074001) and develop color to appropriate level, usually 6-8 hours. After color development level is reached, rinse embryos in NTMT several times to minimize precipitate formation, then continue rinsing in PBT.

Embryo imaging

Whole mount images were taken using a Lecia MZ FLIII. Images were captured using a Spot 25.2 2 Mp Color Mosaic camera using Spot Software V4.6 by Diagnostic Instruments. Images were modified using Photoshop CS2.

3.4 Results:

3.4.1 Targeting the Core Enhancer for deletion:

To define the compensatory abilities of the CE and DRR or to provide data that uncharacterized enhancers exist, the CE was targeted for deletion in mouse embryonic stem cells (ESCs) already lacking the DRR. ESCs were created by the UCHC through mating male DRR^{loxP} male mice, maintained on a 129SvJ genetic background, to the cell culture friendly strain, 129SvEv. Blastocysts created form the mating were collected to create the new ESC line. The targeting vector, p5'FLNeoLF3'tk, was created to precisely replace the 258bp CE with a Neomycin resistance gene, flanked by loxP sites, all of which was flanked by FRT sites (Fig 3-1A). The presence of two different recombinase targets allows for creation of two different lines from the same targeting event, described below. The homology arms of the targeting vector originated from the 129SvJ strain to increase efficiency of targeting the correct chromosome by sequence similarity. Homologous recombination was assayed by southern blot on the 5' side and long range nested PCR on the 3' side (Fig. 3-1B and C).

Following germline transmission of the targeted locus, male offspring were mated with both $R26^{Flp}$ and $Hprt^{Cre}$ females to produce two different lines via recombination. Flippase dependent recombination (Schaft et al., 2001) removes the floxed Neo cassette, leaving a transcriptionally inert FRT site, creating the new line lacking both the CE and DRR, $MyoD^{\Delta CEDRR/+}$. Cre

recombination (Nagy, 2000) of the *MyoD*^{CENeo} allele when located on a *DRR*^{loxP} chromosome, results in removal of the 15kb of DNA from the 5' end of the Neo cassette to the 3' end of the former site of the DRR, called *MyoD*$^{\Delta CE15DRR/+}$ (Fig 3-2A and B). The new lines were expanded by mating with FVB mice. Heterozygous and homozygous mutant mice were all equally viable.

3.4.2 MyoD mRNA expression in *MyoD*$^{\Delta CEDRR/\Delta CEDRR}$ embryos

In order to observe the effect on MyoD expression patterns when both known enhancer elements were removed, *MyoD*$^{\Delta CEDRR/+}$ mice were intercrossed, and embryos from pregnant females were collected between E9.5 and E12.5. Noon following the morning of vaginal plug detection was considered E0.5 for staging purposes. Whole mount in situ hybridization was performed to visualize *MyoD* transcripts. Successful validation of the probe and the sense control probe, a sequence that is identical to *MyoD* mRNA and should not produce a specific signal is shown in Fig 3-3.

Comparisons between wild type and heterozygous embryos show no phenotypic difference, meaning haploinsufficiency is not an issue and allows for heterozygous embryos to be used as a reference point in some figures (Fig 3-4).

Figure 3-1 A

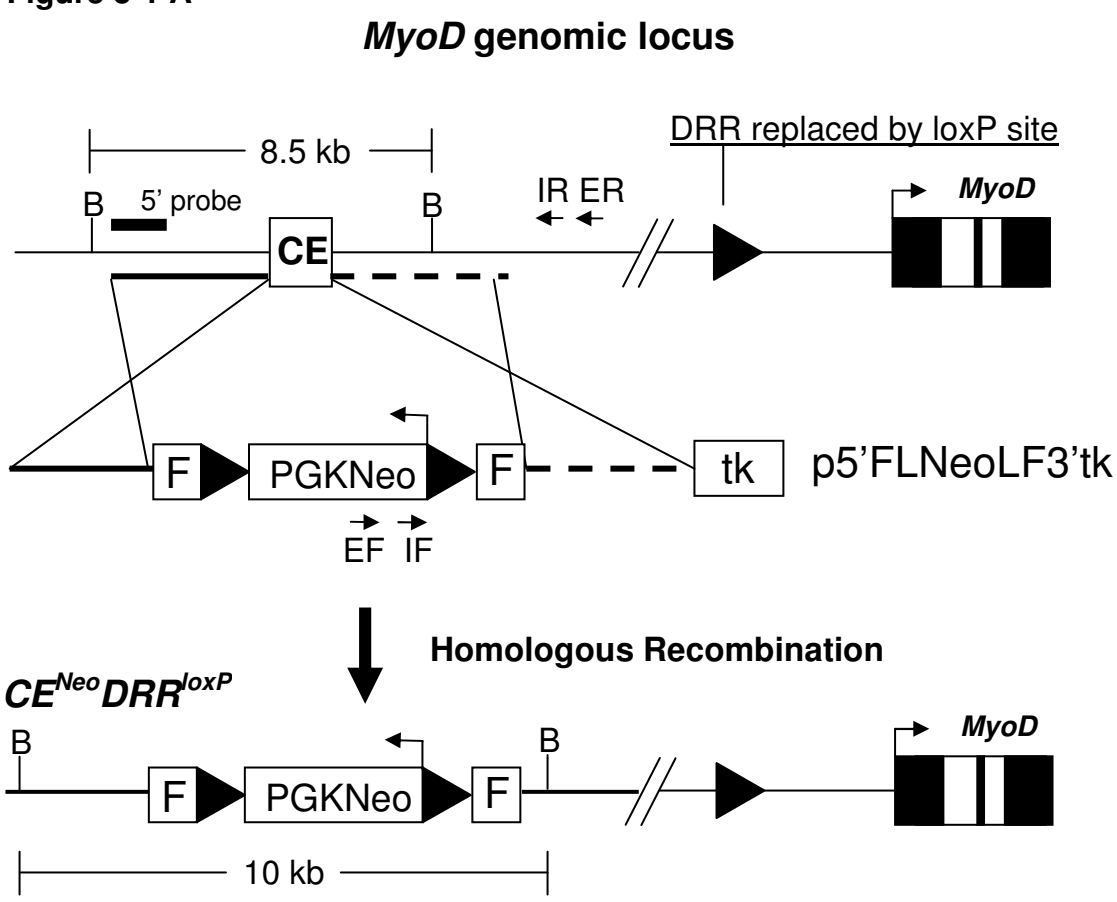
MyoD genomic locus
8.5 kb
DRR replaced by loxP site
B
5' probe
B
IR ER
MyoD
CE
F
PGKNeo
F
tk
p5'FLNeoLF3'tk
EF
IF
Homologous Recombination
CE^{Neo}*DRR*^{loxP}
B
B
MyoD
F
PGKNeo
F
10 kb

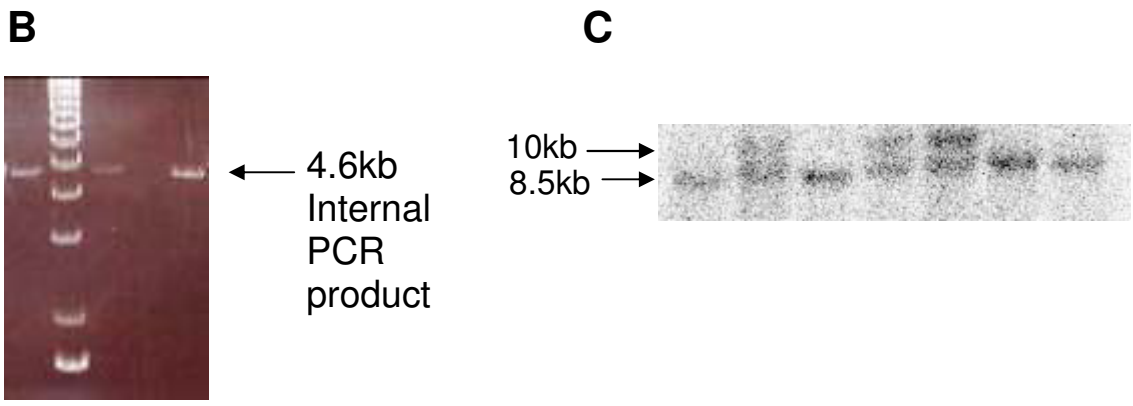
B
C
4.6kb
Internal
PCR
product
10kb
8.5kb

Figure 3-1. Targeting the Core Enhancer for deletion

The 258bp Core Enhancer lies approximately 22 kb upsteam of the *MyoD* locus and was targeted for precise removal by the targeting vector, p5'FLneoLF3'tk. The targeting vector contains a 3.7kb 5' homology arm, ending at the EcoRI site 5' of the CE, and a 3.6kb 3' homology arm, that ends at the XhoI site 3' of the CE. After homologous recombination, the CE is replaced by a PGKNeo cassette flanked by loxP and FRT sites, in reverse orientation in respect to the transcriptional orientation of *MyoD*. Desired recombination on the 3' side was assessed via long range nested PCR, where 3 of the four lanes show the targeted 10kb band size along with the wild type 8.5kb band (Fig 3-1B). Detection of proper recombination was carried out on the 5' end by BclI digest and southern blot using the DNA probe depicted. Fig. 3-1C shows correctly targeted clones in lanes 2, 4 and 5.

Figure 3-2A

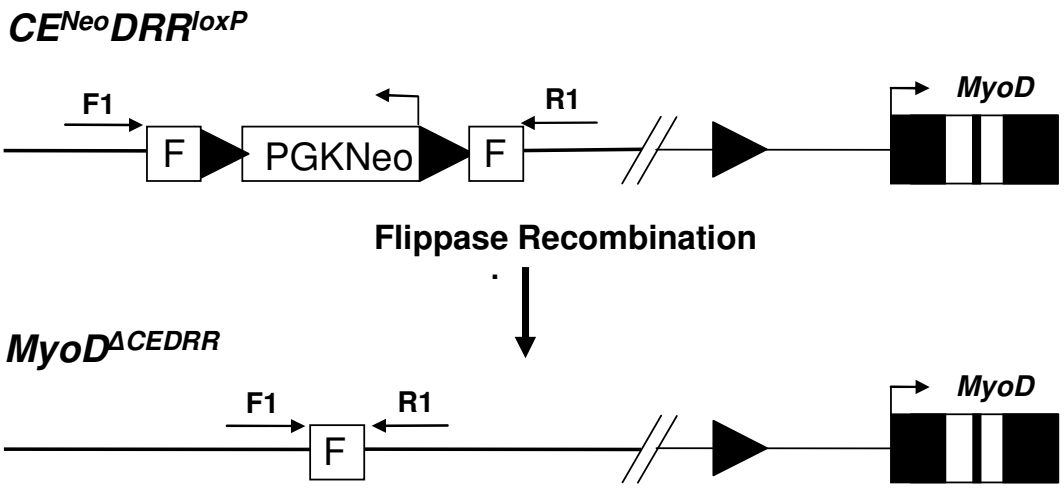

Figure 3-2B

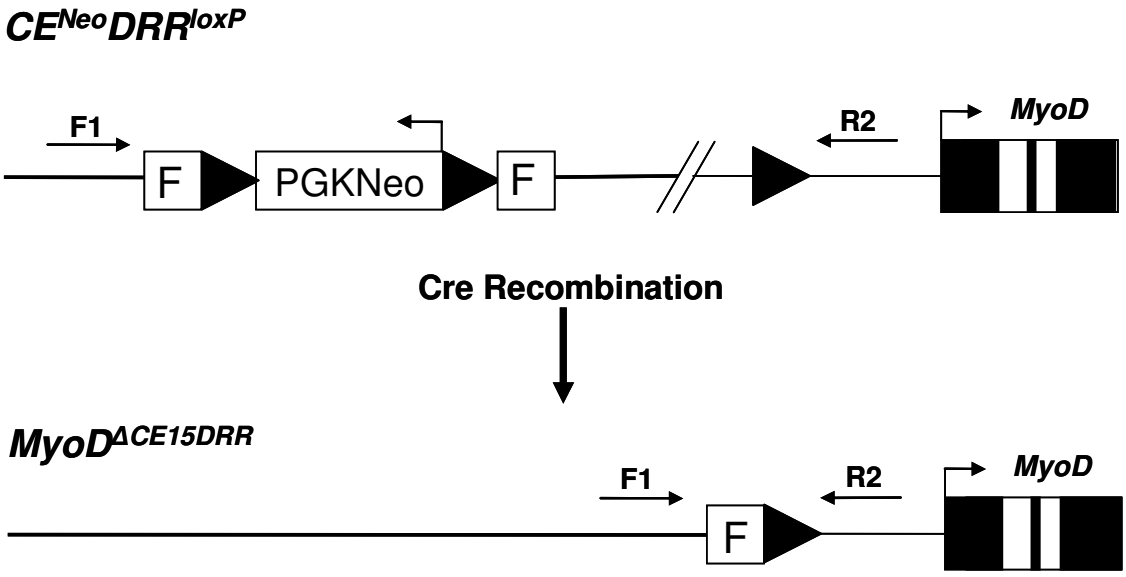

Figure 3-2. Creation of *MyoD*$^{\Delta CEDRR}$ and *MyoD*$^{\Delta CE15DRR}$ mice

Following germline transmission of the *CE*^{Neo} allele, two different recombination events need to take place to create the two new mutant lines. *CE*^{Neo} male mice were mated with R26Flpe female mice to recombine out the PGKNeo cassette, creating the *MyoD*$^{\Delta CEDRR/+}$ line (Fig 3-2A). Appropriate recombination was assessed via PCR using primers F1 and R1, that generate a 210 bp band if recombination took place, while non recombinant alleles would generate an approximate 430bp fragment.

CE^{Neo} male mice crossed with *HprtCre* females to produce the *MyoD*$^{\Delta CE15DRR/+}$ line. Proper recombination was assessed via PCR using primers F2 and R2, to create a 350bp product if recombination took place, and no product if recombination did not take place as the primers lie approximately 15kb away from each other in the genome.

Figure 3-3

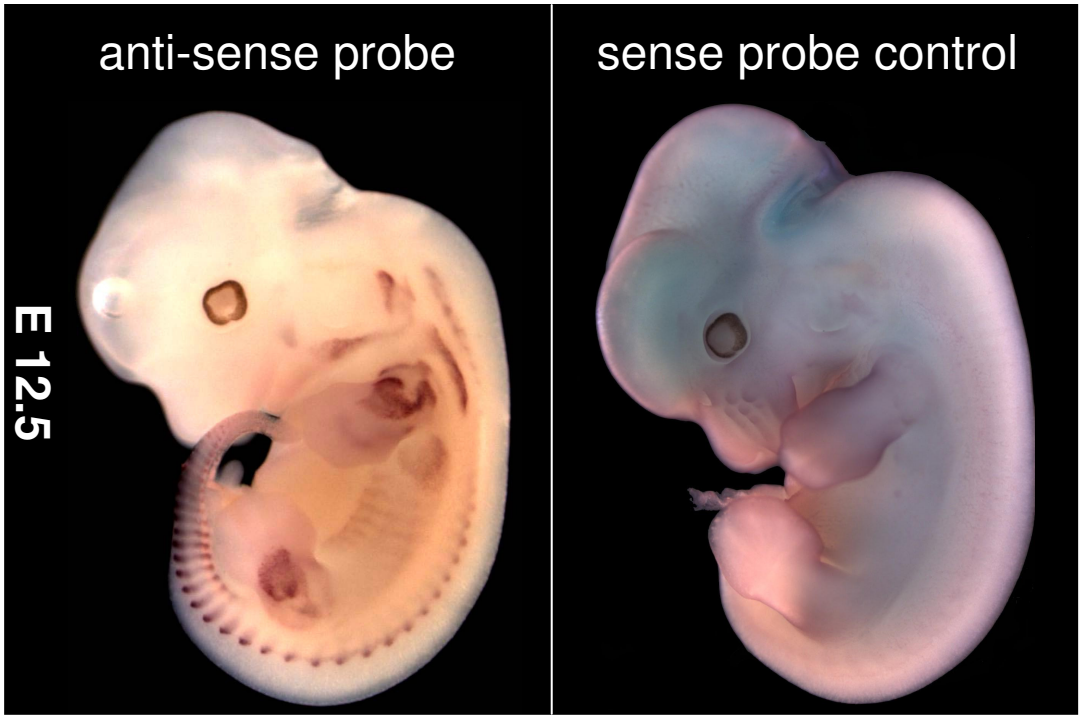

Figure 3-3. Validation of *MyoD in situ* probe

E12.5 littermate embryos hybridized with either the sense or anti-sense RNA probe to detect endogenous *MyoD* mRNA. The antisense probe complimentary base-pairs with *MyoD* transcripts and produces the expected signal profile. The sense probe RNA sequence is identical to *MyoD* transcripts and serves as a control against non specific binding of the anti-sense probe or hybridization to genomic DNA. Note the lack of and real signal, with only minor background, in the sense probe panel.

Figure 3-4

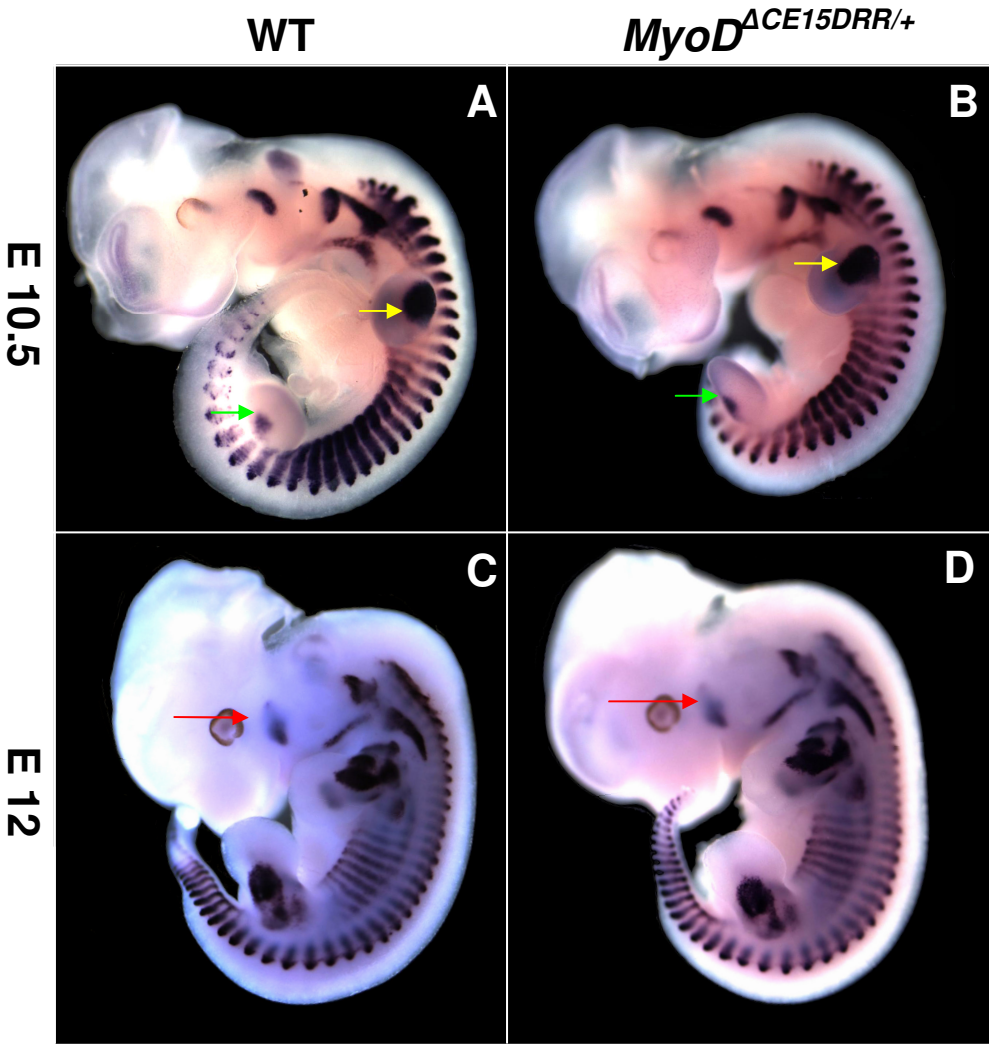

Figure 3-4. *MyoD*$^{\Delta CE15DRR}$ heterozygote and Wild Type *MyoD* mRNA profiles

In situ hybridization for *MyoD* transcripts of heterozygous *MyoD*$^{\Delta CE15DRR/+}$ embryos was compared to wild type embryos to asses any haploinsufficiency. E10.5 (A and B) and E12.5 (C and D) embryos showed no significant differences in timing or intensity of expression between heterozygous and wild type embryos. In panels A and B, the yellow arrows indicate the forelimb buds and the green arrows indicate the hindlimb buds. In panels C and D, the red arrows indicate the branchial arches.

A comparison of *MyoD*$^{\Delta CEDRR/\Delta CEDRR}$ and wild type embryos between E9.5 and E12.5 shows that the CE and DRR are not the only enhancers of *MyoD* and they do not compensate for each other when one is absent. Generally, the phenotype in *MyoD*$^{\Delta CEDRR/\Delta CEDRR}$ embryos is a combination of *CE*^{loxP} and *DRR*^{loxP} single knock out phenotypes, described previously (Chen et al., 2002) (Chen and Goldhamer, 2004b). At the onset of *MyoD* expression in the myotome and branchial arches at E9.5, *MyoD* expression is absent in both areas in the mutant embryos (compare Fig 3-5A to 3-5E). The lack of early myotomal expression is the only significant phenotypic difference between *MyoD*$^{\Delta CEDRR/\Delta CEDRR}$ mutant embryos and either *CE*^{loxP} or *DRR*^{loxP} single mutants. In either single knock out, the timing of myotomal *MyoD* expression is identical to wild type embryos (Chen et al., 2002; Chen and Goldhamer, 2004b). It can now be said that timely activation of myotomal *MyoD* expression is dependent on either the CE or DRR being present. By E10.5, the epaxial signal has largely recovered, with only a mild reduction in signal intensity in the mutant embryos similar to *DRR*^{loxP} embryos. The hypaxial lineage that gives rise to muscle beds in the limb buds and branchial arches still exhibits a pronounced delay, with no signal in limb buds of *MyoD*$^{\Delta CEDRR/\Delta CEDRR}$ embryos at E10.5(Fig 3-5 B and F). At E11.5, *MyoD* expression is largely identical between wild type and mutant embryos, with a slight delay in hindlimb expression in the mutants (Fig 3-5 C, G). The expression profile of *MyoD* eventually recovers in mutant embryos by E12.5 (Fig 3-5 D and H) and is nearly indistinguishable to wild type embryos.

Figure 3-5

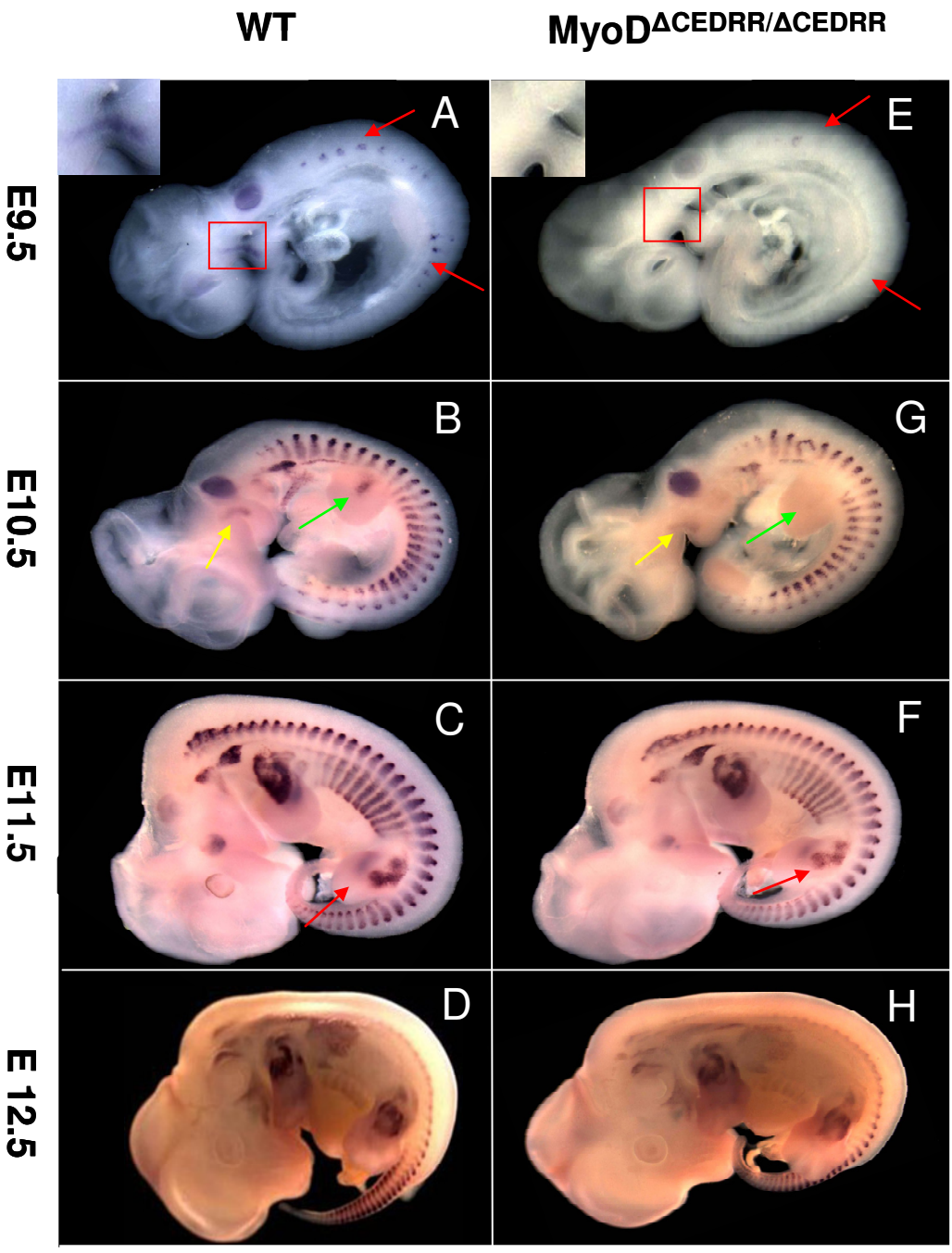

Figure 3-5. Timeline of *MyoD* expression in *MyoD*$^{\Delta CEDRR/\Delta CEDRR}$ and wild type embryos

Whole-mount *in situ* hybridization for *MyoD* mRNA in WT embryos (A-D) and litter mate *MyoD*$^{\Delta CEDRR/\Delta CEDRR}$ embryos (E-H). At E9.5, (A and E) branchial arch expression is present in the wild type embryo and absent in the mutant, as seen in the magnified areas (red boxes). Red arrows indicate early myotome expression in the wild type embryo (A) that is absent in the mutant embryo (E). At E10.5, branchial arch expression (yellow arrow) still lags in mutants. Forelimb signal (green arrows) is present in wild type (B) embryos and lacking in mutant embryos (F). E11.5 forelimb expression is similar between (C) and (G), while hindlimb expression, red arrows, still lags in the mutant. By E12.5, (D and H) embryos have nearly identical expression patterns, although the expression level is slightly reduced in the mutant.

3.4.3 *Pax-3* dependent rescue of *MyoD* expression is independent of the CE and DRR

In the absence of *Myf-5*, *MyoD* expression is delayed in the myotome by approximately 2 days, with no effect on the hypaxial lineages (Tajbakhsh et al., 1997). The factor that rescues *MyoD* expression in *Myf-5* mutants is *Pax3*. In the absence of *Pax3*, limb myogenesis fails, as myogenic progenitors can't migrate from the somite to the limb due lack of activation of downstream target genes, such as *c-met* (Bober et al., 1994b) (Daston et al., 1996a). Embryos lacking both *Myf-5* and *Pax3* fail to activate *MyoD* in the body, due to the dependence of either gene to activate transcription of *MyoD*. *MyoD*$^{\Delta CEDRR/+}$;*Myf-5*$^{Neo/+}$ mice were intercrossed to create *MyoD*$^{\Delta CEDRR/\Delta CEDRR}$;*Myf-5*$^{Neo/Neo}$ embryos in order to determine if the CE and DRR are the only elements responsive to *Pax3* dependent activation. E11.25 embryos lacking only *Myf-5* exhibit the early stages of *Pax3* dependent myotomal *MyoD* expression (Figure 3-6 A,B). In *MyoD*$^{\Delta CEDRR/\Delta CEDRR}$;*Myf-5*$^{Neo/Neo}$ embryos at this stage, myotomal expression is nearly identical to *Myf-5*$^{Neo/Neo}$ embryos. The delay observed in limb expression is due only to the absence of the CE and DRR. By E12.5 (Figure 3-6 C-E), *Pax3* dependent *MyoD* rescue is complete, even with the absence of known *MyoD* enhancers.

3.4.4 The 15kb of DNA between the CE and DRR is not involved in embryonic transcription of *MyoD* or in *Pax3* dependent expression

The results from the discrete enhancer knock outs show that at least one other enhancer exists. This was a possible result, so the targeting vector was designed to allow for precise removal of the CE and DRR, but also for removal of the genomic sequence between the CE and DRR.

In the new line, called $MyoD^{\Delta CE15DRR}$, both the CE and DRR are absent, along with the intervening DNA. The expression profile of homozygous embryos is identical to the that of embryos lacking only the CE and DRR (compare Figures 3-5 to 3-7). The delay and eventual recovery of *MyoD* expression in the hypaxial lineage mirrors that of $MyoD^{\Delta CEDRR/\Delta CEDRR}$ embryos.

We also investigated whether *Pax3* dependent rescue of *MyoD* expression occurs though the sequence between the CE and DRR. Figure 3-8 shows the same delay and rescue kinetics of MyoD expression exists in $MyoD^{\Delta CE15DRR/\Delta CE15DRR}$;$Myf\text{-}5^{Neo/Neo}$ as in $Myf\text{-}5^{Neo/Neo}$ embryos.

Figure 3-6

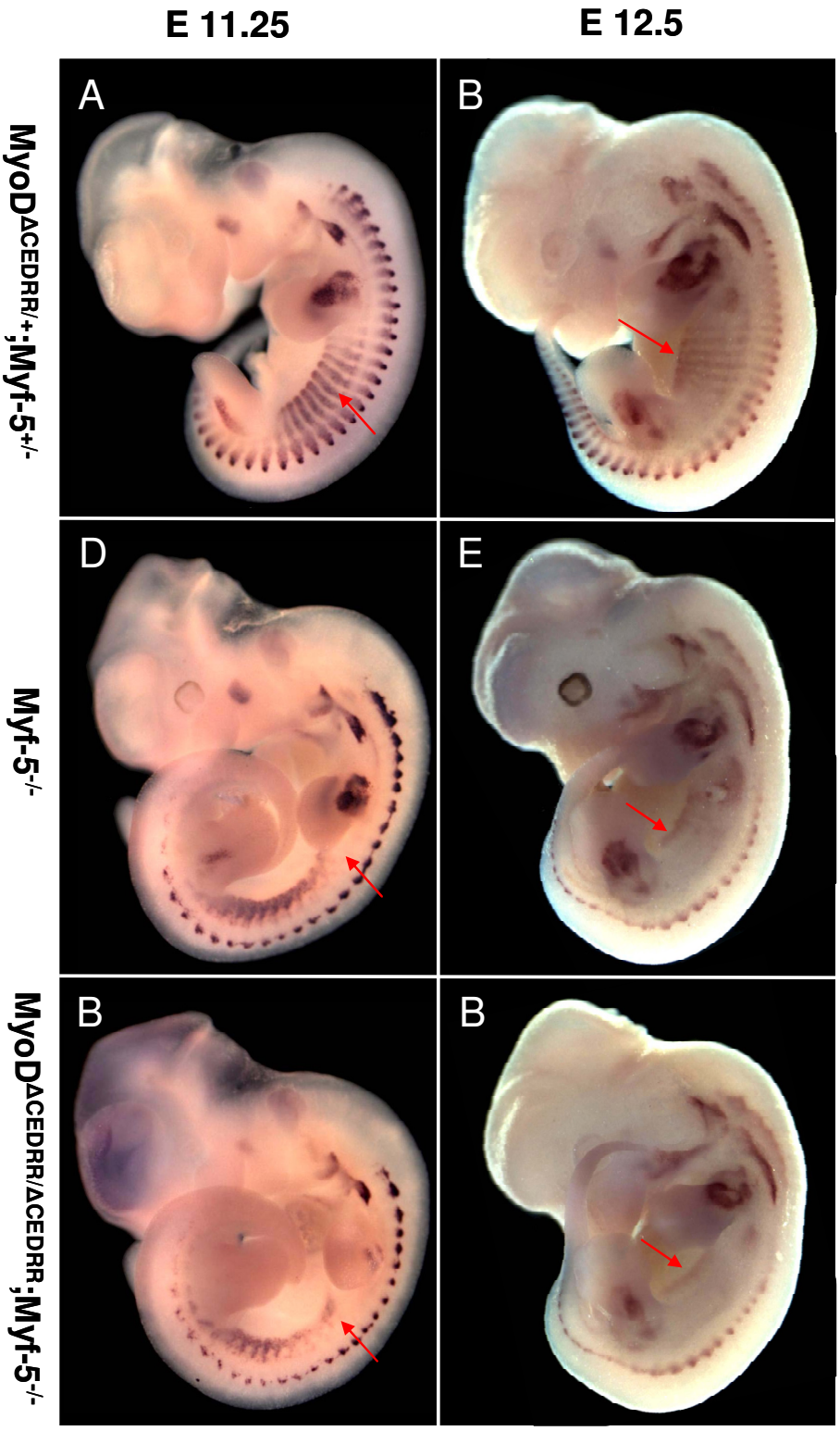
E 11.25
E 12.5
MyoD^ΔCEDRR/+;Myf-5^+/-
Myf-5^-/-
MyoD^ΔCEDRR/ΔCEDRR;Myf-5^-/-
A
B
D
E
B
B

Figure 3-6. Removal of the CE and DRR does not affect *Pax3* dependent rescue of *MyoD* expression

At E11.25 (A-C) early rescue of myotomal *MyoD* expression is underway in *Myf-5*$^{Neo/Neo}$ and *MyoD*$^{\Delta CEDRR/\Delta CEDRR}$;*Myf5*$^{Neo/Neo}$ embryos (red arrows). Delay of *MyoD* expression in limb buds and branchial arches is due to the lack of the CE and DRR, and does not reflect the absence of *Myf-5*. By E12.5 (D-F), the myotomal expression of *MyoD* is similar between *MyoD*$^{\Delta CEDRR/\Delta CEDRR}$;*Myf5*$^{Neo/Neo}$ and *Myf5*$^{Neo/Neo}$ embryos. The aberration in expression in the trunk is due to the rib defect seen in *Myf-5*$^{Neo/Neo}$ only embryos (compare D and E, red arrows).

Figure 3-7

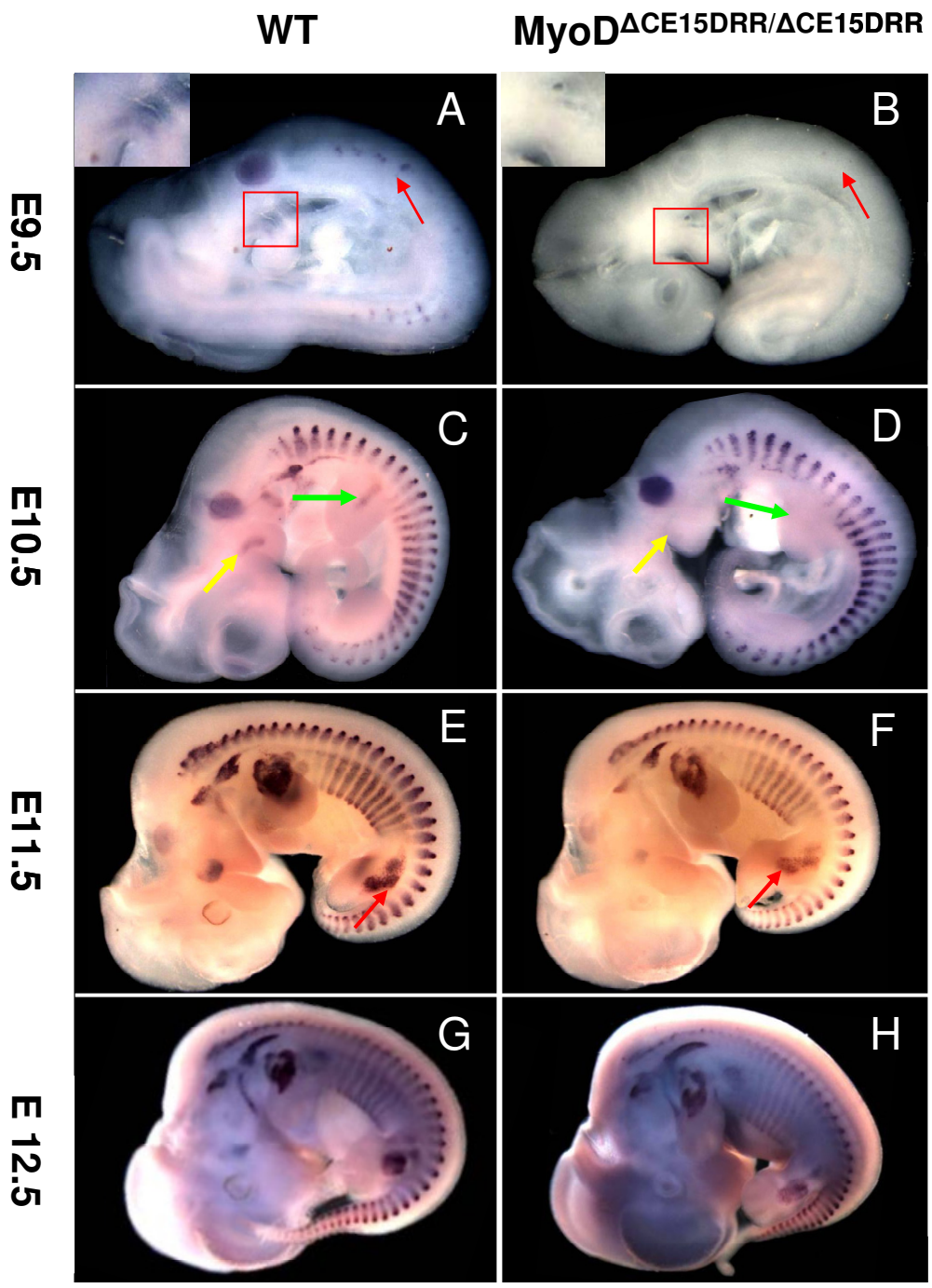

Figure 3-7. Whole mount in situ hybridization for *MyoD* mRNA in *MyoD*$^{\Delta CE15DRR/\Delta CE15DRR}$ and wild type embryos

Wild type embryos (A-D) are compared to *MyoD*$^{\Delta CE15DRR/\Delta CE15DRR}$ embryos (E-H). Red panels in A and D indicate zoomed in areas showing either a presence or absence of *MyoD* signal in the branchial arches. In B and E, branchial arch staining (yellow arrows) is present in the mutant embryo, but is not as advanced as the wild type embryo. Green arrows show the delayed activation of MyoD in the forelimb buds. By E11.5, (C and G), mutant embryos largely mimic the wild type expression pattern. There is less expression in the hindlimbs (red arrow) in mutants than in wild type embryos. At E12.5 (D and H), expression is similar in both embryos.

Figure 3-8

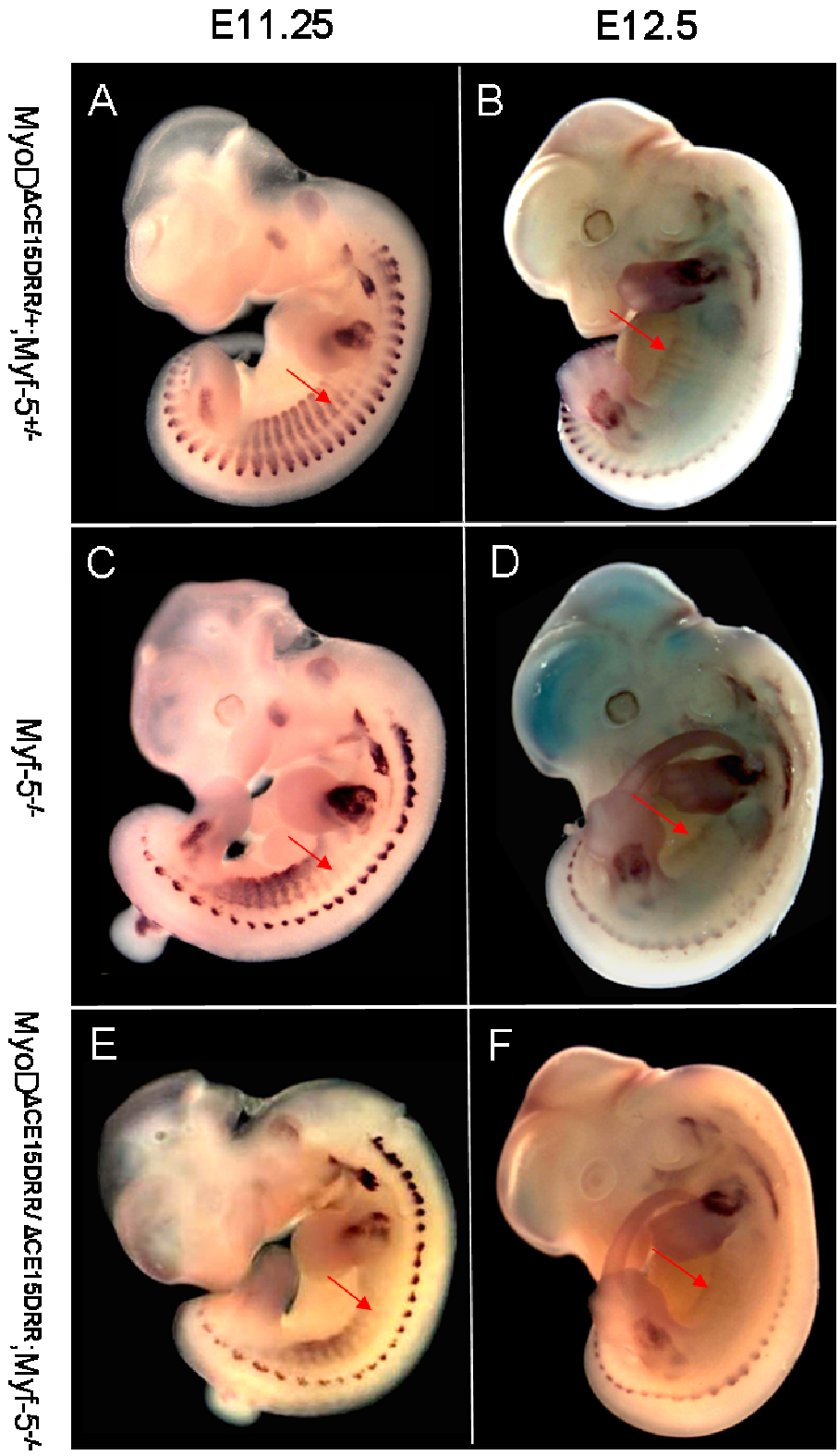
E11.25
E12.5
A
B
C
D
E
F
MyoDΔCE15DRR/+;Myf-5+/-
Myf-5-/-
MyoDΔCE15DRR/ΔCE15DRR;Myf-5-/-

Figure 3-8. *Pax3* dependent *MyoD* expression occurs normally in *MyoD*$^{\Delta CE15DRR/\Delta CE15DRR}$ embryos

At E11.25 (A-C) early myotomal *MyoD* expression in MyoD$^{\Delta CE15DRR/\Delta CE15DRR}$ embryos is identical to embryos with or without the CE and DRR. Limb bud expression differences (B and C versus A) result from the absence of the CE, DRR and intervening sequence. Myotomal expression, dependent on *Pax3* (compare B and C) are identical (red arrows). At E12.5, myotomal *MyoD* expression is nearly identical between *MyoD*$^{\Delta CE15DRR/\Delta CE15DRR}$ and wild type embryos(D-F). The only difference in myotomal expression is due to the *Myf-5*$^{Neo/Neo}$ genotype (red arrows) that causes rib defects involving intercostal muscles.

3.4.5 Genome Database Analysis

The lack of dramatic phenotypes in *MyoD*$^{\Delta CEDRR/\Delta CEDRR}$ and *MyoD*$^{\Delta CE15DRR/\Delta CE15DRR}$ embryos led us to search for enhancer regions using database analysis. Two million bases, centered on the *MyoD* locus, were analyzed for conservation of DNA sequence among mammals (rat, dog, human, orangutan, and horse), a marsupial (opossum), the chicken, and the stickleback fish. Active chromatin markers from C2C12 myoblasts were also considered in the search for enhancer elements.

The Genome Browser, created at The University of California, Santa Cruz, allows for integration of genome data from various groups. We looked for sequence conservation across a number of species, as this is a strong indicator of important sequences. The CE and DRR were known to be conserved between humans and mice, and they are highly conserved among most mammals analyzed (Figure 3-10 A and B). Included in the analysis was the level of mono-, di-, and tri-methylation of the protein tail of histone 3, lysine 4 (H3K4) in the C2C12 cell line. This specific epigenetic marking is indicative of active chromatin, and forced methylation of H3K4 leads to gene activation (Snowden et al., 2002; Towbin et al., 2012). H3K4 methylation is also a strong epigenetic indicator of enhancers (Bernstein et al., 2006). Specifically, H3K4 di and tri-methylation have been proven to mark active enhancers (Pekowska et al., 2011). Using a myoblast cell line gives more relevant data about portions of the genome available for transcription factor binding, and thus transcriptional control.

In the 2 million bases flanking *MyoD*, we found no evolutionarily conserved sequences that were also highly methylated outside of protein coding genes. Some of the conserved genes have active histone modifications, while many did not. The heavily methylated, conserved genes, such as *Emp3*, and *Gys1*, are both expressed in muscle cells. *Emp3* is involved in cell proliferation and *Gys1* encodes a metabolic gene, glycogen synthase (Villarroel-Espíndola et al., 2013). The locally non-methylated, conserved genes encode proteins involved in various non-myogenic organ systems, such as *Otog*, a gene involved in inner ear development (Schraders et al., 2012).

Sequence conservation in non-protein coding regions of the genome indicates important regions that can contain regulatory elements. The four MRFs likely arose from gene duplication and divergence during evolutionary history (Dermitzakis and Clark, 2001). *Myf-5* has high sequence and functional similarity to *MyoD*, and *Myf-5* has important enhancers in its introns (Carvajal et al., 2001). The idea that intronic enhancers may exist for *MyoD* is supported by unpublished observations by Masakazu Yamamoto. In a targeted mutation creating a new *MyoD* allele, the exons and two introns of *MyoD* are flanked by loxP sites, followed by the GFP gene. Following Cre recombination, the *MyoD* gene is removed, and GFP should be driven by the local enhancers. However, GFP expression does not occur in myogenic regions of the embryo, perhaps due to the removal of intronic enhancers. The $MyoD^{iCre}$ allele, used in the previous chapter, shows robust activity in myogenic cells. However, this allele only removes exon 1 and the first 42 nucleotides of intron 1 (Kanisicak et al., 2009).

Interestingly, sequence analysis of *MyoD* shows the highest levels of H3K4 tri-methylation occurring in intron 1. There are also several short regions in intron 1 that are evolutionarily conserved across several mammalian species (Fig 3-9).

Intronic sequences were compared for any similarity between *MyoD* and *Myf-5*, and no significant similarities were found (data not shown). However, transcription factor binding sites, based on sequence only, are plentiful in intron 1 of *MyoD*, and many of these motifs are present in intron 2 (http://jaspar.genereg.net/). Binding sites of interest include Klf4, Sp1, En1, Ap1, Pax2, Sox 5, 10, and 17. Klf4 is an indicator of stem cell like capacity in hESC cultures and is used in formation of induced pluripotent stem (iPS) cells (Tahmasebi et al.). Sp1 is known to regulate expression of many genes involved in cell proliferation, apoptosis, and differentiation (Chu, 2012). En1, or engrailed, is a homeobox containing transcription factor involved in dorso-ventral patterning of the limb field during embryogenesis (Hanks et al., 1998). Ap1 controls cell division and cell death decisions (Alani et al., 1991) and is known to work with Pax2, another vital factor in embryogenesis (Zhang et al., 2012). Sox 5 plays a role in differentiation during embryogenesis and Sox 17 works to inhibit Wnt3a singaling (Vervoort et al., 2012). The computational data indicates that putative binding elements for relevant factors exist within the introns of *MyoD* and warrant further study.

The lack of positive epigenetic modifications, and presence of negative epigenetic changes were also examined in non-myogenic cell types. H3K4 methylation is absent in neural, heart, and liver tissue, as well as erythroblasts

and megakaryocytes. In fact, all non-myogenic cell types exhibited high levels of transcriptionally repressive marks, such as H3K27 and H3K9 tri-methylation (Barski et al., 2007). A marker of active chromatin is acetylation of lysine in H3. C2C12 cells contain H3K9ac, while all other cells types analyzed, including, brain, liver, and heart tissue, lacked this positive epigenetic mark.

Figure 3-9

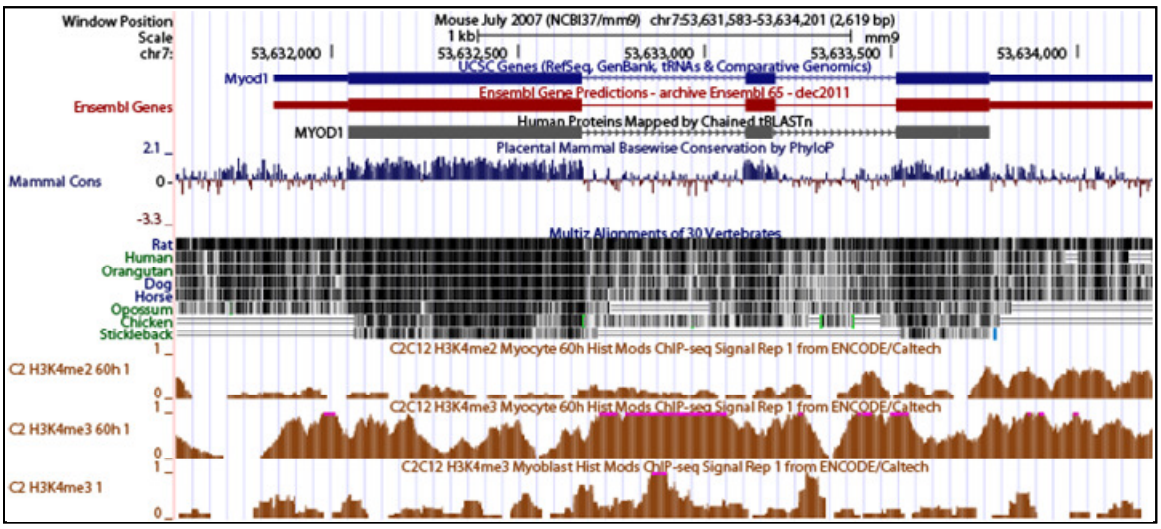
Window Position
Mouse July 2007 (NCBI37/mm9) chr7:53,631,583-53,634,201 (2,619 bp)
Scale
1 kb
mm9
chr7:
53,632,000
53,632,500
53,633,000
53,633,500
53,634,000
Myod1
UCSC Genes (RefSeq, GenBank, tRNAs & Comparative Genomics)
Ensembl Genes
Ensembl Gene Predictions - archive Ensembl 65 - dec2011
MYOD1
Human Proteins Mapped by Chained tBLASTn
2.1
Mammal Cons
0
-3.3
Placental Mammal Basewise Conservation by PhyloP
Multiz Alignments of 30 Vertebrates
Rat
Human
Orangutan
Dog
Horse
Opossum
Chicken
Stickleback
C2C12 H3K4me2 Myocyte 60h Hist Mods ChIP-seq Signal Rep 1 from ENCODE/Caltech
C2 H3K4me2 60h 1
1
0
C2C12 H3K4me3 Myocyte 60h Hist Mods ChIP-seq Signal Rep 1 from ENCODE/Caltech
C2 H3K4me3 60h 1
1
0
C2C12 H3K4me3 Myoblast Hist Mods ChIP-seq Signal Rep 1 from ENCODE/Caltech
C2 H3K4me3 1
1
0

Figure 3-9. Database analysis of the *MyoD* locus reveals sequence conservation across species and positive epigenetic markings

Data obtained from the University of California, Santa Cruz, Genome Browser. Analysis of the genomic sequence surrounding the *MyoD* locus includes sequence conservation across species along with active histone modifications in the C2C12 immortal myoblast cell line. Abbreviations: (STS) sequence tagged site, (EST) expressed sequence tag, (H3K4me3) histone 3, lysine 4, tri-methylation. The *MyoD* coding region shows high sequence similarity across species in exons, with high levels of H3K4me3 in introns 1 and 2. Intron 1 also shows sequence conservation across several species.

Figure3-10

A

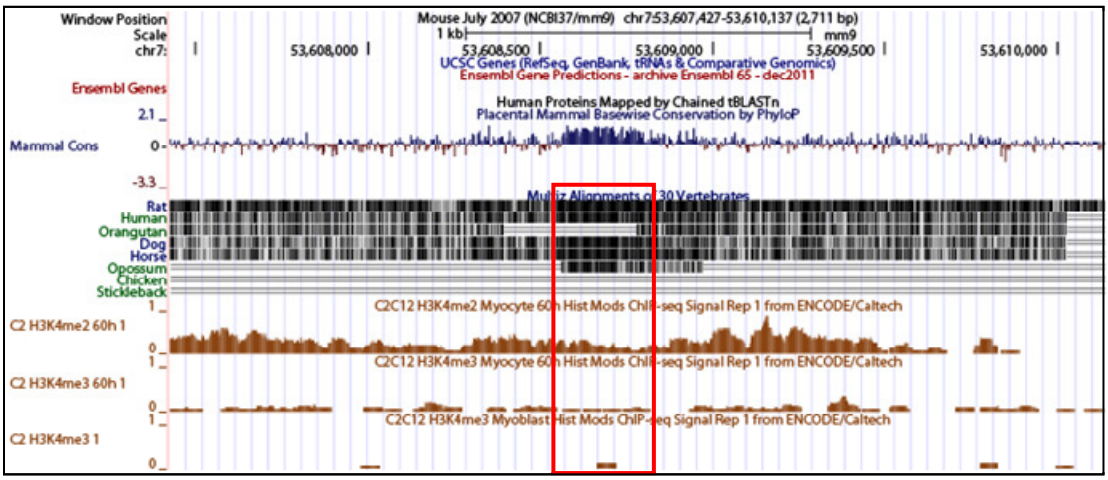

B

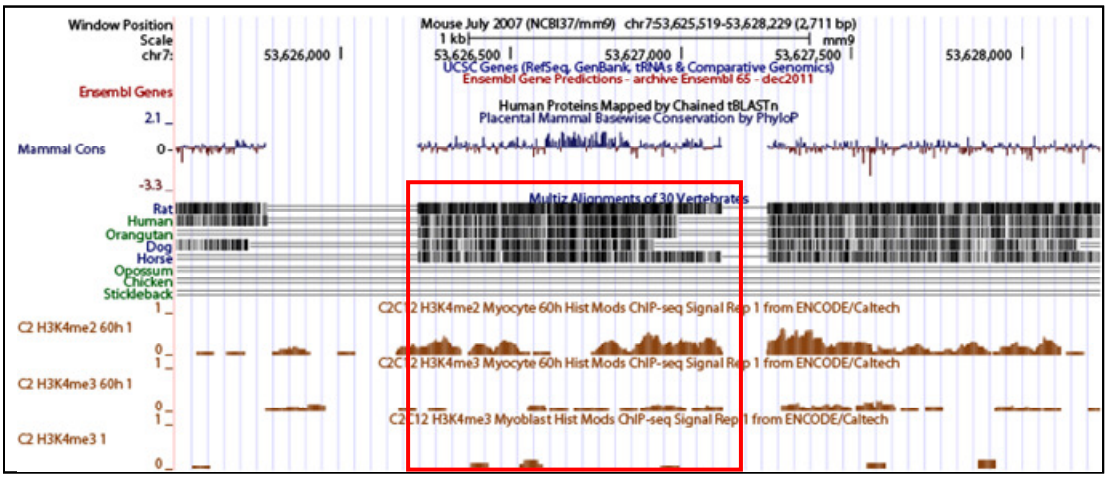

Figure 3-10. Database analysis of the CE and DRR reveals high sequence similarity across species

Sequence images of the murine CE (A) and DRR (B). The discrete enhancer areas are boxed in red. Sequence conservation is high across species and is higher than outside of the boxed regions.

3.5 Discussion:

When the 24 kb of human sequence upstream of *MyoD* is attached to either *GFP* or *lacZ* and placed in the mouse genome, reporter gene expression almost flawlessly mimics endogenous *MyoD* expression (Chen et al., 2001). Other transgenic experiments demonstrated distinct functions between the two known *MyoD* enhancers contained in the 24kb of sequence. The CE transgene showed activity concurrent with initiation of *MyoD* expression, and the DRR was active in differentiating muscle (Chen et al., 2001). When either of the discrete enhancers were eliminated from the mouse genome, only slight defects occurred, leading to the hypothesis that the enhancers could compensate for each other when one was absent (Chen et al., 2002; Chen and Goldhamer, 2004b). In this present study, we have shown that at least one other uncharacterized enhancer exists, and that they are largely responsible for the proper spatio-temporal transcription profile of *MyoD* during embryogenesis. This study is a striking example of necessity versus sufficiency. The known enhancers are sufficient to drive reporter gene expression in a pattern that mimics *MyoD*, but none of the known enhancers are necessary for it.

Recent studies regarding upstream regulators of *MyoD* show pronounced muscular defects after eliminating trans acting regulators that have been shown to bind the CE or DRR. Positive regulators, such as YB1/p32 (Song and Lee, 2010), Six1/4 and Eya1/2 (Grifone et al., 2005), BMAL1/Clock (Andrews et al., 2010) (Zhang et al., 2011), Pitx2 (L'Honore et al., 2010), and the transcriptional

repressor Sim2 (Metz et al. 2006, Havis et al. 2012) have demonstrable effects on *MyoD* transcription. Although binding of these various factors to the CE have been shown in vitro, the CE may not be the only target, and the introns or other DNA elements may be binding sites for these factors. It should be noted that some of the previous studies examined postnatal transcriptional control, and that aspect of myogenesis has not been addressed in this study. The CE's function may be to control the circadian oscillation of *MyoD* expression in adult muscle, via binding of CLOCK1/BAML to the CE, however, only the CE and 6kbs of DNA upstream of *MyoD* were assayed for binding (Andrews et al., 2010). In mice lacking only the CE, $CE^{loxP/loxP}$, MyoD expression oscillation is only dampened, not eliminated (Zhang et al., 2011). In all studies mentioned above, it may be that DNA elements outside of the CE and DRR are involved as well.

In this study, it has been shown that in the absence of both the CE and DRR, MyoD expression is largely unperturbed, with only a delay in MyoD expression in the limb buds and branchial arches. This phenotype was also observed when only the CE is removed (Chen and Goldhamer, 2004b). $MyoD^{\Delta CE15DRR/\Delta CE15DRR}$ embryos displayed MyoD expression identical to the pattern in $MyoD^{\Delta CEDRR/\Delta CEDRR}$ embryos. This result is not unexpected, as there have been no studies implicating the sequence between the CE and DRR as a potent regulator of MyoD expression. Now there is definitive proof that no necessary regulation of MyoD occurs via this DNA sequence. There is a portion of F3 that remains in $MyoD^{\Delta CE15DRR/\Delta CE15DRR}$ animals that may have regulatory abilities. The CE was found to be the most potent portion of F3, but the

approximately 1.5 kb of F3 that remains could partly control transcription (Goldhamer et al., 1995).

The targets of the *Pax3* dependent rescue pathway of *MyoD* expression in the absence of *Myf-5* was investigated in our two now mouse lines. We have shown that the rescue kinetics are similar between wild type embryos and both $MyoD^{\Delta CEDRR/\Delta CEDRR}$ and $MyoD^{\Delta CE15DRR/\Delta CE15DRR}$ embryos. These results are striking when compared to numerous transgenic analyses. In a fine scale transgenic mapping study of the CE, where only the CE and proximal promoter of *MyoD* controll lacZ expression, 15 bases of the CE were replaced with a linker sequence at a time. Two adjacent sequences, when mutated, both resulted in the loss of reporter expression in the myotome and myotome derived muscles. (Kucharczuk et al., 1999) This mutated construct showed no activity in the trunk of *Myf-5 null* embryos, showing the exact portion of the CE that is a target of *Pax3* rescue (Chen and Goldhamer, 2004a), albeit not the only target.

There remains the possibility of regulatory element in the 2kb upstream of the CE. Transgenic studies using 24kb of human DNA upstream of *MyoD*, with a 4kb fragment removed, to drive lacZ expression exhibited reporter gene expression delay throughout the embryo (Chen et al., 2001). Importantly, near the center of this 4kb deleted fragment lies the CE. Both the $MyoD^{\Delta CEDRR/\Delta CEDRR}$ and $MyoD^{\Delta CE15DRR/\Delta CED15RR}$ lines retain the 2 kb portion. Database analysis shows the 2 kbs directly upstream of the CE contain a similar amount of H3K4 tri-methylation as the CE itself, but the amount of sequence conservation between species is higher in the 258 bps of the CE (Figure 3-10A).

Database analysis supports the hypothesis that enhancers exist in the introns of *MyoD*, particularly in intron 1. Sequence analysis of the *MyoD* shows that of all the surrounding sequence analyzed, the highest levels of H3K4 tri-methylation, an epigenetic marker of enhancers, occurs in the introns. There is also a short region in intron 1 that is evolutionarily conserved across several mammalian species and contains multiple, unproven, transcription factor binding sites. These active chromatin modifications are not present in non-muscle cell types. In non-muscle cell types, the entire *MyoD* locus contains repressive chromatin modifications, such as H3K9 and K3K27 tri-methylation. A follow up experiment is warranted to address intronic enhancers. Either a transgenic study where the introns drive reporter gene expression, or targeting the *MyoD* locus to replace the entirety of *MyoD* with a reporter gene can be performed.

The intricate pattern and timing of *MyoD* expression throughout the entire embryo implies a more complex regulatory system than currently known. The regulatory network of the conserved family members, *Myf-5* and *Mrf4*, has proven to be quite complex, and this study indicates that *MyoD* may have similarly complex regulation. *Myf-5* enhancer elements span over 140kb and there are distinct roles for each of the 19 enhancers identified in location of expression, timing of expression, or both (Buchberger et al., 2003; Carvajal et al., 2001; Hadchouel et al., 2003; Summerbell et al., 2000). Also known is that some enhancers of *Myf-5* are contained in the introns (Carvajal et al., 2008). The signaling environments that lead to *MyoD* expression are different at the three main areas of embryonic myogenesis, namely, the head, trunk and limbs

(Moncaut et al., 2013). This variability in regulatory factor environments implies multiple enhancers and is consistent with the findings presented here, as we demonstrated that the embryonic transcriptional regulation of *MyoD* is more complex than previously shown.

3.6 References

Alani, R., et al., 1991. The transactivating domain of the c-Jun proto-oncoprotein is required for cotransformation of rat embryo cells. Molecular and Cellular Biology. 11**,** 6286-6295.

Andrews, J. L., et al., CLOCK and BMAL1 regulate MyoD and are necessary for maintenance of skeletal muscle phenotype and function. Vol. 107, 2010, pp. 19090-19095.

Asakura, A., et al., 1995. The regulation of MyoD gene expression: conserved elements mediate expression in embryonic axial muscle. Dev Biol. 171**,** 386-98.

Barski, A., et al., 2007. High-resolution profiling of histone methylations in the human genome. Cell. 129**,** 823-37.

Bernstein, B. E., et al., 2006. A bivalent chromatin structure marks key developmental genes in embryonic stem cells. Cell. 125**,** 315-26.

Bober, E., et al., 1994a. Initial steps of myogenesis in somites are independent of influence from axial structures. Development. 120**,** 3073-82.

Bober, E., et al., 1994b. Pax-3 is required for the development of limb muscles: a possible role for the migration of dermomyotomal muscle progenitor cells. Development. 120**,** 603-12.

Borycki, A. G., Emerson, C. P., Jr., 2000. Multiple tissue interactions and signal transduction pathways control somite myogenesis. Curr Top Dev Biol. 48**,** 165-224.

Buchberger, A., et al., 2003. Myf5 expression in somites and limb buds of mouse embryos is controlled by two distinct distal enhancer activities. Development. 130**,** 3297-307.

Carvajal, J. J., et al., 2001. A BAC transgenic analysis of the Mrf4/Myf5 locus reveals interdigitated elements that control activation and maintenance of gene expression during muscle development. Development. 128**,** 1857-68.

Carvajal, J. J., et al., Global transcriptional regulation of the locus encoding the skeletal muscle determination genes Mrf4 and Myf5. Vol. 22, 2008, pp. 265-276.

Chen, J. C., Goldhamer, D. J., 2004a. The core enhancer is essential for proper timing of MyoD activation in limb buds and branchial arches. Dev Biol. 265**,** 502-12.

Chen, J. C., et al., 2001. Two upstream enhancers collaborate to regulate the spatial patterning and timing of MyoD transcription during mouse development. Dev Dyn. 221**,** 274-88.

Chen, J. C., et al., Essential and redundant functions of the MyoD distal regulatory region revealed by targeted mutagenesis. Vol. 245, 2002, pp. 213 - 223.

Chen, J. C. J., Goldhamer, D. J., 2004b. The core enhancer is essential for proper timing of MyoD activation in limb buds and branchial arches. Developmental Biology. 265**,** 502-512.

Chu, S., 2012. Transcriptional regulation by post-transcriptional modificationâ€"Role of phosphorylation in Sp1 transcriptional activity. Gene. 508**,** 1-8.

Cossu, G., et al., 1996. Activation of different myogenic pathways: myf-5 is induced by the neural tube and MyoD by the dorsal ectoderm in mouse paraxial mesoderm. Development. 122**,** 429-37.

Daston, G., et al., 1996a. Pax-3 is necessary for migration but not differentiation of limb muscle precursors in the mouse. Development. 122**,** 1017-27.

Daston, G., et al., Pax-3 is necessary for migration but not differentiation of limb muscle precursors in the mouse. Vol. 122, 1996b, pp. 1017-1027.

Dermitzakis, E. T., Clark, A. G., 2001. Differential Selection After Duplication in Mammalian Developmental Genes. Molecular Biology and Evolution. 18**,** 557-562.

Faerman, A., et al., 1995. The distal human myoD enhancer sequences direct unique muscle-specific patterns of lacZ expression during mouse development. Dev Biol. 171**,** 27-38.

Goldhamer, D. J., et al., 1995. Embryonic activation of the myoD gene is regulated by a highly conserved distal control element. Development. 121**,** 637-49.

Goldhamer, D. J., et al., 1992. Regulatory elements that control the lineage-specific expression of myoD. Science. 256**,** 538-42.

Hadchouel, J., et al., 2003. Analysis of a key regulatory region upstream of the Myf5 gene reveals multiple phases of myogenesis, orchestrated at each site by a combination of elements dispersed throughout the locus. Development. 130**,** 3415-26.

Hanks, M. C., et al., 1998. Drosophila engrailed can substitute for mouse Engrailed1 function in mid-hindbrain, but not limb development. Development. 125**,** 4521-4530.

Kablar, B., et al., 1999. Myogenic determination occurs independently in somites and limb buds. Dev Biol. 206**,** 219-31.

Kanisicak, O., et al., 2009. Progenitors of skeletal muscle satellite cells express the muscle determination gene, MyoD. Dev Biol. 332**,** 131-41.

Kassar-Duchossoy, L., et al., 2004. Mrf4 determines skeletal muscle identity in Myf5:Myod double-mutant mice. Nature. 431**,** 466-71.

Kucharczuk, K. L., et al., 1999. Fine-scale transgenic mapping of the MyoD core enhancer: MyoD is regulated by distinct but overlapping mechanisms in myotomal and non-myotomal muscle lineages. Development. 126**,** 1957-65.

L'Honore, A., et al., 2003. MyoD Distal Regulatory Region Contains an SRF Binding CArG Element Required for MyoD Expression in Skeletal Myoblasts and during Muscle Regeneration. Molecular Biology of the Cell. 14**,** 2151-2162.

L'Honore, A., et al., Pitx2 defines alternate pathways acting through MyoD during limb and somitic myogenesis. Vol. 137, 2010, pp. 3847-3856.

Marcelle, C., et al., 1999. In Vivo Regulation of Somite Differentiation and Proliferation by Sonic Hedgehog. Developmental Biology. 214**,** 277-287.

Moncaut, N., et al., 2013. Dial M(RF) for myogenesis. Febs J. 280**,** 3980-90.

Nagy, A., 2000. Cre recombinase: The universal reagent for genome tailoring. genesis. 26, 99-109.

Pekowska, A., et al., 2011. H3K4 tri-methylation provides an epigenetic signature of active enhancers. Embo J. 30, 4198-210.

Pennacchio, L. A., et al., 2013. Enhancers: five essential questions. Nat Rev Genet. 14, 288-295.

Rudnicki, M. A., et al., 1993. MyoD or Myf-5 is required for the formation of skeletal muscle. Cell. 75, 1351-9.

Schaft, J., et al., 2001. Efficient FLP recombination in mouse ES cells and oocytes. genesis. 31, 6-10.

Schraders, M., et al., 2012. Mutations of the Gene Encoding Otogelin Are a Cause of Autosomal-Recessive Nonsyndromic Moderate Hearing Impairment. American journal of human genetics. 91, 883-889.

Snowden, A. W., et al., 2002. Gene-Specific Targeting of H3K9 Methylation Is Sufficient for Initiating Repression In Vivo. Current biology : CB. 12, 2159-2166.

Song, Y. J., Lee, H., 2010. YB1/p32, a nuclear Y-box binding protein 1, is a novel regulator of myoblast differentiation that interacts with Msx1 homeoprotein. Experimental Cell Research. 316, 517-529.

Summerbell, D., et al., 2000. The expression of Myf5 in the developing mouse embryo is controlled by discrete and dispersed enhancers specific for particular populations of skeletal muscle precursors. Development. 127, 3745-57.

Sur, I. K., et al., 2012. Mice Lacking a Myc Enhancer That Includes Human SNP rs6983267 Are Resistant to Intestinal Tumors. Science. 338, 1360-1363.

Tahmasebi, S., et al., Sumoylation of Kruppel-like factor 4 inhibits pluripotency induction but promotes adipocyte differentiation. Journal of Biological Chemistry.

Tajbakhsh, S., et al., 1998. Differential activation of Myf5 and MyoD by different Wnts in explants of mouse paraxial mesoderm and the later activation of myogenesis in the absence of Myf5. Development. 125, 4155-62.

Tajbakhsh, S., et al., 1997. Redefining the genetic hierarchies controlling skeletal myogenesis: Pax-3 and Myf-5 act upstream of MyoD. Cell. 89, 127-38.

Towbin, Benjamin D., et al., 2012. Step-Wise Methylation of Histone H3K9 Positions Heterochromatin at the Nuclear Periphery. Cell. 150**,** 934-947.

Vervoort, S. J., et al., 2012. The role of SRY-related HMG box transcription factor 4 (SOX4) in tumorigenesis and metastasis: friend or foe[quest]. Oncogene.

Villarroel-Espíndola, F., et al., 2013. Muscle glycogen synthase isoform is responsible for testicular glycogen synthesis: Glycogen overproduction induces apoptosis in male germ cells. Journal of Cellular Biochemistry. 114**,** 1653-1664.

Zhang, H.-S., et al., 2012. PAX2 Protein Induces Expression of Cyclin D1 through Activating AP-1 Protein and Promotes Proliferation of Colon Cancer Cells. Journal of Biological Chemistry. 287**,** 44164-44172.

Zhang, X., et al., 2011. A non-canonical E-box within the MyoD core enhancer is necessary for circadian expression in skeletal muscle. Nucleic Acids Research. 40**,** 3419-3430.

Chapter 4 *MyoD* lineage ablation and the role of myogenesis in proper rib development

4.1 Abstract:

In order to address the mode of redundancy between *MyoD* and *Myf-5*, we used the $MyoD^{iCre}$ allele to activate the Cre dependent diphtheria toxin ($R26^{DTA}$) gene resulting in the death of any cell that activates the *MyoD* locus Preliminary data at E18.5 shows the complete absence of skeletal muscle, evidenced by a lack of Myosin Heavy Chain expressing cells. This result is in contrast to previously reported $Myf\text{-}5^{Cre};R26^{DTA}$ embryos, where myogenesis occurs and embryos are born with functional muscle, indicating that all myogenic cells express *MyoD*, but not *Myf-5,* during development. Interestingly, there was an unexpected rib malformation phenotype in $MyoD^{iCre};R26^{DTA}$ embryos. This observation led to analysis of the dependency of rib development on appropriate muscle formation in the myotome. We examined the rib malformation phenotype in $Myf\text{-}5^{loxP/loxP}$;$MyoD^{iCre/Neo}$, $Myf\text{-}5^{Neo/Neo}$;$MyoD^{iCre/Neo}$ and $MyoD^{iCre/+}$;$R26^{DTA}$ embryos, three genotypes known to affect myotome formation and development at different times. It appears that normal rib development requires the timely formation of the myotome, as well as continued presence of intercostal muscles, such that the earlier the perturbation in myotome formation and development, the more severe the rib defect.

4.2 Introduction:

Lineage Ablation

Since the seminal research regarding the genetic control of embryonic myogenesis, there has been an open question regarding the mode of redundancy between *MyoD* and *Myf-5*. These transcription factors are largely similar in DNA sequence, and share an identical DNA binding domain. When either *MyoD* or *Myf-5* is deleted from the mouse genome, myogenesis occurs almost normally, and embryos are born with functional skeletal muscle (Braun et al., 1992; Rudnicki et al., 1992a). However, when both genes are deleted, no skeletal muscle forms in the embryo. (Rudnicki et al., 1993). The question became, are *MyoD* and *Myf-5* functionally redundant in the same cells, or are there redundant lineages, ie a *MyoD* dependent and a *Myf-5* dependent lineage?

Recently, the two separate lineage hypothesis was supported by the diphtheria toxin (DTA) induced cell death after activation of the *Myf-5* locus (Gensch et al., 2008; Haldar et al., 2008). The C*re* gene was knocked into the *Myf-5* locus, where activation results in cre-mediated recombination of $R26^{DTA}$, and diphtheria toxin production, causing cell death by inhibiting protein translation via elongation factor 2 (Ivanova et al., 2005; Pappenheimer, 1977). Skeletal myogenesis still occurs in these embryos, via a *Myf-5* independent lineage.

Putting lineage ablation under the control of the *MyoD* locus was performed using *MyoD*$^{iCre/+}$;*R26*^{DTA} embryos and results in the lack of skeletal muscle at E18.5. This preliminary data shows that all cells of the myogenic lineage activate the *MyoD* locus.

Rib Development

The original *Myf-5* knockout allele, *Myf-5*^{Neo}, resulted in severe, perinatal lethal, rib defects (Braun et al., 1992). However, *MyoD*$^{Neo/Neo}$ embryos did not exhibit a rib phenotype (Rudnicki et al., 1992b). Thought only to control myogenesis, the connection between the allele, and the unexpected rib phenotype was a major point of interest. The *Myf-5*^{Neo} allele retains the PGKNeo selection cassette, and it was hypothesized that the disrupted allele affected expression of other unspecified genes involved in rib development. After a more discrete allele was created, *Myf-5*^{loxP}, it was found that the rib defect was eliminated. The Neo cassette was transcriptionally silencing the physically close myogenic gene, *Mrf4* (Kassar-Duchossoy et al., 2004). *Myf-5* and *Mrf4* control the formation of the myotome, and *MyoD* plays a later role in myotomal development.

Generally, functional muscle aids in proper embryonic bone growth by providing static load and contractions to stimulate osteogenesis (Hamrick, 2010). Aside from the rib truncation phenotype, *MyoD*$^{-/-}$;*Myf-5*$^{Neo/Neo}$ embryos have fused vertebra, malformed mandibles and palate (Rot-Nikcevic et al., 2006), and close

proximity of the radius and ulna (presented in Chapter 2). The rib phenotype appears to be caused by much earlier stages in myogenesis, prior to functionally contractile muscle formation. The close proximity of the developing axial skeleton, arising from the sclerotome, and the myotome, may point to a signaling pathway between the two, such that the lack of a myotome perturbs signaling and results in a malformed rib cage. It has been found that the myotome allows for *PDGFA* and *FGF* expression in the sclerotome, and that this activation is needed to promote rib development (Tallquist et al., 2000; Vinagre et al., 2010). In embryos with compromised muscle differentiation, rib development is still affected. When embryos lack *Mrf4* and have hypomorphic alleles of *Myogenin*, fusion of ribs to the sternum fails, and the ribs are shaped improperly (Vivian et al., 2000). These two genes are not expressed in axial bones nor the early myotome, meaning the resulting rib phenotype is dependent only on the failure of myogenic differentiation.

Here we report that a link between myotome formation and maintenance impacts the extent of rib development, further strengthening the link between skeletal muscle and bone development.

4.3 Materials and Methods:

Mouse breeding and genotyping

All mouse handling, breeding, and sacrificing were done in accordance with our IACUC animal care protocol. All separate lines were maintained by breeding to FVB mice. Cre dependent DTA expressing mice, *R26*^{DTA}, were obtained from Jaxson Labs (ID #006631) and expanded through intercrossing. Offspring were crossed to *MyoD*$^{iCre/+}$ animals. Timed matings were set up by taking the morning of vaginal plug as embryonic day 0.5 or E0.5. The *MyoD*^{iCre} allele was detected by PCR using a forward primer (5′-GCGGATCCGAATTC GAAGTTCC-3′) that lies at the 3′ end of the icre/+2pA cassette and a reverse primer in intron 1 of *MyoD* (5′-TGGGTCTCCAAAGCGACTCC-3′), generating a product of 149 bp. No genotyping was required for the DTA allele, as mice received were homozygous and the presence of the allele in embryos is evident based on EGFP expression in the non-recombined allele. The *MyoD*^{Neo} allele was detected with the forward primer 5'- TGGATGTGGAATGTGTGCGAG-3' and the reverse primer 5'- TCACTGTAGTAGGCGGTGTCGTAG-3' to create a 420 bp product. The *Myf-5*^{Neo} allele was detected using the primers 5'-CGTTGG CTACCCGTGATATT-3' and 5'- CAGCTCAGCTTTGTGTGCTC-3' creating a 410 bp product. *Myf-5*^{loxP} was detected using the primers 5'- GGTGTCT CCTCTCTGCTGAATCCAGGTAT-3' and 5'-AGGTGCACGCACGTGCTCA CTGTCTGA-3' to create a 349 bp band.

Cryostat sectioning

Embryos were isolated and fixed with 4% paraformaldehyde for 3.5 hours at 4^{o}C. The embryos were rinsed with 4^{o}C PBS 4 times for 20 minutes each. The fixed muscle was processed through a sucrose gradient of 15% sucrose in PBS overnight, followed by 30% sucrose in PBS overnight all at 4^{o}C . The processed tissue was placed into OCT compound and quickly frozen in dry ice cooled isopentane. The frozen tissue was cryosectioned at 10 µm and either stored at -80^{o}C, or immediately processed for observation.

Immunofluorescence

Skeletal muscle was detected using a mouse anti-Myosin antibody at a 1:250 dilution (Millipore # MAB1628) and a secondary goat anti-mouse red fluorescent antibody 1:500 dilution (Invitrogen # A-21422). Vector labs MOM kit (# BMK-2202) was used as per manufacturers instructions after antigen retrieval. The retrieval process entails a 6 min. soak in -20^{o}C methanol, followed by a 30 minute incubation in 95^{o}C 10mM sodium citrate pH 6. A standard block (1% BSA, 10% goat serum, 0.1% Tween in PBS) was performed for 2 hours at room temperature, followed by a 2 hour primary antibody incubation, also at room temperature.

4.4 Results:

Embryonic day 18.5 *MyoD*$^{iCre/+}$*;R26*^{DTA} embryos were collected as an end point assay to determine the size of the *MyoD* expressing lineage. At this stage, there was no muscle visible. The gross appearance of the embryos (Fig 4-2) was similar to the amyogenic embryos in Chapter 2. Sectioning of the embryos followed by antibody detection of myosin heavy chain, a muscle specific marker, revealed a complete lack of skeletal muscle in the embryo (Fig 4-1)

The rib defect phenotype seen in *MyoD*$^{iCre/+}$*;R26*^{DTA} embryos was not as severe as in *Myf-5*$^{Neo/Neo}$*;MyoD*$^{iCre/Neo}$ embryos. Myf-5$^{Neo/Neo}$;MyoD$^{iCre/Neo}$ embryos also have a transcriptionally repressed *Mrf4* gene, and in the absence of primary myogenesis, no muscle forms and only rib rudiments or 'nubs' are formed (Figure 4-2 A red arrow). In *MyoD*$^{iCre/+}$*;R26*^{DTA} embryos, early myotome development occurs normally. Early myotome formation is under the control of *Myf-5* and *Mrf4* as they are turned on at E9, while MyoD is not turned on robustly until E10. Cell death does not occur instantly, as Cre must be produced, the *R26*^{DTA} locus must be recombined and produce the toxin to kill the cell, which takes at least 24 hours (Saito et al., 2001). This window of myogenesis allowed for rib outgrowth, however myogenesis ends and the ribs are still severely truncated (Figure 4-2 B red arrow). In *Myf-5*$^{loxP/loxP}$*;MyoD*$^{iCre/Neo}$ embryos, primary myogenesis is completely dependent on *Mrf4*. In these embryos, rib outgrowth is the most advanced. These embryos still die at birth and have very

little organized muscle. However, the continual presence of muscle allows for rib outgrowth (Figure 4-2 C).

Figure 4-1

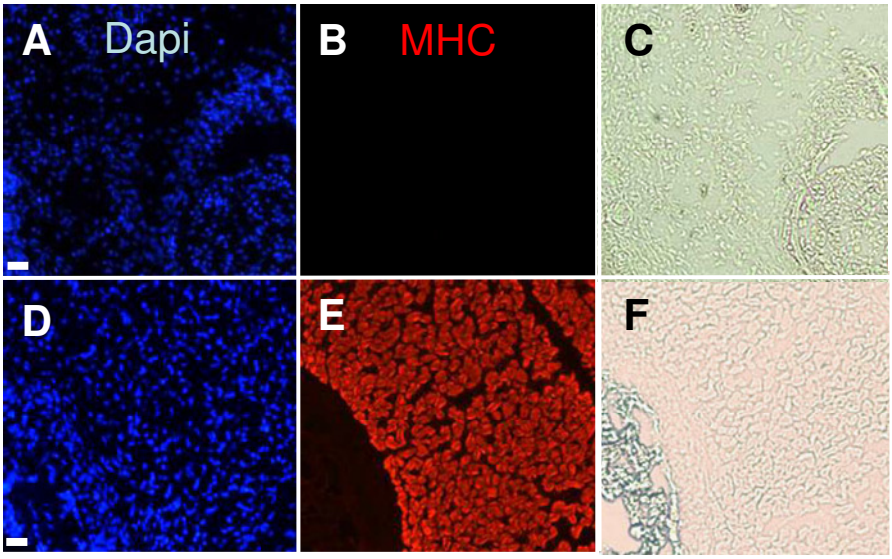

Figure 4-1. Lack of Muscle in limb of E18.5 *MyoD$^{iCre/+}$;R26^{DTA}* embryos

10 μm cryostat sections of wild type (D-F) and *MyoD$^{iCre/+}$;R26^{DTA}* limbs at E18.5. Myosin Heavy Chain antibody detection (B and E) show the absence of any myogenic cells in *MyoD$^{iCre/+}$;R26^{DTA}* embryos. Dapi is used to visualize nuclei (A and D) while (C and F) show phase images. The forearm bones are seen as an absence of staining in B and in the phase images (C and F). Scale bar represents 30 μm.

Figure 4-2

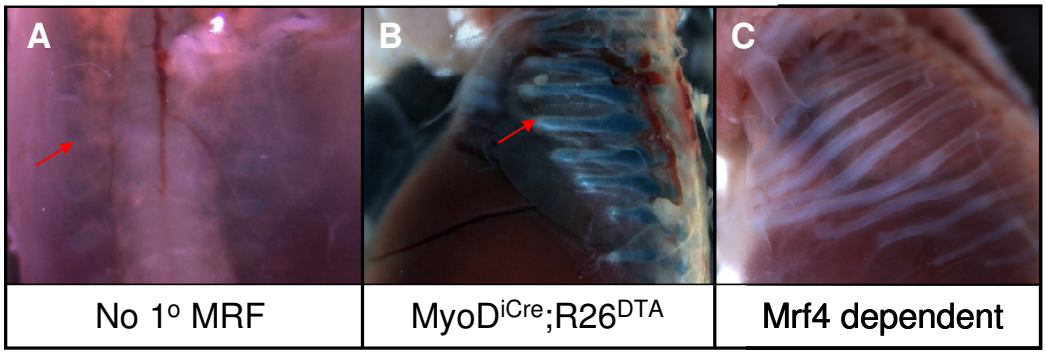

Figure 4-2. Rib Abnormality Phenotype in E18.5 Embryos with different MRF mutations

Comparison of rib development in embryos with various myogenic mutations. There is no *MyoD*, *Myf-5*, or *Mrf4* expression in (A) and rib development does not produce more than nubs (red arrow in A). Rib development progresses more in B (red arrows) when early myotome formation is dependent on *Myf-5* and *Mrf4* until the onset of *MyoD* expression causing cell death. In *Myf-5*$^{loxP/loxP}$*;MyoD*$^{iCre/Neo}$ embryos (C) the only factor driving myogenesis is *Mrf4* and produces the most 'normal' rib phenotype in comparison to the other genotypes.

4.5 Discussion:

Given the preliminary status of these experiments, it is difficult to draw many concrete conclusions. However, given the striking phenotype when the *MyoD* expressing lineage is ablated, it can be assumed that every cell in the myogenic lineage activates the MyoD locus during embryonic development. This follows closely on the heels of the finding that all satellite cells activate the *MyoD* locus during embryogenesis (Kanisicak et al., 2009). As an endpoint assay, it is striking to find no differentiated muscle at E18.5 in $MyoD^{iCre/+};R26^{DTA}$ embryos. A detailed timeline of DTA dependent cell death needs to be performed in order to fully characterize this phenomenon.

When analyzing the $MyoD^{iCre/+};R26^{DTA}$ E18.5 embryos, the rib phenotype was impossible to miss. The lack of skeletal muscle and limb phenotype was identical to the $MyoD^{iCre/Neo};Myf\text{-}5^{Neo/Neo};R26^{lacZ}$ phenotype described in chapter 2, yet rib growth was much more pronounced, although still extremely poor in respect to wild type embryos. The different rib phenotypes in the three genotypes analyzed, where myogenesis is disrupted at various time points, supports the hypothesis that rib growth is dependent on the myotome. $MyoD^{iCre/Neo};Myf\text{-}5^{Neo/Neo}$ embryos have silenced *Mrf4* expression, lack myoblast and myotome formation, and have the most severe rib truncation phenotype as myogenesis never begins (Kablar et al., 2003; Rudnicki et al., 1993). In $MyoD^{iCre/+};R26^{DTA}$ embryos, early myotome formation occurs, under the control of *Myf-5* and *Mrf4*, until *MyoD* is activated at approximately E10, after which, all

muscle and myoblasts die and rib outgrowth stops. This window of myogenesis appears to allow for more rib development. In the third genotype examined, *Myf-5$^{loxP/loxP}$;MyoD$^{iCre/Neo}$* embryos have only *Mrf4* to drive early myogenesis, which is not enough to form viable newborn mice (Kassar-Duchossoy et al., 2004). However, myogenesis occurs during embryogenesis and ribs develop much more than any other genotype analyzed here. A more detailed analysis of these animals during development will show exactly when myogenesis fails and confirm signaling disruption between the sclerotome and myotome, and the resulting axial skeleton defects linked to those genotypes.

4.6 References

Braun, T., et al., 1992. Targeted inactivation of the muscle regulatory gene Myf-5 results in abnormal rib development and perinatal death. Cell. 71**,** 369-82.

Gensch, N., et al., 2008. Different autonomous myogenic cell populations revealed by ablation of Myf5-expressing cells during mouse embryogenesis. Development. 135**,** 1597-604.

Haldar, M., et al., 2008. Two cell lineages, myf5 and myf5-independent, participate in mouse skeletal myogenesis. Dev Cell. 14**,** 437-45.

Hamrick, M., 2010. JMNI special issue: basic science and mechanisms of muscle-bone interactions. J Musculoskelet Neuronal Interact. 10**,** 1-2.

Ivanova, A., et al., 2005. In vivo genetic ablation by Cre-mediated expression of diphtheria toxin fragment A. Genesis. 43**,** 129-35.

Kablar, B., et al., 2003. Myf5 and MyoD activation define independent myogenic compartments during embryonic development. Dev Biol. 258**,** 307-18.

Kanisicak, O., et al., 2009. Progenitors of skeletal muscle satellite cells express the muscle determination gene, MyoD. Dev Biol. 332**,** 131-41.

Kassar-Duchossoy, L., et al., 2004. Mrf4 determines skeletal muscle identity in Myf5:Myod double-mutant mice. Nature. 431**,** 466-71.

Pappenheimer, A. M., Jr., 1977. Diphtheria toxin. Annu Rev Biochem. 46**,** 69-94.

Rot-Nikcevic, I., et al., 2006. Myf5-/- :MyoD-/- amyogenic fetuses reveal the importance of early contraction and static loading by striated muscle in mouse skeletogenesis. Dev Genes Evol. 216**,** 1-9.

Rudnicki, M. A., et al., Inactivation of MyoD in mice leads to up-regulation of the myogenic HLH gene Myf-5 and results in apparently normal muscle development. Vol. 71, 1992a, pp. 383 - 390.

Rudnicki, M. A., et al., 1992b. Inactivation of MyoD in mice leads to up-regulation of the myogenic HLH gene Myf-5 and results in apparently normal muscle development. Cell. 71**,** 383-90.

Rudnicki, M. A., et al., 1993. MyoD or Myf-5 is required for the formation of skeletal muscle. Cell. 75**,** 1351-9.

Saito, M., et al., 2001. Diphtheria toxin receptor-mediated conditional and targeted cell ablation in transgenic mice. Nat Biotechnol. 19**,** 746-50.

Tallquist, M. D., et al., 2000. Early myotome specification regulates PDGFA expression and axial skeleton development. Development. 127**,** 5059-5070.

Vinagre, T. n., et al., 2010. Evidence for a Myotomal Hox/Myf Cascade Governing Nonautonomous Control of Rib Specification within Global Vertebral Domains. Developmental Cell. 18**,** 655-661.

Vivian, J. L., et al., 2000. Thoracic Skeletal Defects in Myogenin- and MRF4-Deficient Mice Correlate with Early Defects in Myotome and Intercostal Musculature. Developmental Biology. 224**,** 29-41.

Chapter 5: Conclusions and Future Directions

5.1 Conclusions

All chapters of this thesis focus primarily on one member of the MRF gene family, *MyoD*. In an attempt to refine the roles of the known cis-regulators of *MyoD* transcription, the CE and DRR, we have shown these DNA elements are not necessary to direct *MyoD* mRNA expression in a predominantly faithful manner compared to wild type embryos. In embryos lacking the CE and DRR, aside from an approximately one day delay in initiation of *MyoD* expression in the limb buds and branchial arches, and a shorter delay in activation in the early myotome, *MyoD* expression occurs normally during development. Knowing that the vast majority of transcriptional regulation does not lie in the CE and DRR, or the 15kb in between them, begins a new search for vital regulatory regions of this important gene.

These current experimental outcomes are the epitome of necessity vs. sufficiency. The CE (258bp) and DRR (720bp) are sufficient to activate and maintain reporter gene transcription in a pattern nearly identical to *MyoD's* expression profile (Chen et al., 2001; Goldhamer et al., 1995; Kablar et al., 1999). When these elements are deleted, we find they are not necessary for proper regulation of the *MyoD* locus. We have shown that the recently published reports focused on *MyoD* regulation via transcription factor binding to the CE are incomplete as this element is quite disposable for proper regulation (Andrews et

al., 2010; Havis et al., 2012; L'Honore et al., 2010; Yamamoto et al., 2007; Zhang et al., 2011). It should be noted that these studies looked much more deeply into MyoD mRNA levels in their tissue or environment of interest than we did. Our analysis ended at E12.5, when the global MyoD mRNA profile appeared equivalent to wild type embryos. Both of our new lines, *MyoD*$^{\Delta CEDRR}$ and *MyoD*$^{\Delta CE15DRR}$, are viable and healthy, but they may exhibit unknown postnatal transcriptional phenotypes. The response these animals have to injury and regeneration may also be affected, and should be investigated in the future. Also, our genomic deletions have not led to improper, ectopic expression of *MyoD*, leaving no known areas that are capable of repressing *MyoD* transcription. The state of chromatin surrounding the *MyoD* locus may control repression, as *MyoD* was discovered after demethylating fibroblasts, that in turn activate the *MyoD* locus and form muscle (Taylor and Jones, 1979).

These findings ignite the search for new enhancer regions. The location of possible enhancers abound, but based on the current knowledge of the locus, one may be slightly upstream of the CE, where a portion of F3 fragment remains. The F3 fragment has been shown to drive faithful reporter gene expression, and part of this fragment contains the CE (Goldhamer et al., 1995; Goldhamer et al., 1992)). Another possible regulatory target are the introns of *MyoD*. This hypothesis is based on intronic enhancers in *Myf-5* , sequence conservation across species, putative binging sites for transcriptional activators, and preliminary data from Dr. Yamamoto, whose work showed that replacement of the open reading frame of *MyoD* with the GFP gene results in an unexpected

absence of GFP in the myogenic lineage. Whether this result is an artifact of the targeting design, or disruption of a new regulatory mechanism, should be pursued. Intron 1 of *MyoD* appears to be involved in regulation also based on H3K4 tri-methylation levels. A transgenic mouse embryo with intron one driving a reporter gene's expression can be performed to address that possibility.

Replacement of the *MyoD* gene with the *MyoD* cDNA in mouse embryos will determine if introns are regulating *MyoD* expression. To begin an unbiased search for enhancers, large scale BAC transgenes can be employed. The BACs should contain the genomic DNA surrounding the MyoD gene and contain a reporter gene, with its own minimal promoter. Large portions of the BAC can then be removed, followed by integration into the genome of murine ESCs to develop embryos and assayed for aberrant reporter gene expression. Ultimately, the large deletions can be refined to discrete elements. Chromatin Immunoprecipitation can also be used to identify trans-acting regulators, which are largely unknown, but several have been implicated in the introns of *MyoD*. Many recent studies have show transcription factors of interest binding the CE, but we now know that this interaction is not necessary for embryonic *MyoD* expression, and other regions should be investigated.

Linage tracing experiments presented in this thesis show strong support for *MyoD* being a determination factor in the trunk. Observation of cells that normally would have contributed to skeletal muscle instead forming brown fat, cartilage and bone in the absence of *MyoD* shows these cells are not determined before *MyoD* expression. The interpretation is complicated due to the absence

of the *Myf-5* gene. In embryos lacking only *MyoD*, all recombined cells contribute to the developing skeletal muscle. Based on the preliminary data in Chapter4 and *Myf-5* lineage ablation studies (Gensch et al., 2008; Haldar et al., 2008), some portion of the recombined cells presumably express only *MyoD* and not *Myf-5*. These cells may have fused to *Myf-5* dependent muscle.

The difference in phenotype of progenitors in the limb versus the trunk should also be investigated. Trunk progenitors can assume various fates, yet limb progenitors remain physically distinct from the surrounding fibroblastic mesenchyme, yet some express markers of the mesenchyme. FACS isolation of recombined cells that arrive in the limb at different time points can be used for heterotopic transplantation to further assess the determination status of these cells. Due to the long range migration, and lack of MRF expression before reaching the limb field, these cells may be strongly specified to the myogenic lineage while in the somite. The contribution of labeled cells to bone in the trunk may be due to both lineages arising from paraxial mesoderm. In the limb, bone progenitors come from the lateral plate mesoderm, and may be somehow refractory to contribution from somitically derived cells.

Also, if the genotype were changed such that the *Myf-5*^{loxP} allele replaces the *Myf-5*^{Neo} allele, information regarding *Mrf4* dependent myogenesis could be uncovered. In this scheme, *Mrf4* expression is not compromised and myogenesis occurs, but not to the extent of myogenic rescue (Kassar-Duchossoy et al., 2004). Looking for a fate change of the recombined cells in an embryo with some myogenesis would be informative as to the overlap between *Mrf4* and

MyoD expression. I would like to see if the recombined cells all contribute to the muscle, or if some still escape and become fat or cartilage. The limb field is of particular interest, as minimal reports are available on the limb phenotype in *MyoD*/*Myf-5* double mutants when the *Mrf4* locus is unperturbed.

The $MyoD^{iCre};R26^{DTA}$ results add support to the new theory that all myogenic progenitors express *MyoD* during development. Previous reports imply that there is a *Myf-5* dependent lineage and a *Myf-5* independent lineage. Now that all myoblasts and satellite cells (Kanisicak et al., 2009) express *MyoD* prenatally, it is even more interesting that *MyoD* null animals are viable and have reasonably normal muscle. Some uncertainty exists when comparing $Myf\text{-}5^{Cre}$ studies to the current $MyoD^{iCre}$ studies. The $Myf\text{-}5^{Cre}$ allele may be ectopically expressed. Given the sensitivity of the *Myf-5* locus to targeting, cells that should activate the allele may not, while other may activate it when inappropriate. We have internally tested the $MyoD^{iCre}$ allele for specificity, and it appears to faithfully mimic *MyoD* mRNA expression.

The observation that the longer the myotome exists, the more complete rib development occurs requires extensive experimental refinement. A developmental time courses during embryogenesis is needed to analyze exactly when myotome growth, and the resulting intercostal muscles, starts and stops in the various genotypes used in these preliminary studies. Our endpoint assay only shows a correlation, and is light on cause and effect. Others have reported that PDGFR alpha and FGF signaling between the myotome and sclerotome is disrupted when the myotome is absent and this is the cause of the rib phenotype

(Tallquist et al., 2000). Detection of these growth factors should be performed during development in the three genotypes analyzed here. Also of interest is a study that shows terminal rib malformations in embryos lacking the two differentiation factors, *Mrf4* and a reduced function version of *Myogenin* (Vivian et al., 2000). This supports the hypothesis that myotome formation and the maintenance of muscle is needed throughout rib development.

5.2 References

Andrews, J. L., et al., CLOCK and BMAL1 regulate MyoD and are necessary for maintenance of skeletal muscle phenotype and function. Vol. 107, 2010, pp. 19090-19095.

Chen, J. C., et al., 2001. Two upstream enhancers collaborate to regulate the spatial patterning and timing of MyoD transcription during mouse development. Dev Dyn. 221**,** 274-88.

Gensch, N., et al., 2008. Different autonomous myogenic cell populations revealed by ablation of Myf5-expressing cells during mouse embryogenesis. Development. 135**,** 1597-604.

Goldhamer, D. J., et al., 1995. Embryonic activation of the myoD gene is regulated by a highly conserved distal control element. Development. 121**,** 637-49.

Goldhamer, D. J., et al., 1992. Regulatory elements that control the lineage-specific expression of myoD. Science. 256**,** 538-42.

Haldar, M., et al., 2008. Two cell lineages, myf5 and myf5-independent, participate in mouse skeletal myogenesis. Dev Cell. 14**,** 437-45.

Havis, E., et al., 2012. Sim2 prevents entry into the myogenic program by repressing MyoD transcription during limb embryonic myogenesis. Development. 139**,** 1910-20.

Kablar, B., et al., 1999. Myogenic determination occurs independently in somites and limb buds. Dev Biol. 206**,** 219-31.

Kanisicak, O., et al., 2009. Progenitors of skeletal muscle satellite cells express the muscle determination gene, MyoD. Dev Biol. 332**,** 131-41.

Kassar-Duchossoy, L., et al., 2004. Mrf4 determines skeletal muscle identity in Myf5:Myod double-mutant mice. Nature. 431**,** 466-71.

L'Honore, A., et al., Pitx2 defines alternate pathways acting through MyoD during limb and somitic myogenesis. Vol. 137, 2010, pp. 3847-3856.

Tallquist, M. D., et al., 2000. Early myotome specification regulates PDGFA expression and axial skeleton development. Development. 127**,** 5059-5070.

Taylor, S. M., Jones, P. A., 1979. Multiple new phenotypes induced in 10T12 and 3T3 cells treated with 5-azacytidine. Cell. 17**,** 771-779.

Vivian, J. L., et al., 2000. Thoracic Skeletal Defects in Myogenin- and MRF4-Deficient Mice Correlate with Early Defects in Myotome and Intercostal Musculature. Developmental Biology. 224**,** 29-41.

Yamamoto, M., et al., 2007. Cloning and characterization of a novel MyoD enhancer-binding factor. Mechanisms of Development. 124**,** 715-728.

Zhang, X., et al., A non-canonical E-box within the MyoD core enhancer is necessary for circadian expression in skeletal muscle. Vol. 40, 2011, pp. 3419-3430.